

Berichte

zur Polar-
und Meeresforschung

628

2011

Reports
on Polar and Marine Research



The Expedition of the Research Vessel "Polarstern"
to the Antarctic in 2010 (ANT-XXVII/1)

Edited by
Karl Bumke
with contributions of the participants



ALFRED-WEGENER-INSTITUT FÜR
POLAR- UND MEERESFORSCHUNG
in der Helmholtz-Gemeinschaft
D-27570 BREMERHAVEN
Bundesrepublik Deutschland

ISSN 1866-3192

Hinweis

Die Berichte zur Polar- und Meeresforschung werden vom Alfred-Wegener-Institut für Polar- und Meeresforschung in Bremerhaven* in unregelmäßiger Abfolge herausgegeben.

Sie enthalten Beschreibungen und Ergebnisse der vom Institut (AWI) oder mit seiner Unterstützung durchgeführten Forschungsarbeiten in den Polargebieten und in den Meeren.

Es werden veröffentlicht:

- Expeditionsberichte (inkl. Stationslisten und Routenkarten)
- Expeditionsergebnisse (inkl. Dissertationen)
- wissenschaftliche Ergebnisse der Antarktis-Stationen und anderer Forschungs-Stationen des AWI
- Berichte wissenschaftlicher Tagungen

Die Beiträge geben nicht notwendigerweise die Auffassung des Instituts wieder.

Notice

The Reports on Polar and Marine Research are issued by the Alfred Wegener Institute for Polar and Marine Research in Bremerhaven*, Federal Republic of Germany. They appear in irregular intervals.

They contain descriptions and results of investigations in polar regions and in the seas either conducted by the Institute (AWI) or with its support.

The following items are published:

- expedition reports (incl. station lists and route maps)
- expedition results (incl. Ph.D. theses)
- scientific results of the Antarctic stations and of other AWI research stations
- reports on scientific meetings

The papers contained in the Reports do not necessarily reflect the opinion of the Institute.

The „Berichte zur Polar- und Meeresforschung“
continue the former „Berichte zur Polarforschung“

* Anschrift / Address

Alfred-Wegener-Institut
für Polar- und Meeresforschung
D-27570 Bremerhaven
Germany
www.awi.de

Editor in charge:
Dr. Horst Bornemann

Assistant editor:
Birgit Chiaventone

Die "Berichte zur Polar- und Meeresforschung" (ISSN 1866-3192) werden ab 2008 ausschließlich als Open-Access-Publikation herausgegeben (URL: <http://epic.awi.de>).

Since 2008 the "Reports on Polar and Marine Research" (ISSN 1866-3192) are only available as web-based open-access publications (URL: <http://epic.awi.de>)

The Expedition of the Research Vessel "Polarstern" to the Antarctic in 2010 (ANT-XXVII/1)

**Edited by
Karl Bumke
with contributions of the participants**

**Please cite or link this publication using the identifier
hdl:10013/epic.37742 or <http://hdl.handle.net/10013/epic.37742>**

ISSN 1866-3192

ANT-XXVII/1

25 October - 26 November 2010

Bremerhaven – Las Palmas - Cape Town

Chief scientist

Karl Bumke

Coordinator

Eberhard Fahrback

Contents

1. Zusammenfassung und Fahrtverlauf	2
Itinerary and summary	4
2. Weather conditions	6
3. Autonomous measurement platforms for energy and material exchange between ocean and atmosphere (OCEANET) - atmosphere component	10
3.1 Energy and material exchange between ocean and atmosphere: The OCEANET atmosphere observatory	10
3.2 Aerosol measurements with hand-held MICROTOPS II sunphotometer	18
3.3 Cloud detection by full-sky imaging polarimetry	20
4. Autonomous measurement platforms for energy and material exchange between ocean and atmosphere (OCEanet): Ocean	23
5. Autonomous measurement platforms for energy and material exchange between ocean and atmosphere (OCEanet): Biology - Biogeographical distribution and activity of diazotrophs	26
6. Sea trial and tests of the underwater navigation system “POSIDONIA 6000“ after modification of the protective window	29
7. Calibration of the new echosounder system Atlas Hydrosweep DS3	38
7.1 Analysis of the distance between MINS and GPS Antennas	39
7.2 Determination of sound velocity profiles using VALEPORT SVP	43
7.3 Calibration of time latency, roll, pitch and yaw angle	46
7.4 Quality determination of the HYDROSWEEP DS3	49
8. Halocarbon Air Sea Transect – Atlantic (HalocAST-A) – Fall	53

9. Investigation of brominated and organophosphorus flame retardants and monitoring of legacy POPs in the Atlantic and the southern ocean	57
10. (A) On-board testing of a newly developed seagoing membrane-inlet mass spectro-meter (MIMS) and setup of pCO₂/iron experiments with natural Southern Ocean phytoplankton populations; (B) Sampling of POM for biomarker analysis	63
11. Installation and data taking of a cosmic muon detector on <i>Polarstern</i>	65
12. Cavity-enhanced DOAS measurements of iodine monoxide in the marine atmosphere	67
13. MAPS: marine mammal perimeter surveillance	69
Annex	
A.1 Teilnehmende Institute / participating institutions	77
A.2 Fahrtteilnehmer / cruise participants	79
A.3 Schiffsbesatzung / ship's crew	80
A.4 Stationsliste / station list PS 77	81

1. ZUSAMMENFASSUNG UND FAHRTVERLAUF

Karl Bumke

Leibniz-Institut für Meereswissenschaften IFM-GEOMAR, Kiel

Am 25. Oktober 2010 begann der Fahrtabschnitt ANT-XXVII/1 von Bremerhaven nach Kapstadt (Abbildung 1.1) mit 43 Wissenschaftlern an Bord. Die Fahrt diente zur kontinuierlichen Messung atmosphärischer und ozeanographischer Parameter, der Erprobung von weiterentwickelten und neuen Geräten im Einsatz auf See sowie der Wechselwirkung Ozean-Atmosphäre.

In der Nordsee wurde das Navigations-System MINS ausgiebig getestet. Auf dem weiteren Weg in die Biskaya herrschte windiges Wetter, aber rechtzeitig für die Kalibrierung und Abnahmetests des weiterentwickelten Hydrosweep-Systems in der Biskaya legte sich der Wind. So konnten alle Testzyklen erfolgreich abgeschlossen werden, bevor die Windgeschwindigkeit Sturmstärke erreichte und die Wellenhöhen anwuchsen. Auf dem Weg zur nächsten Station im Südwesten der Iberischen Halbinsel besserte sich das Wetter zusehends. Nach Durchführung der Tests des modifizierten Unterwasser-Navigations-Systems POSIDONIA nahmen wir Kurs auf Las Palmas, wo wir am 6. November anlegten. 12 Wissenschaftler verließen dort FS *Polarstern* und 3 kamen an Bord. Am Nachmittag legten wir wieder ab und verließen Las Palmas in Richtung der Romanche Bruchzone. Dort wurden die Pitch-Kalibrierungen des Hydrosweep-Systems wiederholt und Profile zur Kartierung des Ozeanbodens gefahren. Auf dem weiteren Weg zum Angola-Becken war das Wetter ruhig. Dort wurde mit Hilfe des Hydrosweep-Systems eine geeignete Stelle zur Verankerung eines akustischen Rekorders für Untersuchungen von Wal-aufzuchtgebieten festgelegt. Auf dem weiteren Weg nach Kapstadt nahm der Wind stetig zu und erreichte schließlich wieder Sturmstärke.

Während des gesamten Fahrtabschnittes wurden kontinuierliche Messungen der Energie- und Materialflüsse zwischen Ozean und Atmosphäre, der Bewölkung und Aerosolverteilung in der Atmosphäre, von Temperatur- und Wasserdampfprofilen sowie des Flüssigwassergehalts der Troposphäre und eine Reihe von biologischen und chemischen Untersuchungen in Atmosphäre und Ozean durchgeführt. Letztere befassten sich mit Stickstoff, Sauerstoff, persistenten organischen Schadstoffen, Jod-Monoxid, Stickstoff-Dioxid, Kohlenstoff-Dioxid und reaktiven Halogenen. Biogeographische Messungen der Primärproduktion und Stickstoff-Fixierung wurden ebenfalls durchgeführt. Im Nasslabor wurde ein für den Einsatz auf See neu entwickeltes Massenspektrometer installiert und in Betrieb genommen. Auf dem Krähennest wurde ein automatisches Walbeobachtungs-System aufgebaut und ebenfalls umfangreichen Tests unterzogen. Ergänzt wurden die Messungen noch durch Bestimmungen der Rate kosmischer Teilchen.

Alle geplanten Messungen, Kalibrierungen und Gerätetests unter Einsatzbedingungen auf See konnten wie geplant durchgeführt werden. Am 26. November erreichte *Polarstern* Kapstadt.

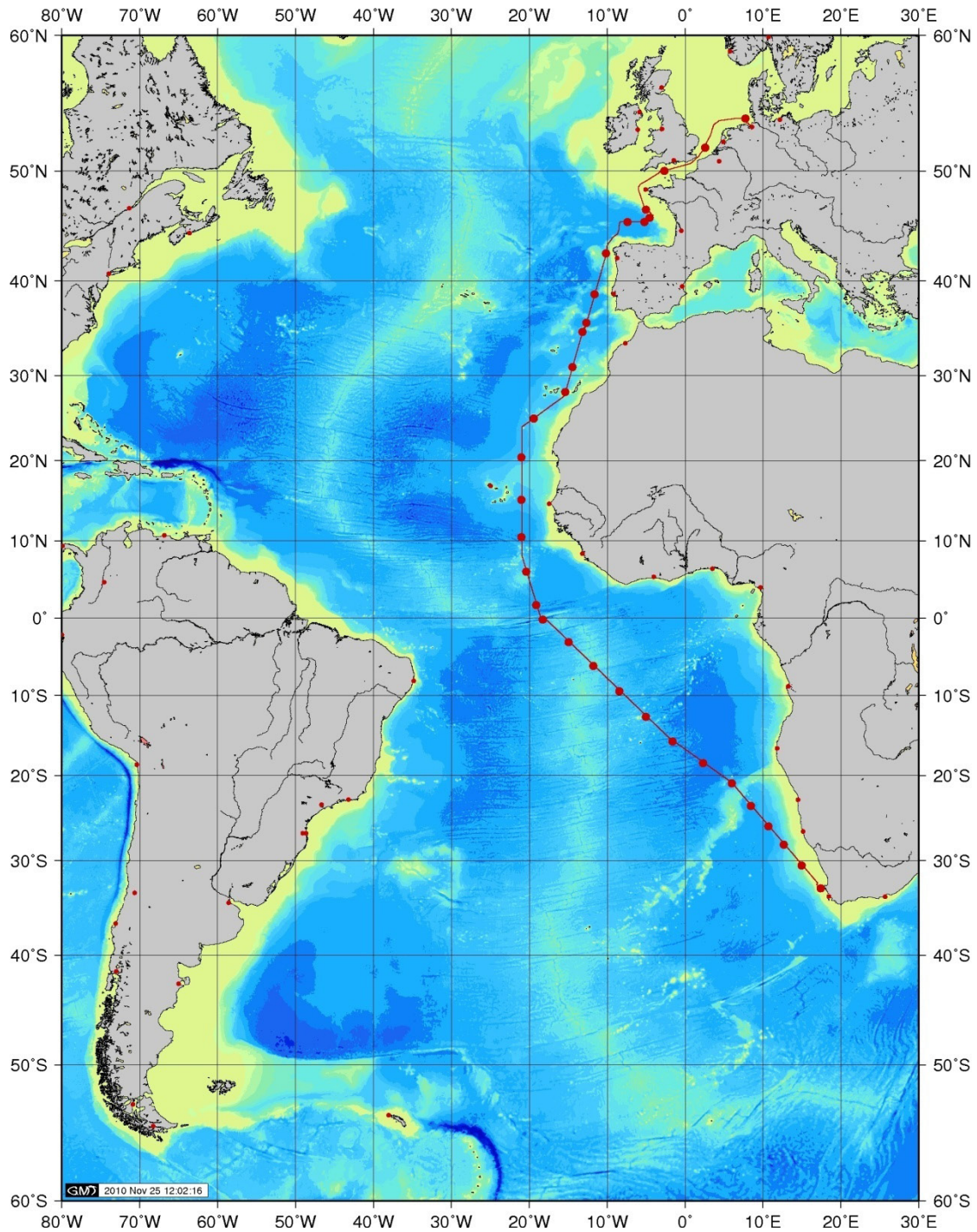


Abb. 1.1: Kurs der FS Polarstern Reise ANT-XXVII/1

Fig. 1.1: Cruise track of Polarstern during the expedition ANT-XXVII/1

ITINERARY AND SUMMARY

On 25 October 2010 *Polarstern* started its Atlantic transfer ANT-XXVII/1 from Bremerhaven to Cape Town (Fig. 1.1) with 43 scientists on board. The cruise was utilized for continuous investigations of atmospheric and marine properties, sea acceptance tests of modified and new instruments as well as for ocean and atmosphere interaction studies.

In the North Sea the navigation system MINS was extensively tested. On the cruise to the Bay of Biscay we had windy weather, but just in time for the calibration and the sea acceptance test of the improved Hydrosweep system winds slowed down. So all tests could be successfully finished just in time before wind speeds reached gale force and wave heights increased again. Steaming towards the next station southwest of the Iberian Peninsula weather became kind. Tests of the improved underwater navigation system POSIDONIA were carried out before we took course on Las Palmas. We berthed there on 6 of November. 12 scientists went off board and 3 entered the *Polarstern*. At noon we left Las Palmas and steamed towards the Romanche Gap. At this station we repeated the pitch calibration of the Hydrosweep system and took several profiles to estimate the seafloor orography. Weather remained kind on our way towards the Angola Basin. With the aid of the Hydrosweep system we searched for a suitable position to deploy a mooring equipped with a voice recorder to improve our knowledge about whales' breeding grounds. At the end of our cruise leg to Cape Town wind speeds again reached gale force. During the whole cruise a number of underway measurements were carried out. These were meteorological measurements of the energy and material fluxes, monitoring of cloudiness and aerosol distribution in the atmosphere, and measurements of the tropospheric state with respect to temperature, humidity, and liquid water content as well as a number of experiments regarding air and marine chemistry. These comprised estimates of nitrogen and oxygen, persistent organic pollutants, Iodine monoxide, nitrogen dioxide, carbon dioxide, and reactive halogens. Bio-geographical measurements of primary production and nitrogen fixation were also performed. In the wet laboratory a new developed mass spectrometer (MIMS) for the use on sea was installed and was put into operation. On the crow's nest a whale observation system was mounted and extensively tested. Measurements were completed by estimates of cosmic particles rates.

All measurements, calibrations, and sea acceptance tests were carried out according to the planning. On 26 November 2010 *Polarstern* arrived in Cape Town.

2. WEATHER CONDITIONS

Hartmut Sonnabend
Deutscher Wetterdienst

Associated by strong to stormy winds and lively shower activity *Polarstern* left Bremerhaven in the morning of 25 October 2010 to start with a station for test purposes in the vicinity of Helgoland. In the rear of a complex low pressure system over Scandinavia a wave depression tracked from the northern North Sea across Denmark towards the Western Baltic. During its approach the shower activity was tied up soon and the wind increased quickly up to gale force 8 Bft from west-north-west. The corresponding wind sea rose to 4 meters. Directly after having finished the test station *Polarstern* headed for the next working area in the Bay of Biscay. Until the morning of the next day the wind decreased to 5 - 6 Beaufort shifting to southwest and south-southwest later on. Before having reached the Strait of Dover the wind increased once more up to gale force 8 and 9 at times during the approach of a warm front belonging to a new large gale centre over the North Atlantic. A rough wind sea of around 3.5 meters formed quickly. The passage of the Strait of Dover happened in the evening of 26 October 2010 with rain, drizzle and reduced visibilities. After the passage of the following cold front during the next morning, the wind and weather conditions improved gradually over the remaining areas of the English Channel.

The investigation area in the Bay of Biscay was reached in the morning of 28 October 2010 with sunny skies, moderate winds from the south and a north-westerly swell of about 3 meters which did not hamper station works. Unfortunately these fine conditions did not last for a long time. A cold front belonging to a storm depression west of Scotland crossed the working area between noon and afternoon of the following day inducing a rise of wind force up to 7 - 8 from south-southwest for some hours. This marked the prelude for significant cyclonic activity during the next few days. The next storm depression following in the very active frontal zone reached the Bay of Biscay in the morning of 30 October 2010 with strong to stormy winds from southerly directions and some rain at times. After the passage of its frontal system in the afternoon the wind shifted to southwest remaining strong to stormy. The following maritime cold air mass triggered high reaching convection with numerous strong showers partly associated with thunderstorms. During the whole day a rough wind sea of around 3.5 meters moved over the still existing westerly swell of about 3 to 4 meters inducing uncomfortable pitching and rolling.

After having finished all tests and investigations in the Bay of Biscay in the early morning hours of 31 October 2010, *Polarstern* headed towards the test area for the Posidonia system lying on its course to Las Palmas. This day brought the spectacular development predicted well by all forecast systems. During the centre of the storm depression started to track from its position west of Britain towards the Western Mediterranean Sea slowly,

a high pressure ridge from the North Atlantic subtropical high spread east, quickly forming a sharp pressure gradient especially over the western and south-western parts of Biscay. After a short break in the morning the wind increased soon reaching gale force 8 from northwest until noon. While shifting to the north-northwest, the wind still increased up to 9 Beaufort reaching its maximum in the early evening when gale force 9 - 10 with gusts up to Bft 11 were measured for a short period. At the same time the wave maximum passed the course of *Polarstern* with heights between 7 to 8 meters on average. The west-northwest swell with heights of about 4.5 to 5 meters was quickly superimposed by the wind sea up to 7 m with some single waves reaching heights of around 10 m or even more. Shortly after having reached their maxima, wind and sea started to decrease - slowly at first and rapidly down to Bft 6 until the early morning of 1 November, shortly after *Polarstern* had circumnavigated Cape Finisterre, the north-western tip of Spain. Influenced by increasing high pressure influence the wind finally decreased to north-northwest 4 - 5 Bft while subsequently the swell dropped to 3 - 4 meters during the same day. As a contrast that day brought a lot of sunshine. The air pressure rose from 987 hPa in the morning of 31 October 2010 to a value of 1025 hPa until noon of 1 November 2010.

This change was due to this transition from the North Atlantic frontal zone into the area of the subtropical high. After having passed the axis of a large high propagating from the Azores towards Northern Spain and Southern France the northeast trade wind set in during the morning of 3 November 2010 at the latitude of the Strait of Gibraltar. Between the high in the north and a flat trough south of the Canary Islands the northeast trade wind increased up to force 6 Bft for this day and as a relict of the North Atlantic frontal zone a long north-westerly swell with a maximum height of about 3.5 to 4 meters passed *Polarstern* when carrying out the Posidonia station. But these slightly rough conditions did not persist for a long time and before having finished station work, wind and swell started to decrease. The weather conditions became very fine on the final miles to Las Palmas and light winds from the east and sunny skies dominated during *Polarstern*'s short stay there.

These conditions lasted for the rest of the day after the ship had left the harbour towards its next waypoint at 24°N/21°W. As the days before, the visibilities were reduced slightly by contamination of dust from the Sahara Desert. Induced by a new high that formed over the sea areas between Newfoundland and the Azores the north-easterly trades increased for a while to force 5 - 6 Bft favouring the course with winds from the aft. While proceeding south *Polarstern* left the southern flank of the North Atlantic high and encountered an area with very weak pressure gradients. The northeast trade wind decreased and became light to variable for a while, recovering slightly up to Beaufort 3 - 4 during the next two days, while *Polarstern* was approaching the northern parts of the Intertropical Convergence Zone (ITCZ). The water temperatures rose continuously reaching values of about 29°C at 11°N.

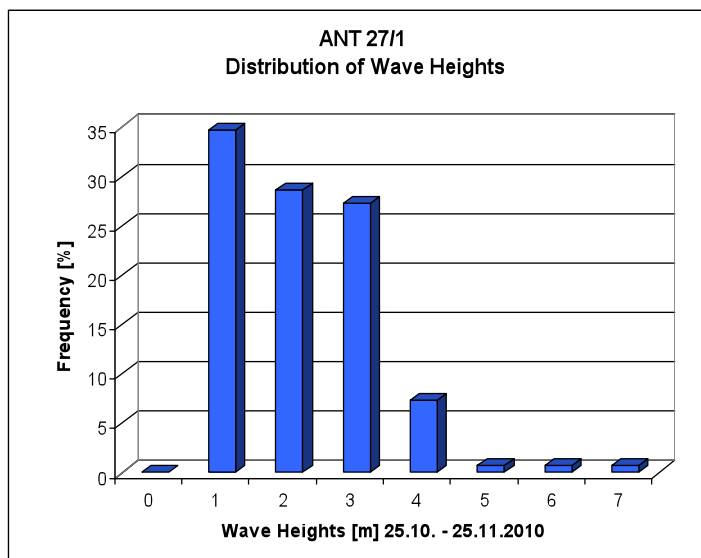
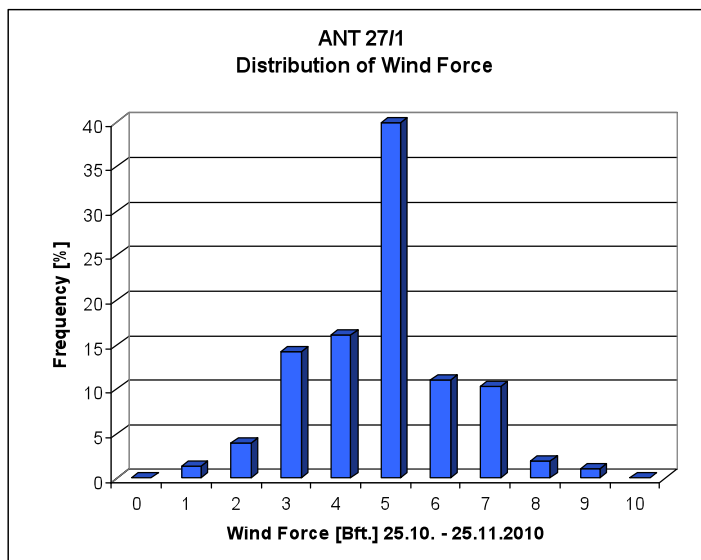
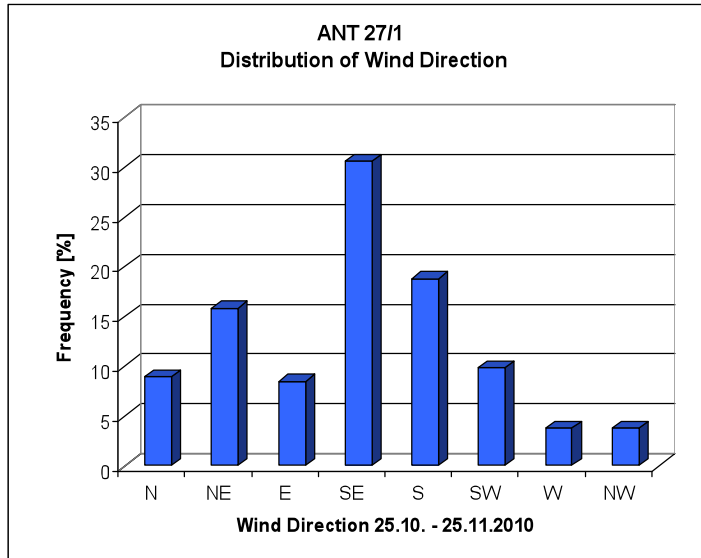
Polarstern encountered the northern most activity zone of the ITCZ in the early afternoon of 10 November 2010 at 10°N with a short "welcome rain shower" of weak intensity. Nevertheless this event induced the wind to shift from northeast to southeast performing the change to the southern hemispheric trade wind system. During the night to 11 November 2010 a large cloud cluster with numerous embedded strong convective cells crossed the cruise track of *Polarstern*. However, none of the active

cells with their heavy rainfall encountered *Polarstern* and so only an imposing firework of sheet lightning to all directions was observed during the night. This changed until noon of 11 November 2010, after the large cluster had drifted north-westward and widely scattered moderate convection was triggered above the up to 29.3°C warm water. Until the early morning of the following day these small sized convective cells provided several short but heavy rain showers, partially associated with lightning and thunder.

Under the regime of a fresh southeast trade wind mainly sunny weather interrupted only by some light and isolated showers dominated the final course towards the working area located a few miles south of the equator. Since having passed the ITCZ, water temperatures dropped from around 29°C to 27°C near equator. After having carried out the Hydrosweep station the cruise was continued towards Cape Town with moderate south-easterly winds and a swell of around 1.5 – 2 meters in the early afternoon of 13 November 2010. Corresponding with a well defined air pressure gradient between the South Atlantic subtropical high and the equatorial trough the southeast trade wind freshened up slightly during the following night reaching 5 Bft and occasionally force Bft 6 during the following 3 days. From the noon of the 15 November until the morning of the 18 November 2010, *Polarstern* crossed a large area of stratocumulus clouds belonging to a significant trade wind inversion which is typical for these sea areas. In the meantime the high that had been responsible for the trade winds blowing along the cruise line, propagated towards the Indian Ocean. As a result of this the gradient between the remaining ridge in the southwest and the seasonal thundery lows over the southern Africa weakened and subsequently the wind calmed down to a gentle breeze from southerly directions between 18 and 20 of November. Besides this the persistent cloud cover broke up partially and gave place for some longer sunny periods. These fine weather conditions continued within the following days, favouring the work at the mooring position on Walvis Ridge.

Nevertheless the last days on the way to Cape Town the trade wind showed its rough face and blew very strong and even stormy at times. This development was initialized by a large and mighty anticyclone which propagated slowly along 40°S eastward towards the Greenwich meridian during the remaining days. Between this high and the seasonal trough over the Kalahari Desert und Southern Namibia a sharp air pressure gradient formed like a bottleneck along our cruise line. As a result of this the southeast wind increased to 6 - 7 Bft rapidly during the night to 22 November 2010 and up to gale force 8 at times in the late evening of the 23 November. The sea became very rough reaching wave heights up to 4.5 meters. The following day brought a lot of sunshine but only little improvement concerning wind conditions and sea state. After a short break in the morning of 25 November 2010, the southeast wind soon increased during afternoon and evening of the same day, reaching force Bft up to gale force 8 for the final approach to Cape Town, where *Polarstern* arrived in the early morning of 26 November 2010. The statistics of wind force and direction as well as of sea state are summarized in Fig. 2.1.

Fig. 2.1: Statistics of wind directions, wind force, and wave heights for the cruise leg ANT-XXVII/1



3. AUTONOMOUS MEASUREMENT PLATFORMS FOR ENERGY AND MATERIAL EXCHANGE BETWEEN OCEAN AND ATMOSPHERE (OCEANET) ATMOSPHERE COMPONENT

Andras Barta¹⁾, Karl Bumke²⁾,
Akos Horvath³⁾, Gabor Horvath¹⁾,
John Kalisch²⁾, Thomas Kanitz⁵⁾,
Henry Kleta⁴⁾, Andreas Macke⁵⁾
(not on board), Yann Zoll²⁾

¹⁾Eötvös
²⁾IFM-GEOMAR
³⁾MPI
⁴⁾DWD
⁵⁾Ift

Objectives

The determination of energy and mass budget at the air-sea interface is still a running task with respect to climate research. One of the biggest obstacles in our understanding of the coupled ocean-atmosphere system are the clouds. Climate models have still difficulties to model clouds correctly with respect to their spatial and temporal distribution. The small scale variability of clouds necessitates parameterizations for a correct description of radiative transfer on subgrid-scales. A combined observation of cloud properties, energy and mass fluxes, and atmospheric parameters and properties are a requirement to validate these parameterizations.

Most of the measurements are part of the Leibniz network-project OCEANET (chapter 3.1). Within this project a 20 - feet sea container has been developed which is equipped with *in-situ* and remote sensing instruments to measure all quantities to estimate and model the energy and mass budget at the air-sea interface. This OCEANET atmosphere observatory was placed the second time on the monkey deck of Polarstern during an Atlantic transect.

Other measurements related to OCEANET are independent estimates of atmospheric aerosol by hand-held sun-photometers (chapter 3.2) and the use of another new type of a full-sky imager (chapter 3.3).

3.1 Energy and material exchange between ocean and atmosphere: THE OCEANET atmosphere observatory

Karl Bumke¹⁾, John Kalisch¹⁾,
Thomas Kanitz²⁾, Henry Kleta³⁾,
Andreas Macke²⁾ (not on board),
Yann Zoll¹⁾

¹⁾IFM-GEOMAR
²⁾Ift
³⁾DWD

Objectives

As mentioned above the OCEANET container is equipped with instruments to measure directly the energy and mass budget at the air sea interface. Measured energy fluxes

are the sensible and latent heat fluxes as well as the down-welling solar radiation and long-wave counter radiation. Simultaneous cloud information is given by a full sky imager every 15 seconds. For modelling and parameterization purposes meteorological standard parameters are measured as well as vertical profiles of the temperature, humidity, and aerosol content. These measurements are completed by estimations of the integrated atmospheric liquid water and information about cloud heights. This gives a comprehensive data set for a detailed analysis of air sea interaction and validation studies of climate analyses.

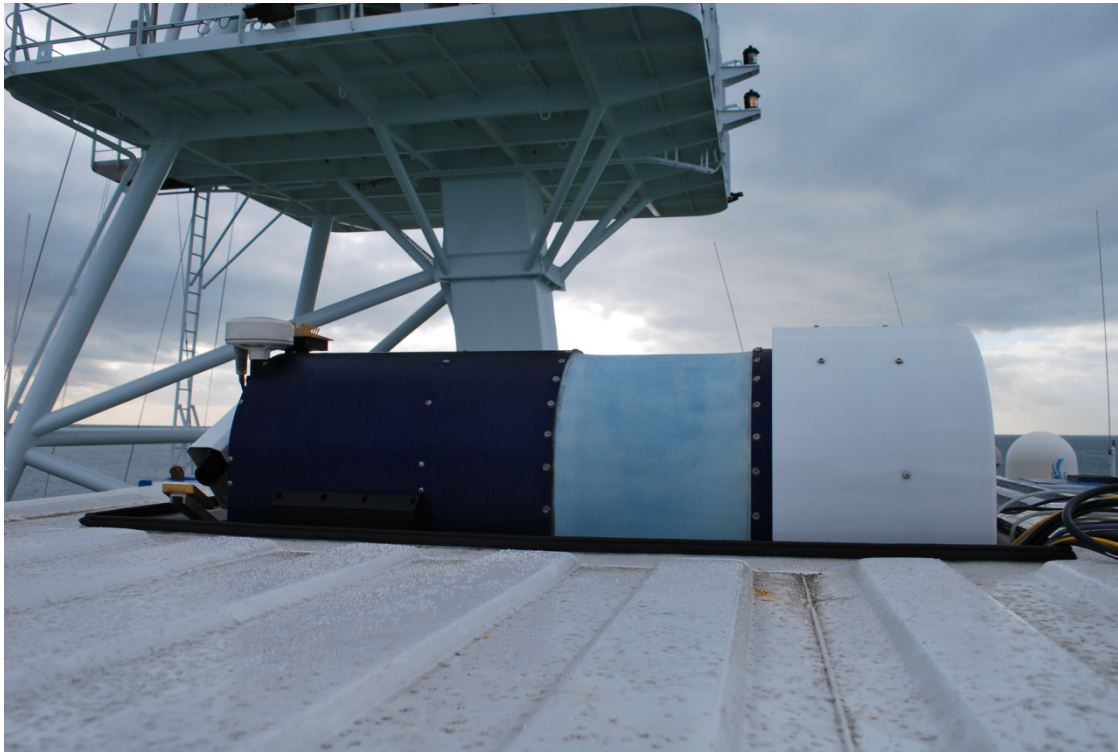


Fig. 3.1.1: Microwave radiometer HATPRO on the top of the OCEANET-atmosphere observatory (photo by Karl Bumke).

Work at sea

After lifting the OCEANET atmosphere container onto the observation deck all instruments were launched while *Polarstern* was still at the pier. The OCEANET atmosphere container comprises the following instruments (bold letters):

- The upward looking **pyranometer** Kipp&Zonen CM 21 and the **pyrgeometer** CG 4 operated by IFM-GEOMAR have provide the broadband downwelling shortwave radiation (DSR) and the downwelling longwave radiation (DLR) with a resolution of roughly 2 seconds.
- Every 15 seconds **full sky images** were obtained from a weatherproof digital camera system manufactured at IFM-GEOMAR. This enables a detailed analysis of the influence of cloud cover and cloud type on the radiation budget at the sea surface.

- As for the previous 6 *Polarstern* Atlantic transects a multi-channel **microwave radiometer** (HATPRO, Radiometer Physics, Fig. 3.1.1) was utilized for continuous observations of atmospheric temperature and humidity profiles as well as liquid water and precipitable water path.

Together with ceilometer measurements of cloud bottom height, sun photometer measurements of aerosol optical thickness, the data from the microwave radiometer provide a unique set of information to interpret the amount of down-welling solar and thermal radiation at the sea surface.

- For the second time an **absorption hygrometer** (Licor) in combination with a Metek **sonic anemometer** was installed, which allows to derive turbulent fluxes of momentum, sensible heat, and water vapour (latent heat). An older measurement system (Another Metek sonic anemometer and a M100) for observations of turbulent fluxes of momentum, sensible and latent heat was installed in addition on the crow's nest. Due to a rough sea state this system was mounted only since the entrance to the Bay of Biscay. Both instrumental systems were functioning properly during the entire cruise.
- **The Polly^{XT} Lidar-system** of the IfT Leipzig for vertical profiling of aerosols and cirrus clouds was also part of the OCEANET container. Whenever weather conditions were appropriate measurements were performed. The used Polly^{XT}, which had been developed at the IfT Leipzig, emits laser pulses at 1064, 532 and linear polarized light at 355 nm into the atmosphere and measures the backscattered elastic light at 180° scattering angle. Additionally, the Raman method is utilized by detecting molecular scattering of nitrogen at 387 and 607 nm. The opportunity of observing depolarization at 355 nm rounds up the system. The scattered light at each wavelength is measured every 30s up to 30 km height at a range resolution of 30 m. Thus it provides the possibility of a high temporal and range resolved description of the vertical aerosol distribution.

The analysis of the retrieved optical and microphysical properties allows the characterization of separated aerosol layers with high vertical resolution. In combination with a radiative transfer model the results will help to quantify the solar aerosol radiative forcing above oceans.

As a by-product Polly^{XT} provides cloud base and top height, the latter for thin clouds only.

- Within the OCEANET project a shipborne automatic weather station has been developed. The System (**SCAWS**) is based on standard hardware (Campbell Scientific) and autonomously measures the following parameters: time, position, speed and course over ground, heading, barometric pressure, temperature, rel. humidity, wind (direction and speed) and radiation (short- and longwave). During the cruise the system was tested under various conditions and was prepared to operate fully independently during the following cruises ANT-XXVII/2 to 4 of *Polarstern*.

The used sensors are standard within the maritime network of DWD. The system provides a complete set of data every second (proprietary NMEA 0183 protocol) and

an hourly weather report (FM13 SHIP) which is transmitted ashore via DCP.

In addition to these standard outputs SCAWS monitors the power supply of the sky imager installed on top of the OCEANET atmosphere container. This information is included with mean values of the connected radiation sensors and transmitted ashore as well, thus allowing real-time monitoring of the radiation fluxes and the status of the sky imager mounted on the OCEANET container.

Preliminary results

Fig. 3.1.2 shows the time series of the integrated water vapour (IWV) and liquid water path (LWP) along the cruise. The *in-situ* IWV derived from the daily radio soundings, which were performed by the DWD, are shown for comparison. The agreement with the indirectly obtained micro-wave products is generally good.

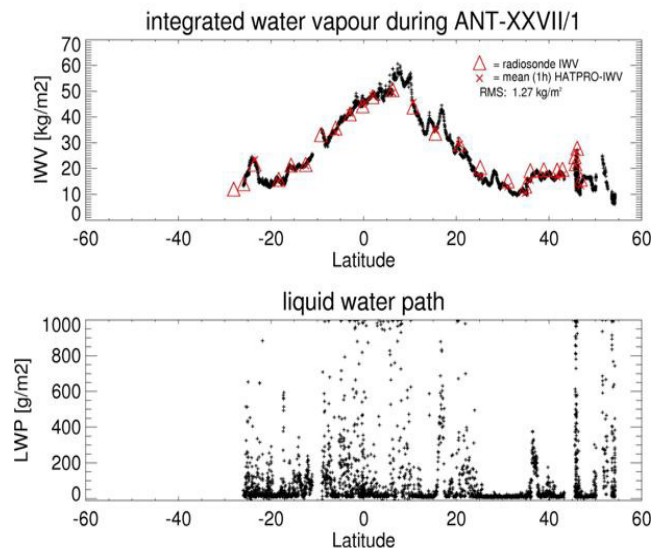


Fig. 3.1.2: Time series of integrated water vapour (upper diagram) and liquid water path (lower diagram) from the HATPRO microwave radiometer. The water vapour path from the radiosonde measurements is also shown.

Largest water vapour paths are observed at the thermal equator reaching about 60 gm². The cloud liquid water path is given by the occasional data points above a background noise. They need to be corrected during a later analysis by making use of the full sky camera images and measurements of the upward looking infrared radiometer to identify clear sky conditions directly above the ship during day time.

The meridional temperature profiles and corresponding humidity profiles are depicted in Figs. 3.1.3 and 3.1.4 and show the typical variations caused by the different climate regimes.

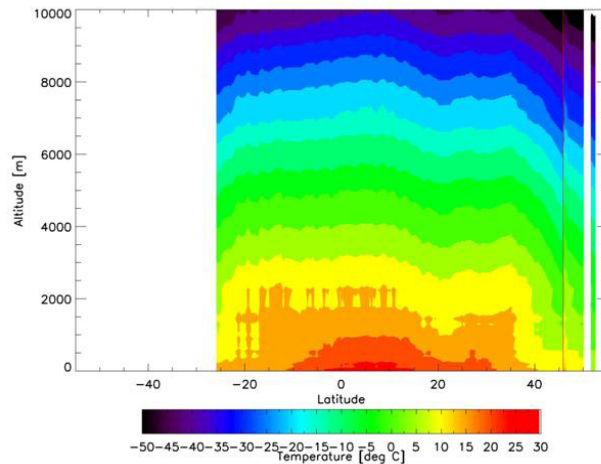


Fig. 3.1.3: Vertical profiles of temperature retrieved from the microwave radiometer along the cruise track, shown as a function of latitude.

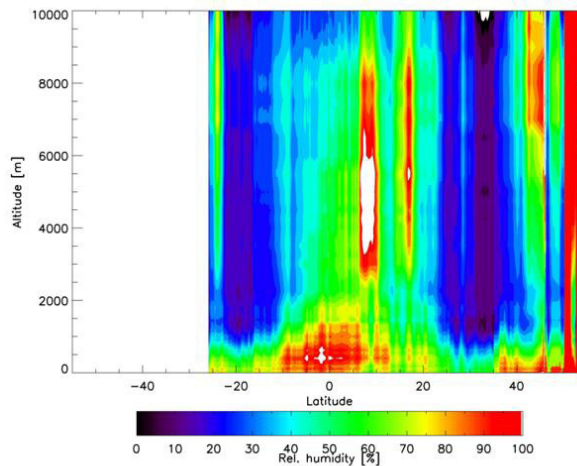


Fig. 3.1.4: Vertical profiles of relative humidity retrieved from the microwave radiometer along the cruise track, shown as a function of latitude.

An example for a daily time series of the down-welling shortwave and longwave radiation is given in Fig. 3.1.5. As a reference, the theoretical curves for clear sky shortwave radiation at the surface (blue) and extraterrestrial shortwave radiation at the top of the atmosphere (grey) are also shown. The measured maximum of the down-welling shortwave radiation is about 1863 Wm^{-2} and exceeds considerably even the extra-terrestrial value of 1370 Wm^{-2} , which is shown at a higher temporal resolution in Fig. 3.1.6.

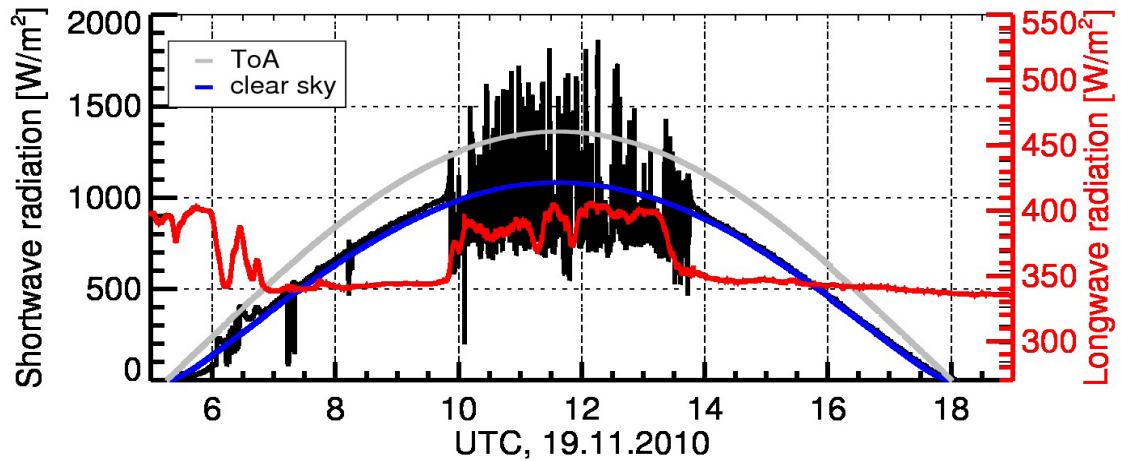


Fig. 3.1.5: Time series of down-welling broadband solar (black) and thermal (red) radiation from 19 November 2010. The reference clear sky radiation at sea level (blue) and at the top of the atmosphere (grey) is shown for comparison.

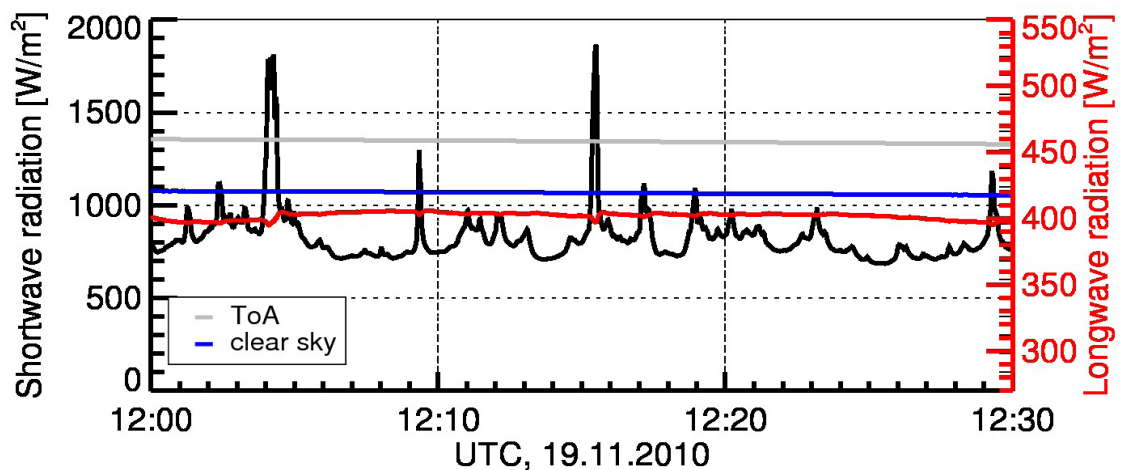


Fig. 3.1.6: High-resolution zoom of the down-welling broadband solar (black) and thermal (red) radiation from 19 November 2010, 12:00 until 12:30 UTC. The reference clear sky radiation at sea level (blue) and the top of the atmosphere (grey) is shown for comparison.

The measured value is the highest ever measured on *Polarstern* since the beginning of our radiation measurements in 2007. Such occasions of a radiation excess can be found often. They are attributed to the increased diffuse down-welling radiation during broken cloud conditions (because of this termed as “broken cloud effect”). The corresponding image of the full sky imager is given in Fig. 3.1.7. It clearly shows that it requires nearly overcast skies with broken alto cumulus clouds where the full solar disk can be seen through a cloud gap. Thus, the direct irradiance is not attenuated by clouds. The additional white diffuse down-welling scattering at the clouds’ sides, in particular in the vicinity of the solar disk, produces the strong enhancements. Further analysis will test the correlation between the observed cloud properties like cloud cover and liquid water path, and the surface radiation budget.

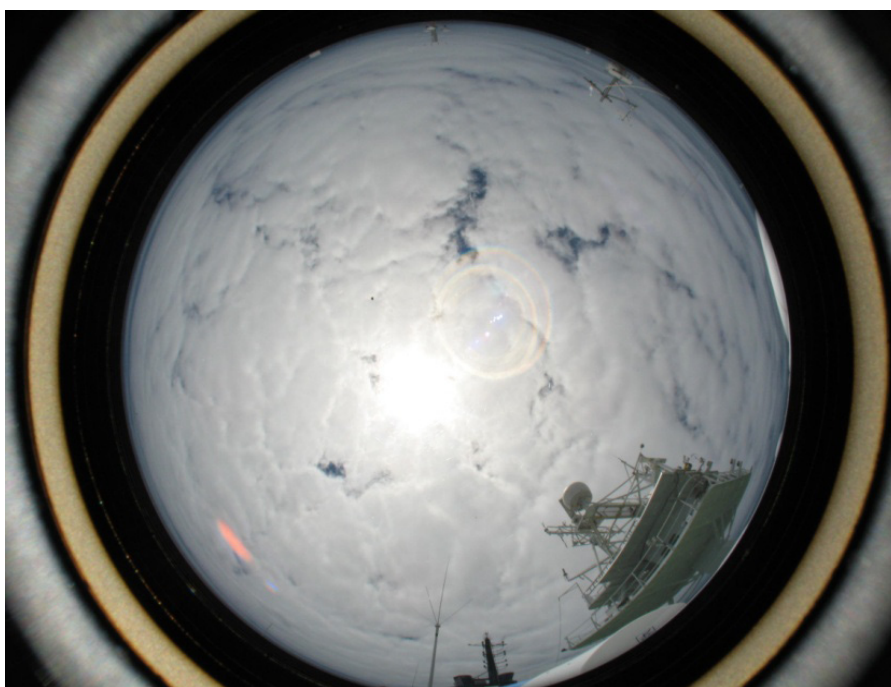


Fig. 3.1.7: Full sky image during the maximum of solar down-welling radiation at the surface measured (Fig. 3.1.6, 12:16 UTC) during this cruise. (photo by John Kalisch)

The measurements of the energy budget at the sea surface is complemented by measurements of turbulent fluxes of sensible heat and of latent heat (water vapour flux). The high frequency measurements of wind, humidity and temperature require a careful quality check and a time consuming numerical analysis before they can be converted into turbulent fluxes. A detailed analysis of turbulence measurements by instruments installed directly on the OCEANET container showed that measurements at this position are hampered by flow distortion. However, measurements at the crow's nest allow derivation of turbulent fluxes using the inertial dissipation method. Results of all measurements (ANT-XXIV/4 until ANT-XXVII/1), expressed in terms of bulk coefficients reduced to 10 m height and neutral stratification, are given in Figs. 3.1.8 and 3.1.9. In general results are close to earlier results of Large and Pond (1981 and 1982). Since turbulence measurements are only possible under conditions with the wind coming over the bow, derived bulk coefficients have to be used to parameterize heat fluxes from measurements of meteorological standard parameters to get continuous estimates of the energy budget at the sea surface.

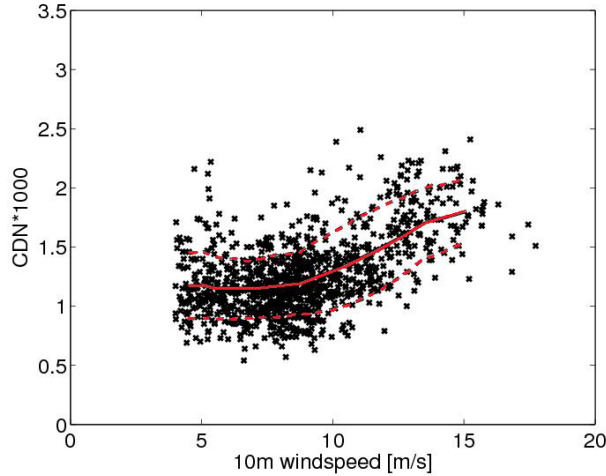


Fig. 3.1.8: Bulk coefficient for the flux of momentum reduced to neutral stratification and 10 m height derived from measurements at the crow's nest and standard meteorological parameters as a function of wind speed u . The lines give averages and standard deviations for each 1ms^{-1} interval. Estimated values of C_{DN} are $1.12 \cdot 10^{-3}$ up to $u=9\text{ms}^{-1}$ and $(0.64 + 0.053 \text{ sm}^{-1} \cdot u) \cdot 10^{-3}$ for $u>9\text{ms}^{-1}$.

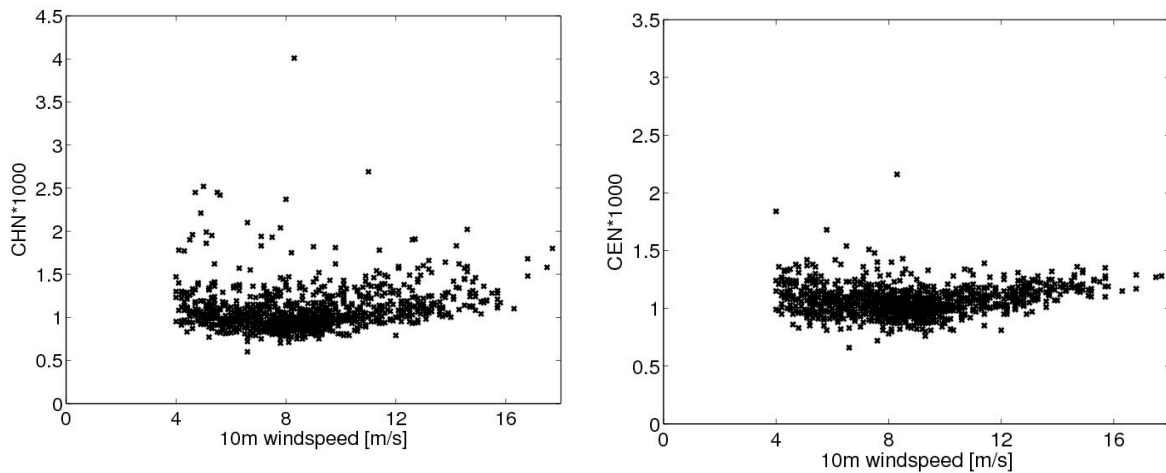


Fig. 3.1.9: Bulk coefficients for the flux of sensible heat (left) and latent heat (right) reduced to neutral stratification and 10 m height derived from measurements at the crow's nest and standard meteorological parameters as a function of wind speed. Average values are $C_{HN}=1.08 \cdot 10^{-3}$ and $C_{EN}=1.02 \cdot 10^{-3}$.

The lidar measurements show that on average the marine boundary layer reached an altitude of 500 m and that the signal intensity strongly depended on wind velocity. A Saharan dust plume has been observed at 5 November 2010 near the Canary Islands. Fig. 3.1.10 shows the range corrected signal at 1064 nm at a logarithmic scale as a function of height from 4 to 5 November. Polarstern entered the plume at midnight. The plume was in a height of 600 to 1,300 m in the beginning and consisted until about seven o'clock in the evening.

Upon arrival in Cape Town the lidar will be parked at a host institute, and will be picked up again for the spring cruise 2011 when Polarstern will be heading back to Bremerhaven.

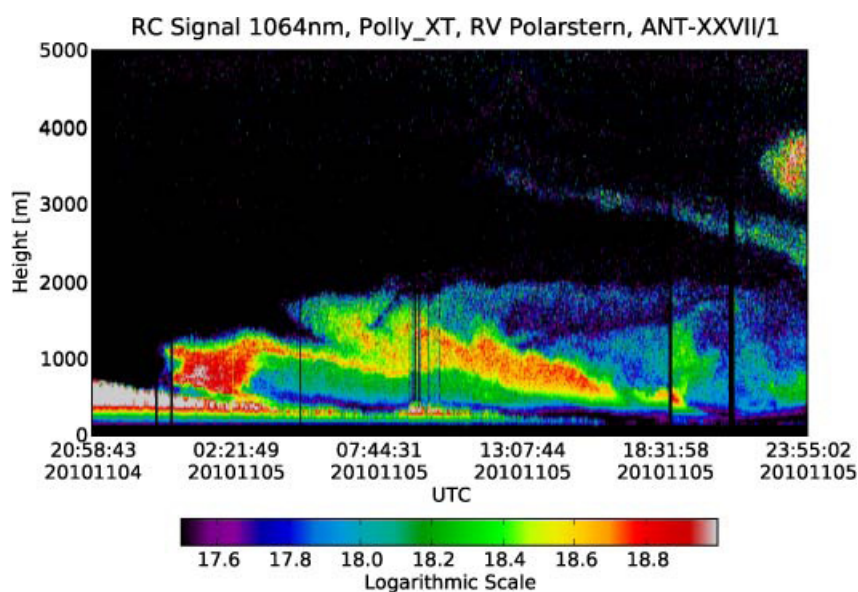


Fig. 3.1.10: Saharan Dust Plume near to Canary Islands.

To check the quality of the data provided by the autonomous meteorological measurement system SCAWS the data have been compared to those of the operational weather station on board *Polarstern*. The overall agreement is good. This system will measure autonomously during the following cruise ANT-XXVII/2 to 4.

References

- Large, W.G. and S. Pond, 1982: Sensible and latent heat flux measurements over the ocean, *J. of Physical Oceanography* 12, 464-482.
- Large, W.G. and S. Pond, 1981: Open ocean momentum flux measurements in moderate to strong winds, *J. of Physical Oceanography* 11, 324-336.

3.2 Aerosol measurements with hand-held MICROTOPS II sunphotometer

Ákos Horváth, Stefan Kinne (not on board)
MPI

Objectives

A large number of different aerosols exist, differing e.g. in type or number density. They play an important role in the atmospheric radiative transfer and influence the cloud formation as well as cloud properties. Furthermore atmospheric water vapour interacts with the aerosols. Therefore there are still large uncertainties in climate modeling with respect to aerosols. Thus, aerosol measurements are an important complement to observations of clouds and air sea interaction (3.1 and 3.3) to improve our knowledge about atmospheric processes influenced by aerosols.

During ANT-XXVII/1 aerosol optical depth (AOD), Angstrom parameter, and columnar

water vapor measurements were obtained with a hand-held 5-channel MICROTOPS II sunphotometer whenever we had clear sky and sea conditions allowed it.

Work on board

Sunphotometer measurements were conducted within the framework of the Maritime Aerosol Network (MAN), a component of AERONET, and OCEANET. For this type of observation it was crucial to avoid any cloud contamination, especially by thin cirrus clouds. In addition, twice per week the front window of the instrument was cleaned with compressed air in order to remove dust and other particles that might have accumulated on it. Raw data were sent on a daily basis to Dr. Alexander Smirnov of Sigma Space Corporation, NASA Goddard Space Flight Center (alexander.smirnov-1@nasa.gov) for post-processing.

Preliminary results

Data taken on and after 19 November showed an unexpected change in the spectral dependence of AOD. Suddenly, AOD₄₄₀ became greater than AOD₃₈₀ contrary to expectations. One possible explanation was that a significant amount of dust had accumulated on the front window. Visual inspection revealed some particle accumulation, but nothing out of the ordinary. Nevertheless, the front window was photographed and cleaned once again with compressed air. Another possibility was that surface pressure was significantly different from the standard pressure of 1013 hPa applied to the instantaneous data that day. This possibility was checked and ruled out as NCEP forecast data became available. Currently, the most likely explanation is that calibration of the 440 nm channel has shifted slightly (within 0.01). Post-field calibration and analysis of the front window photographs by Dr. Smirnov will clear up this discrepancy once the instrument is sent back to NASA GSFC.

Apart from this relatively minor issue, the data looked reasonable. Fig. 3.2.1 shows Level 1.5 (cloud-screened) AOD₅₀₀ measurements taken as of 22 November. AOD was below 0.1 (blue) as *Polarstern* cruised along the European and northwest African coast. After Las Palmas, Canary Islands, AOD first increased to 0.1-0.2 (green) and then reached its maximum of 0.3 - 0.5 (orange) west of Senegal and Guinea, probably due to Saharan dust. Afterwards, as *Polarstern* headed further away from continental sources AOD showed a gradual decline first to 0.1-0.2 then below 0.1. The full dataset is available at the following public domain web-based archive: http://aeronet.gsfc.nasa.gov/new_web/cruises_new/Polarstern_Fall_10.html.

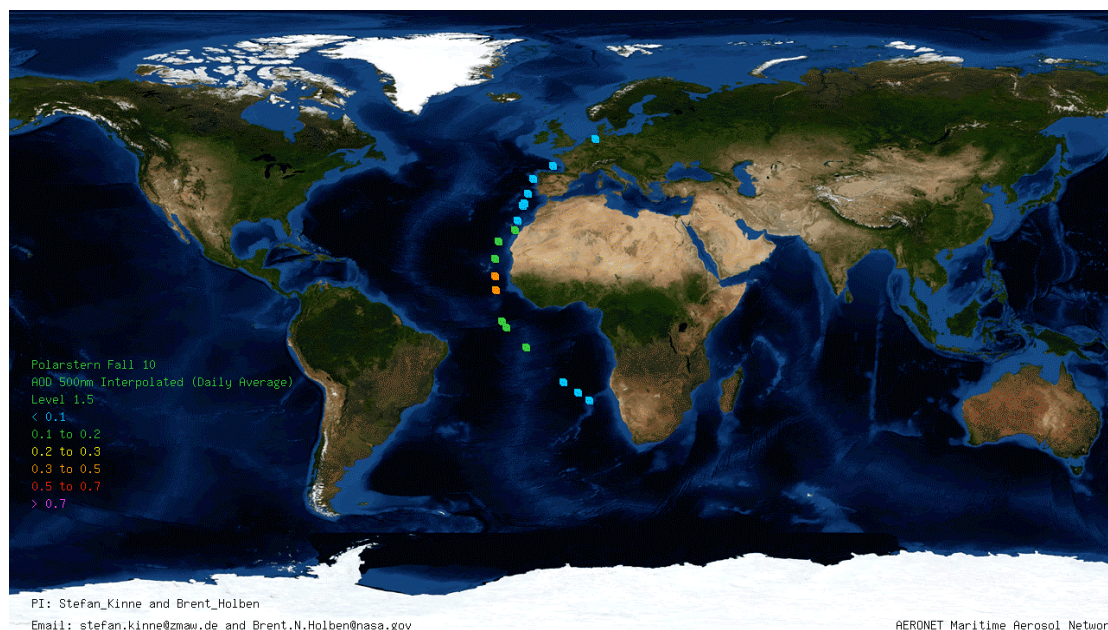


Fig. 3.2.1: Level 1.5 (cloud-screened) AOD_{500} measurements taken during the Atlantic transect ANT-XXVII/1

3.3 Cloud detection by full-sky imaging polarimetry

András Barta¹⁾, Gábor
Horváth²⁾, Ákos Horváth³⁾

¹⁾Eötvös&Estrato
²⁾Eötvös
³⁾MPI

Objectives

The objective was to test the second generation, automatic, sequential, rotating-analyzer, full-sky, imaging polarimetric cloud detector on board *Polarstern* under conditions at sea. The field of view of the camera is 180° (full sky). The rotating wheel contains three linear polarizers with three differently oriented transmission axes (0°, 45°, 90° from the radial direction) and an infrared filter. The instrument takes five photographs of the full sky: One through the infrared filter, one without any filters, and three through the polarization filters. The most important polarization images are taken within 0.5 second. The instrument is supplied by 230 V and controlled remotely through an ethernet cable from a passenger cabin of the ship. Its internal air volume is hermetically separated from the outside environment and contains a Peltier-element cooler for temperature control, and 1 kg silica gel for moisture control. An algorithm detects the position of the sun on the circular color picture of the sky and sets the shadow-disc into this position. Its shade eliminates disturbing internal reflections from the fisheye-lens surfaces that could otherwise lead to artifacts during evaluation of the polarization images. Using the three polarization images, an algorithm calculates the patterns of intensity, degree of polarization, and angle of polarization of skylight in the red (650 nm), green (550 nm), and blue (450 nm) parts of the spectrum. From these parameters another algorithm classifies each pixel as either clear or cloudy, thereby obtaining the cloud mask of the full sky.

Work on board

During the expedition ANT-XXVII/1 the instrument was set up on top of a container on the monkey-deck in the immediate vicinity of the full-sky photometric cloud detector of the OCEANET team (Fig. 3.3.1).

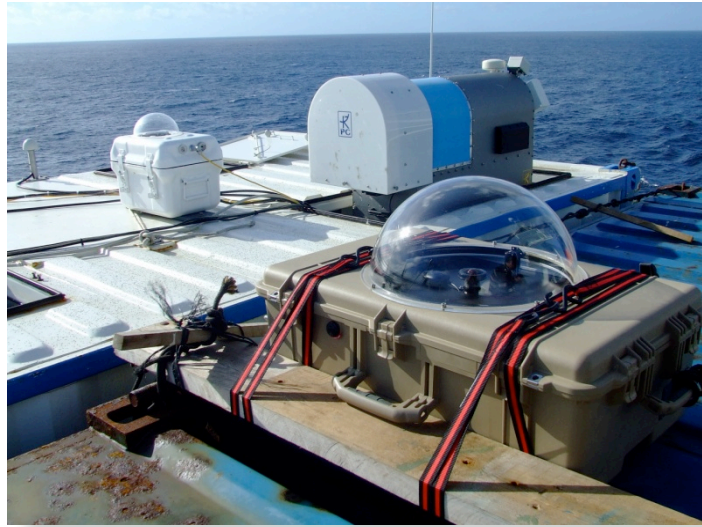


Fig. 3.3.1: Full-sky polarimetric cloud detector (right) in the vicinity of the full-sky photometric cloud detector of the OCEANET team (left) on top of the OCEANET container.(photo by András Barta)

The instrument (Fig. 3.3.2) functioned excellently during the 3-week test period. It passed successfully the sea acceptance tests with regard to water-, moisture-, sun-, and temperature proofes. Occasionally, the transparent plastic hemispheric cover above the fisheye-lens had to be cleaned by fresh water in order to remove salt crystals accumulated from sea spray. The only significant measurement difficulty was encountered during high seas, when rapid changes in the ship's attitude introduced a motion artifact (blurring) during the sequential acquisition of the three polarization images with a single camera. In our 3rd generation instrument this problem will be eliminated by obtaining simultaneous polarization images with three separate cameras.

Preliminary results

- Post-processing of the data will be performed at home. By using a cloud mask, visually-derived by an expert as baseline, the accuracies of a conventional photometric cloud detection algorithm will be compared to several different polarimetric cloud detection algorithms developed at the Budapest university. From the measured pattern of the degree of linear polarization of skylight the distribution of the relative cloud base height in the whole sky will be calculated. Using the cloud base height measured by LIDAR at a given point of the sky, the relative cloud base height values can be transformed into absolute altitude values. This algorithm can be validated by making use of the LIDAR data.
- On the basis of our field experience gathered during the expedition ANT-XXVII/1

3.3. Cloud detection by full-sky imaging polarimetry

the 3rd generation of the instrument will be developed containing three full-sky fisheye-lenses with fixed linear polarizers. This instrument will take three polarization images of the full sky simultaneously and, thus, will eliminate the problem of motion artifact.



Fig. 3.3.2: Close-up photograph of the full-sky polarimetric cloud detector. (photo by András Barta)

4. AUTONOMOUS MEASUREMENT PLATFORMS FOR ENERGY AND MATERIAL EXCHANGE BETWEEN OCEAN AND ATMOSPHERE (OCEANET): OCEAN

Henry Bittig¹⁾, Mario
Hoppema (not on board)²⁾,
Arne Körtzinger (not on
board)¹⁾, Tobias Steinhoff¹⁾, S.
van Heuven (not on board)³⁾

¹⁾IFM-GEOMAR

²⁾AWI

³⁾NIOZ

Objectives

The aim of the WGL-PAKT-Initiative OCEANET is to develop new autonomous instruments for the investigation of energy and matter exchange at the air-sea interface. The multi-institutional participants from IFM-GEOMAR, HZG, and AWI intend to build up a sensor network that investigates atmospheric and surface ocean properties. In order to meet the growing demand for increased spatial and temporal data, autonomous sensor networks that can be deployed on merchant vessels are needed. Tests of new instruments and measuring techniques as well as the installation of instrumentation aboard Polarstern are essential components of the project.

The oceanic component of this study focuses on the marine carbon cycle in the surface ocean which is of high climate relevance but at the same time susceptible to climate change. The surface ocean's CO₂ source/sink function is maintained by a complex interaction of physical and biological processes. Therefore its understanding requires measurement of various different parameters as it is pursued within OCEANET.

During ANT-XXVII/1 the work carried out during the earlier transit expeditions (ANT-XXIV/4, ANT-XXV/1 and 5, ANT-XXVI/1 and 4) was continued. During the first OCEANET cruise the feasibility of autonomous underway measurements was assessed for a wide range of instruments for measurement of physical (temperature, salinity, turbidity), chemical (CO₂ partial pressure (pCO₂), pH, oxygen, total gas tension, nutrients), and biological parameters (chlorophyll a, photosynthetic parameters) and small intercomparison for measurements of pCO₂ and oxygen took place. Within the second cruise the focus was on intercomparison measurements of CO₂ partial pressure with diverse autonomous underway flow-through as well as submersible systems. The work on the third transit dealt with the closer investigation of a commercial submersible pCO₂-sensor and included CTD casts with the instrument. Underway pCO₂-measurements were run as a reference. Nitrate and nutrient determinations were part of the work as well.

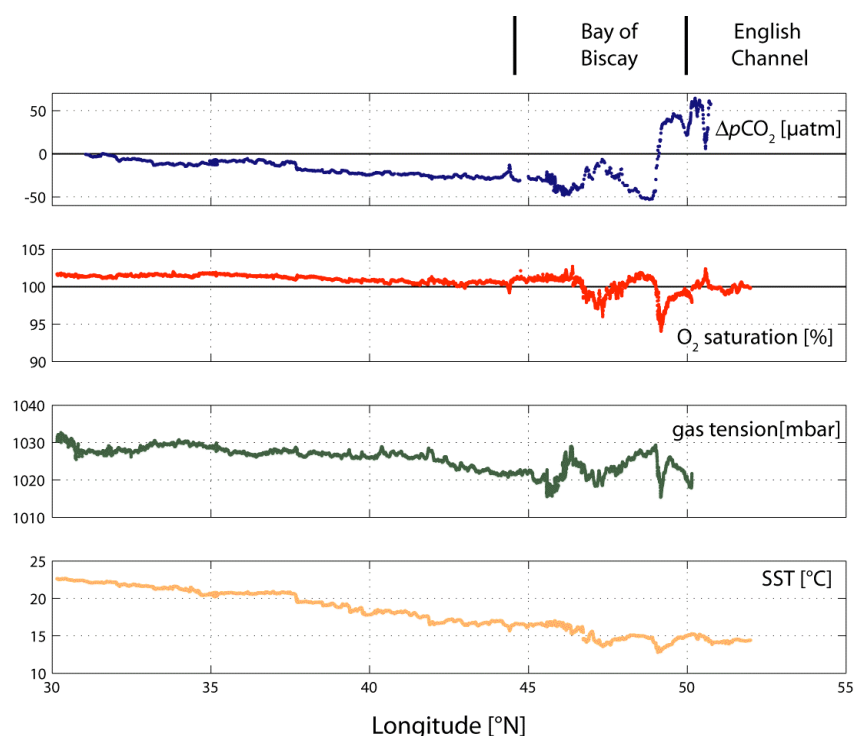
During ANT-XXVII/1 the "standard setup" of proved sensors was installed. These standard sensors include pCO₂ measurements by the classical equilibrator system installed on board and measurements of dissolved oxygen and total gas tension.

Work at sea

We operated four different underway instruments which were all connected to the ships seawater supply. The water was pumped from approximately 11 m depth to the laboratory and was divided to the different instruments.

We used the $p\text{CO}_2$ instrument installed on board as our reference system. It is a commercially available instrument (General Oceanics, Miami, USA) using a classical spray head equilibrator to equilibrate an air portion with the continuous water flow. After the equilibration process the sample gas is dried and subsequently measured via NDIR using a LICOR 7000 gas analyzer. The LICOR is calibrated approximately every 3 h with 3 standard gases ranging from 184 to 744 ppm CO_2 . A detailed description of the instrument can be found in Pierrot et al. (2009).

Fig. 4.1: Preliminary underway data of $\Delta p\text{CO}_2$, Oxygen saturation, gas tension and SST on the transect from Bremerhaven to the Canary Islands.



In addition an oxygen optode (Aanderaa instruments, Bergen, Norway) and a gas tension device (Pro Oceanus, Halifax, Canada) were deployed into a flow-through box that was flushed with approximately 10 L min^{-1} . A newly developed CO_2 sensor (Franatech, Lüneburg, Germany) was also connected to the seawater supply for comparison with the standard $p\text{CO}_2$ instrument (GO system, see above).

For further validation of the $p\text{CO}_2$ results and calculation of the marine carbonate system, discrete samples for dissolved inorganic carbon (DIC) and total alkalinity (TA) were taken every 8 h for analysis at the IFM-GEOMAR in Kiel. The samples were drawn into 500 ml glass bottles and poisoned with saturated mercuric chloride solution

Preliminary (expected) results

Fig. 4.1 shows the preliminary results. Only data of the first part of the cruise track were

used. Shown are the $\Delta p\text{CO}_2$ (difference between seawater $p\text{CO}_2$ and atmospheric $p\text{CO}_2$), Oxygen saturation state, the total pressure of all dissolved gases (gas tension) and sea surface temperature (SST).

The combined patterns of DpCO_2 , oxygen saturation and gas tension along the cruise track can be interpreted in terms of the driving forces of which the seasonal cycles of sea surface temperature and net community production are the most important ones. Their effect on surface disequilibria of CO_2 and O_2 is very different owing to the two gases very different air-sea equilibration time scales (roughly 1 year vs. 1 month). The observed pattern of DpCO_2 shows supersaturation on the continental shelf and slight undersaturation from the Bay of Biscay until the Canary Islands. These observations are in good agreement with Takahashi et al. (2009) and Thomas et al. (2004), who found this supersaturation of CO_2 on the continental shelf. However, the data will be analyzed together with the data of the former Polarstern cruises from 2008 until 2010 and will be published at the Carbon Dioxide Information Center (CDIAC, <http://cdiac.ornl.gov>).

Furthermore the data of the newly developed CO_2 sensor will be compared to the measurements of the GO-system to validate the performance of this system and its possible application for autonomous operation.

References

- Pierrot, D., C. Neill, K. Sullivan, R. Castle, R. Wanninkhof, H. Lüger, T. Johannessen, A. Olsen, R. A. Feely, C. E. Cosca (2009). Recommendations for autonomous underway $p\text{CO}_2$ measuring systems and data-reduction routines. *Deep-Sea Res. II*, 56, 512-522.
- Takahashi, T, S.C. Sutherland, R. Wanninkhof, C. Sweeney, R.A. Feely, D.W. Chipman, B. Hales, G. Friederich, F. Chavez, C. Sabine, A. Watson, D.C.E. Bakker, U. Schuster, N. Metzl, H. Yoshikawa-Inoue, M. Ishii, T. Midorikawa, Y. Nojiri, A. Körtzinger, T. Steinhoff, M. Hoppema, J. Olafsson, T.S. Arnarson, B. Tilbrook, T. Johannessen, A. Olsen, R. Bellerby, C.S. Wong, B. Delille, N.R. Bates und H.J.W. de Baar (2009). Climatological mean and decadal change in surface ocean $p\text{CO}_2$, and net sea-air CO_2 flux over the global oceans. *Deep-Sea Res. II*, 56, 554-577.
- Thomas, H., Y. Bozec, K. Elkalay, and H.J.W. de Baar (2004). Enhanced open ocean storage of CO_2 from shelf sea pumping. *Science*, 304, 1005-1008.

5. AUTONOMOUS MEASUREMENT PLATFORMS FOR ENERGY AND MATERIAL EXCHANGE BETWEEN OCEAN AND ATMOSPHERE (OCEANET): BIOLOGY - BIOGEOGRAPHICAL DISTRIBUTION AND ACTIVITY OF DIAZOTROPHS

Wiebke Mohr, Benjamin Weigel, Julie LaRoche (not on board)
IFM-GEOMAR

Objectives

The main objectives of this project are to assess the abundance, activity and diversity of diazotrophic microorganisms and the determination of the rates of primary production and dinitrogen (N_2) fixation along the meridional transect. Regular 6-h time interval samples during the ship's sailing time provide a roughly 1-1.5° latitudinal resolution enabling the assignment of biogeographical regions for the different diazotrophic groups to be analyzed. The analysis of *nifH* gene expression patterns will be correlated to environmental conditions such as temperature or light. The molecular analysis of the sample seawater will be supplemented with analytical flow cytometry samples as well as the determination of rates of N_2 fixation and primary production using the stable isotopes $^{15}N_2$ and $NaH^{13}CO_3$, respectively. The overall data set will provide a spatial and temporal distribution of the abundance and activity of diazotrophs throughout the Atlantic Ocean.

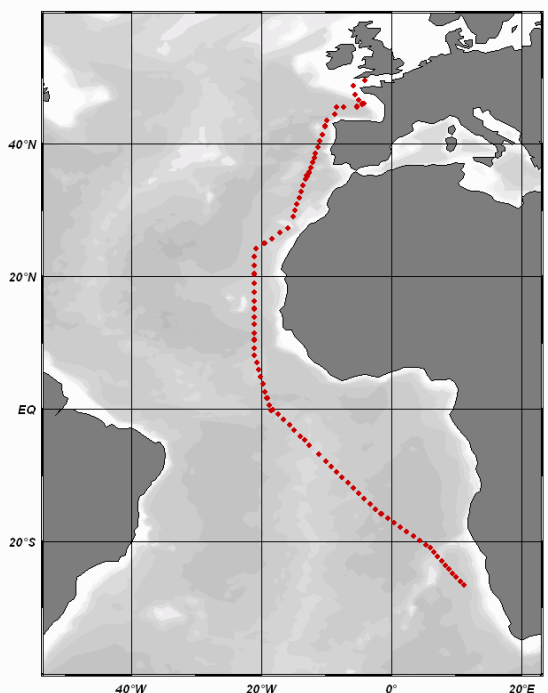
Work at Sea

The first surface seawater samples using the ship's clean seawater supply were obtained in the evening on 27 October 2010 just outside the western English Channel (Fig. 5.1). From thereon, samples were taken at regular 6-h intervals throughout the cruise until 22 November 2010 off the coast of Southern Africa. In summary, a total of 95 stations were sampled for molecular analysis of the diazotrophic community during the cruise. In specific, these surface seawater samples were filtered onto Durapore membrane filters (0.22 μm pore size, 47 mm diameter) within 30 min time, frozen immediately and stored at $-80^\circ C$ until further analysis in the molecular laboratory at the IFM-GEOMAR in Kiel. To supplement the molecular analysis, analytical flow cytometry (AFC) samples were taken in parallel to the seawater filtrations.

To complement the molecular and AFC analysis of the diazotrophic community, on-deck 24-h seawater incubations were performed to determine rates of N_2 fixation (using two different methods: Montoya *et al.* 1996 and Mohr *et al.* 2010) and primary production using the stable isotopes $^{15}N_2$ and $NaH^{13}CO_3$, respectively. In specific, two times triplicate 4-L polycarbonate bottles were filled with seawater from the clean seawater supply. The stable isotopes were added to the bottles which were placed in

on-deck incubator with ambient surface seawater flow-through for about 24 h. Non-amended seawater incubations for the analysis of the natural abundance of ^{15}N and ^{13}C were included for each incubation. After the incubation time, the samples were filtered onto pre-combusted GF/F filters, dried at $\sim 50 - 60^\circ\text{C}$ and stored at room temperature until bulk mass spectrometric analysis.

Fig. 5.1: Sampling stations for molecular biological analysis of the diazotrophic community along the ANT-XXVII/1 cruise transect.



Preliminary Results

Using molecular biological techniques (quantitative PCR), we will obtain abundance estimates for about six different phylotypes of diazotrophs using specific probes for the *nifH* gene which encodes the iron-subunit of the nitrogenase enzyme complex. *nifH* gene expression analysis on these samples will reveal (potential) activity patterns of diazotrophs during the cruise. The combination of the 6-h regular interval sampling and the sailing of the ship will provide a horizontal and temporal distribution of the abundance and activity of diazotrophs. The results of the horizontal distribution will reveal biogeographical information of diazotrophs throughout the Atlantic Ocean including areas of highest dust deposition, *i.e.* the Eastern North Atlantic and upwelling areas, *i.e.* off the coast of Namibia. While passing the area south of the Cape Verde Islands, some atmospheric dust could be observed. Dust has previously been shown to stimulate N_2 fixation (Mills *et al.* 2004) by providing iron and possibly phosphorus to the surface ocean microbial community (Baker *et al.* 2007). Both elements are considered to be limiting nutrients for N_2 fixation. As on ANT-XXVI/1 and ANT-XXVI/4 rates of N_2 fixation and primary production will be obtained through laboratory-based mass spectrometric analysis. The combination of these data sets will show possible seasonal fluctuations with certain environmental or hydrographic conditions.

References

- Baker AR, Weston K, Kelly SD, Voss M, Streu P, Cape JN (2007) Dry and wet deposition of nutrients from the tropical Atlantic atmosphere: Links to primary productivity and nitrogen fixation. *Deep-Sea Res Pt I* 54: 1704-1720.
- Mills MM, Ridame C, Davey M, LaRoche J, Geider RJ (2004) Iron and phosphorus co-limit nitrogen fixation in the eastern tropical North Atlantic. *Nature* 429: 292-294.
- Mohr W, Großkopf T, Wallace DWR, LaRoche J (2010) Methodological underestimation of oceanic nitrogen fixation rates. *PLoS ONE* 5(9): e12583. doi:10.1371/journal.pone.0012583
- Montoya JP, Voss M, Kähler P, Capone DG (1996) A simple, high-precision, high-sensitivity tracer assay for N₂ fixation. *Appl Environ Microbiol* 62(3): 986-993.

6. SEA TRIAL AND TESTS OF THE UNDERWATER NAVIGATION SYSTEM “POSIDONIA 6000“ AFTER MODIFICATION OF THE PROTECTIVE WINDOW

Werner Dimmler¹, Saad El
Naggar², Peter Gerchow²,
Mattias Monsees²,

¹Fielax
²AWI

Objectives

The underwater navigation system POSIDONIA was upgraded during the ship yard stay of *Polarstern* in Bremerhaven between 20 May 2008 and 8 June 2008. Therefore newly designed hard and software were installed and tested at the harbour in Bremerhaven, a new acoustic array and window were fixed installed nearby the moon pool in addition to the mobile acoustic array as well as a complete new electronic cabinet was installed, modified and tested.

The first operational test under real conditions at sea was carried out during the cruise ARK-XXIII/1+2. A final sea trial and calibration were planned to be carried out during the cruise ANT-XXV/1 on the way to Las Palmas in the mean time between 3 November 2008 and 10 November 2008 at water depths of more than 3,000 m. The planned calibration and sea trials could not be carried out during ANT-XXV/1 due to the technical problems occurred to the system. The system was faulty and not operational.

The system was repaired by IXSEA in Bremerhaven during the ship-yard stay of *Polarstern* from 24 May 2009 to 20 June 2009, where the damaged acoustic array and window were replaced by new components. Then POSIDONIA was successfully used during ARK-XXIV cruise, but it was noticed that the new acoustic array was not useable due to the diffraction occurred by the protection window. Thus, the system was not able to correctly locate the target within the expected errors.

A new sea trial and calibration were done on both POSIDONIA systems during ANT-XXVI/1 and on the way between Bremerhaven and Las Palmas (16 October 2009 – 27 October 2009). The tests showed that the new fixed installed acoustic array was not fully operational and could not be calibrated. The protection window underwent a lot of disturbances by transponder positioning. So there was a need of further investigations to improve the acoustical characteristic of the fixed array.

During ANT-XXVI/4 on the way from Las Palmas to Bremerhaven (8 May 2010 – 17 May 2010) new calibration tests were carried out on the new POSIDONIA system after removal of the protective window in Punta Arenas in April 2010. The main objectives here were to eliminate the effects of the protective window on the system, to check and to calibrate the system without the protective window. The sea trials showed that the fixed installed acoustic array worked properly without the protective window.

Positioning data obtained were within the specifications and good enough to carry out the calibration.

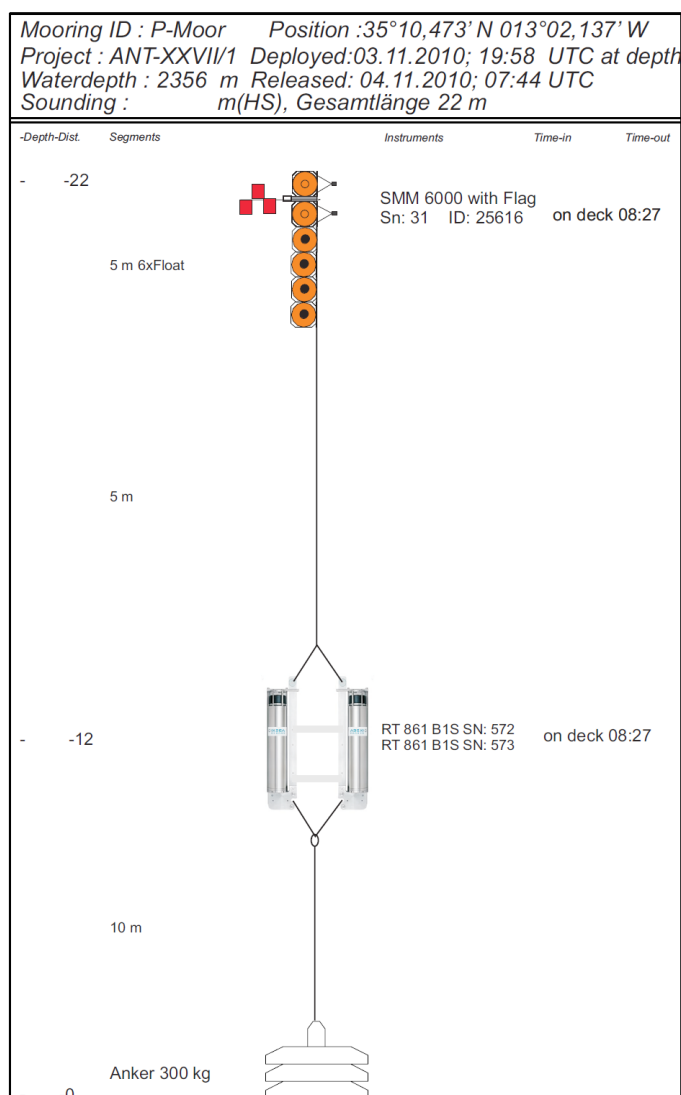


Fig. 6.1: Mooring configuration

The housing of the acoustic array was modified during the next ship yard stay of *Polarstern* in Bremerhaven 17 October 2010 – 6 October 2010) and the acoustic window was reinstalled again. A new calibration and trials including a calibration of the mobile acoustic array and the modified acoustic window were done during ANT-XXVII/1 on the way Bremerhaven - Las Palmas on 3 November 2010 and 4 November 2010 nearby the Ampère Seamount at 35° 10.477' N; 13° 02.139' W and at water depth of 2,356 m. The navigation platforms MINS I were replaced by MINS II between the 10 October 2010 and 25 October 2010 in Bremerhaven. Therefore a recalibration of all POSIDONIA's acoustic arrays was necessary and carried out on this cruise.

Work at sea

During the cruise the following work was carried out:

- The installation of the mobile acoustic array and the system operational check including transponder tests were successfully carried out on the 2 November 2010.
- A suitable place for a mooring was searched by the Multibeam Sonar (Hydrosweep).
- The transponder mooring with two releasers (Fig. 6.1) was prepared and deployed on 3 November 2010, 19:31 UTC, at the surface position 35° 10.472' N; 13° 02.135' W.
- The final position at sea floor was 35° 10.477' N; 13° 02.139' W at a water depth of 2,356 m.
- A sound velocity profile was measured up to 2,000 m water depth using the new Sound Velocity Profiler (SVP) and was used for the calibration (Fig. 6.2).
- Sea trials according Fig. 6.3 were carried out two times for each acoustic array.
- The mooring recovery occurred on 4 November 2010, 08:25 UTC.
- Data analysis and validations.

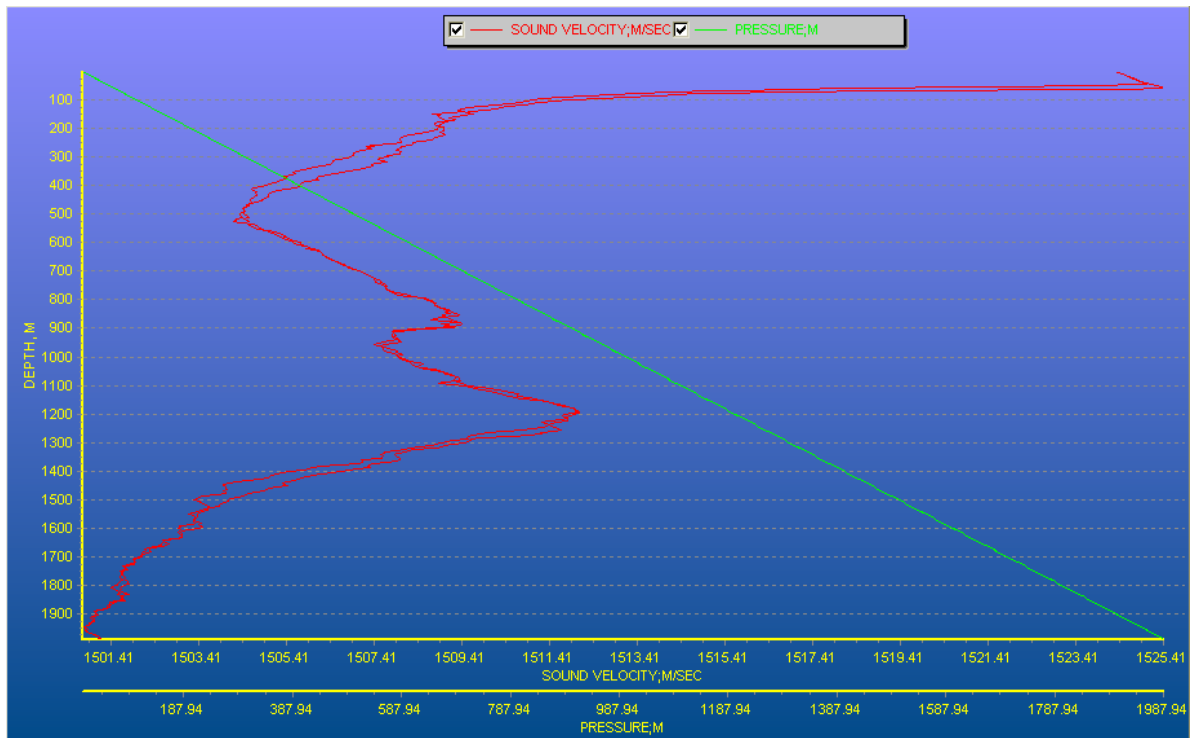


Fig 6.2: Sound velocity profile

Preliminary results

General conditions during the calibration and tests:

Date:	2010-11-03 and 2010-11-04
Transponder Position:	35° 10.477' N; 13° 02.139' W
Transponder depth:	2356 m
Water temperature:	20.5° C
Air temperature:	19.5° C
Sea state:	3.5 to 4.0 m swell
Wind speed:	10.7 m/s
Wind direction:	63°
Track circle diameter:	about 1800 m
Ship speed during measurement:	3 Knots
All other acoustic systems were OFF	
Start of Tests:	2010-11-03; 19:31 UTC
End of Tests:	2010-11-04; 08:12 UTC
Station number	PS 77/10 - 1

Mooring configuration (Fig. 6.1):

Two transponders (RT861 B1S; No 572 and 573), transponder 572 was activated.

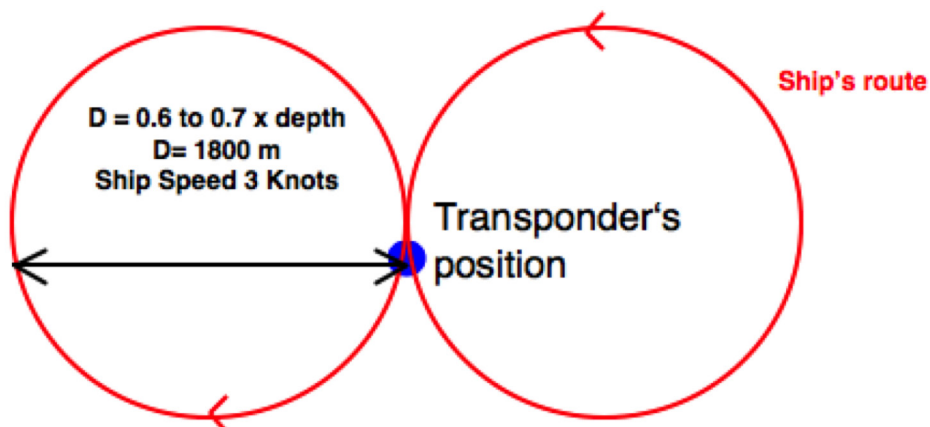


Fig. 6.3: Ship's track performed over the transponder as 8 shapes

Principle of calibration

The calibration of a POSIDONIA system consists in measuring the bias of the antenna relative to the ship's axes. This is done by performing a statistical calculation on a set of transponder position measurements. This calculation provides heading, roll and

pitch offsets.

The set of positions is obtained by doing an 8 shape with the ship above the transponder position (Fig. 6.3). Here the start point of the measurement does not matter. The orientation of the track or the sailing direction are relative. The diameter of the circles composing an 8 shape depends on the depth of the transponder (60 to 70% of the transponder depth). To obtain good calibration accuracy, it is recommended to deploy the transponder at depths between 2,000 and 2,500 m, which gives the best compromise between a wide enough range to get good results and a moderate range to get a high SNR and, consequently, a high positioning accuracy. After having performed the first test track describing an 8, the calibration offsets are calculated and entered in the system. Then, a second test track has to be done to confirm the accuracy of the measurement. If the results of the second test are not as good as expected, other tests have to be performed.

Calibration of the mobile acoustic array:

Used acoustic array: Mobile array, moon pool installation

Used POSIDONIA system: New POSIDONIA system 6000, ABYSS 1.49

The first calibration track for this configuration was carried out according to Fig. 6.4. The positioning performance was found to be good. Only less than 10% of the positions were out of the expected range.

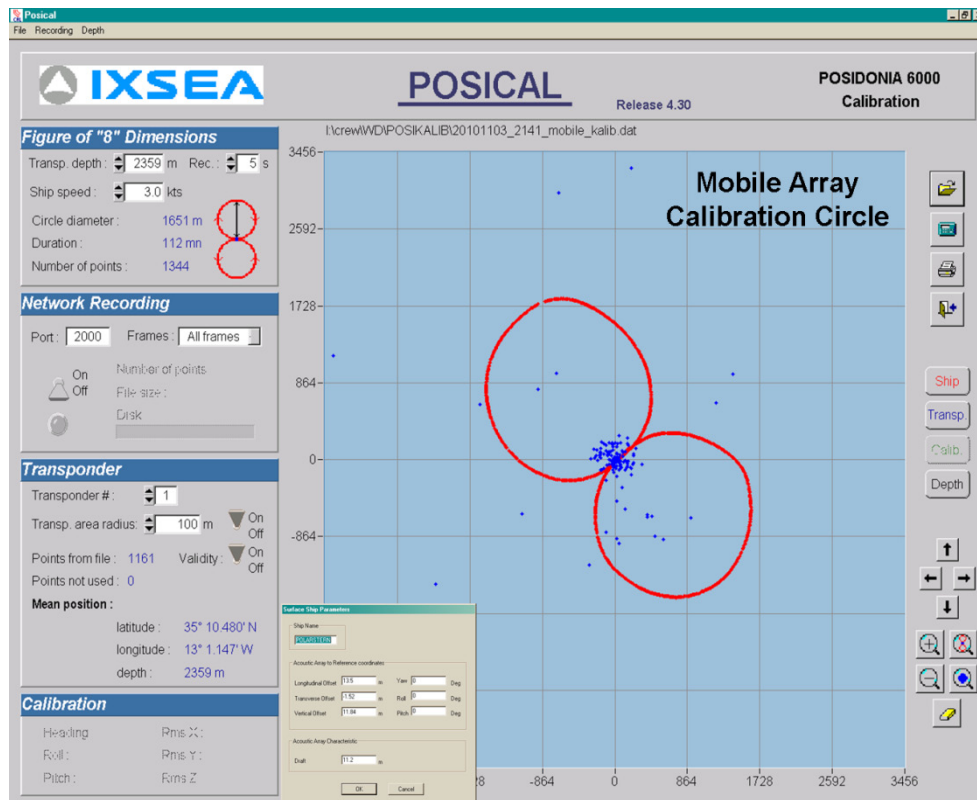


Fig. 6.4: Calibration of the mobile Acoustic Array. Red line = ship's track, blue dots = detected transponder positions.

The calculation of the calibration parameters was carried out using the ABYS-procedure.

The calibration was successful. Accuracy was about ± 15 m (Fig. 6.5). The following calibration parameter set was found for the mobile acoustic array:

Parameter	Parameter set Old	Parameter Set New
Heading	- 0.61°	- 0.38°
Roll	+ 0.17°	+ 0.09°
Pitch	- 0.04°	- 0.02°

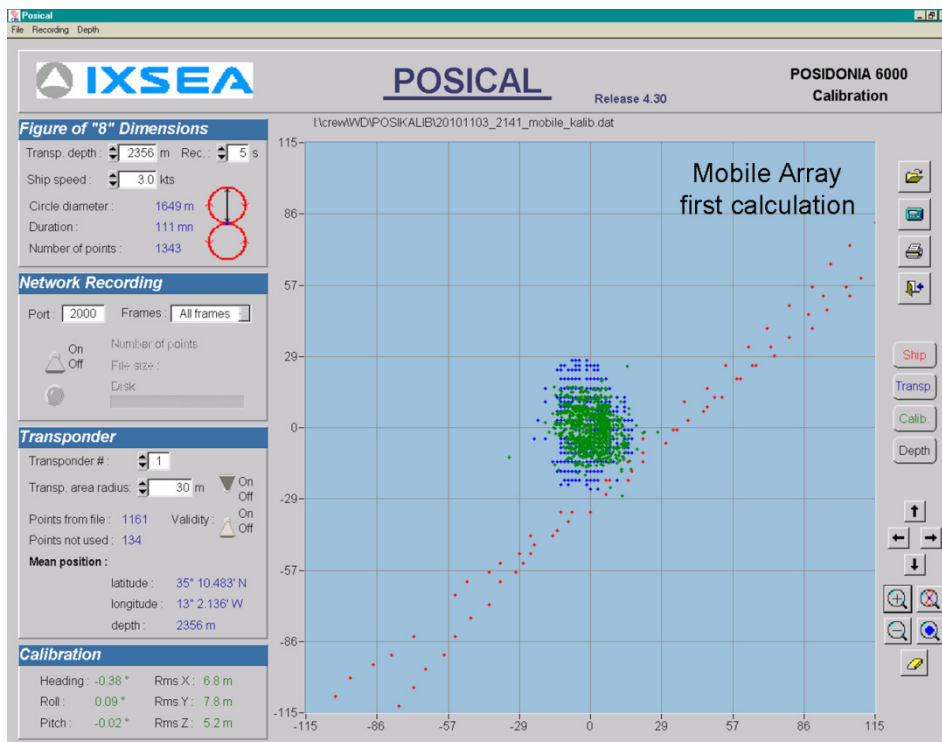


Fig. 6.5: Calibration Mobile Antenna, first loop (8 shape), first calculation. Blue dots are positions before correction and green dots are recalculated positions after the correction. Positioning distributions were reduced from ± 30 m to ± 15 m.

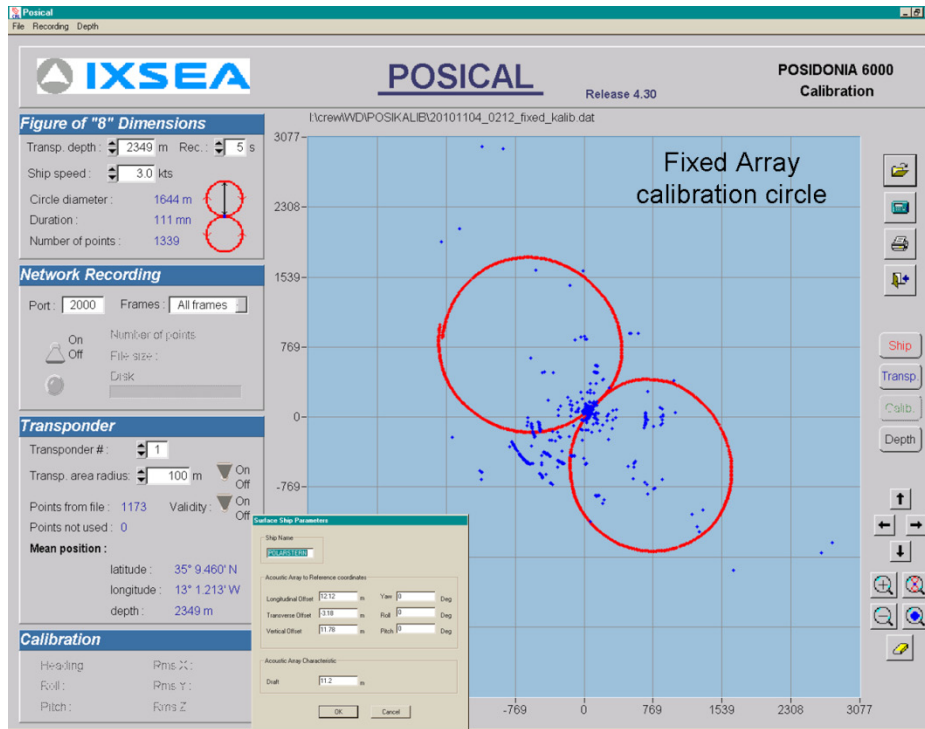


Fig. 6.6: Calibration of the fixed acoustic array with the modified window on ANT-XXVII/1 on 4 November 2010. Red line=ship's track, blue dots=detected transponder positions.

The verification of the parameter set was carried out by repeating the first ship's track. No significant change of the parameter set was found.

Calibration of the fixed acoustic array:

Used acoustic array: Fixed array with modified protection window
 Used POSIDONIA system: New system POSIDONIA 6000, ABYSS 1.49

The first calibration track for this configuration was carried out according to Fig. 6.6. A moderate positioning performance was found. About 30% of all positions were out of the expected range. However, the data set obtained was good enough to perform the calibration. The calculation of the calibration parameters was carried out again using the ABYS-procedure. The calibration was successful. The accuracy was about ± 30 m (see Fig. 6.7)

The following calibration parameter set was found for the fixed acoustic array:

Parameter	Parameter set without protective window	Parameter Set with protective window
<i>Heading</i>	- 0.62°	- 0.34°
<i>Roll</i>	- 0.25°	- 0.34°
<i>Pitch</i>	- 0.44°	- 0.50°

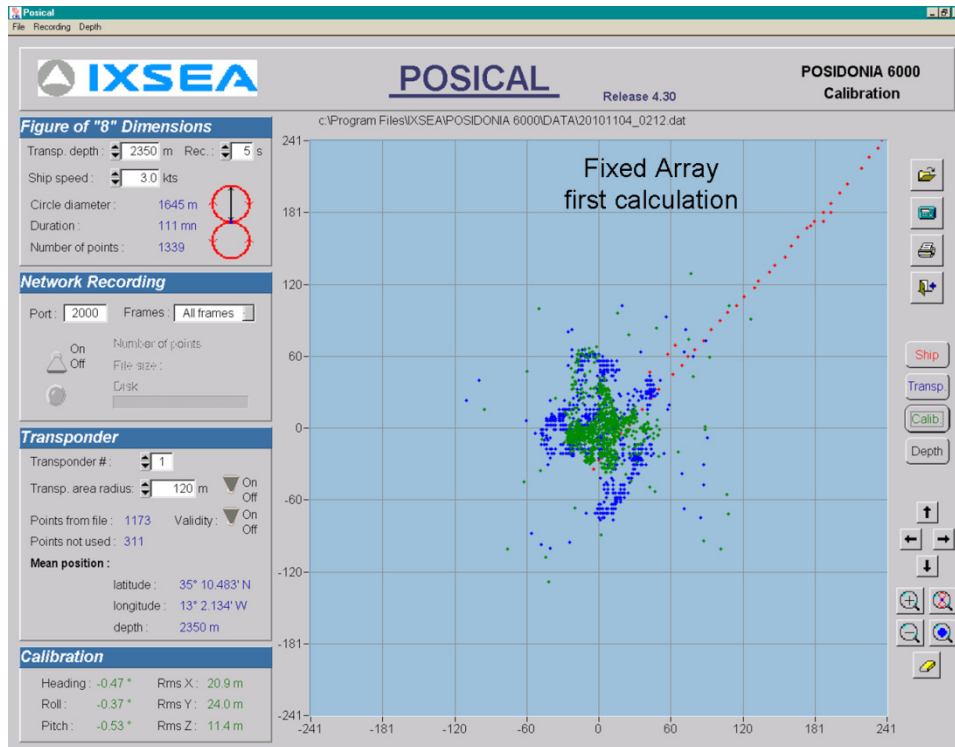


Fig. 6.7: Calibration of the fixed array with modified window. Blue dots are positions before correction and green dots are recalculated positions after the correction. The scatter of the positions was reduced from ± 60 m to ± 30 m.

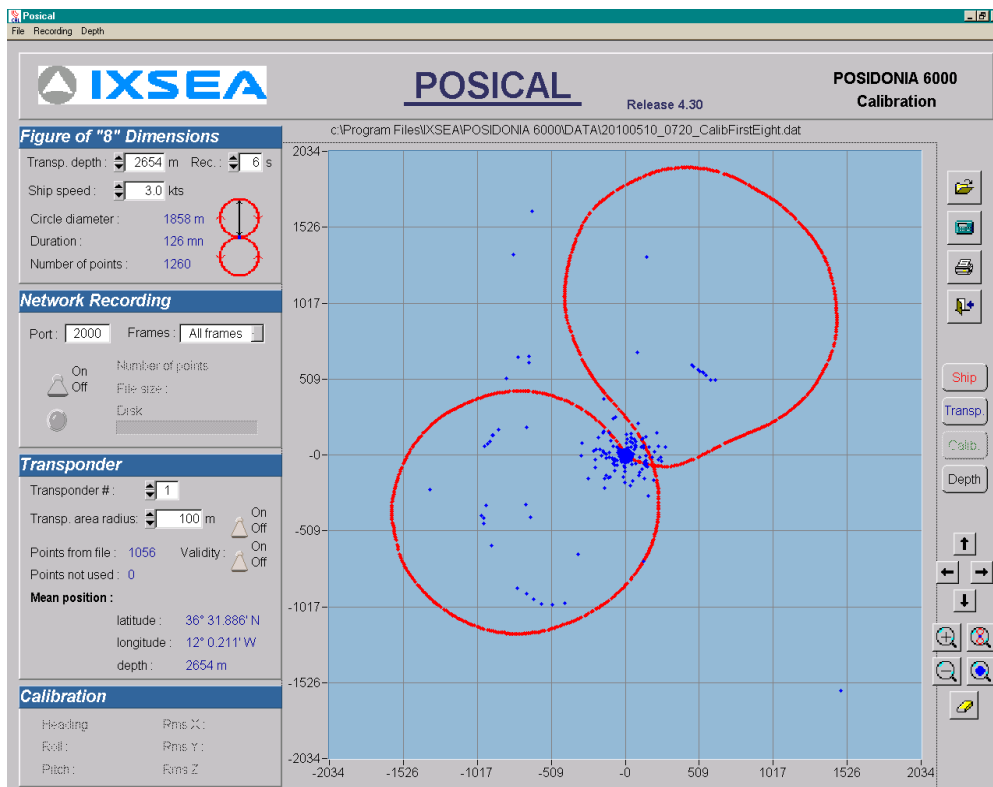


Fig. 6.8: Calibration of the fixed acoustic array without window on ANT-XXVI/4 5 October 2010. Red line = ship's track, blue dots = detected transponder positions.

The verification of the parameter set was carried out again by repeating the ship’s track in 8 shapes. No significant change of the parameter set was found.

The acoustical characteristic of the fixed array was significantly improved by the modification of the protective window. The sound reflections between the antenna and the inner side of the protective window were successfully attenuated by using special foam as insulation material. The previously occurred disturbances of the positioning were reduced significantly.

Fig. 6.8 shows the results of the calibration without window carried out on 10 May 2010 and Fig. 6.9 the same results using the protective window without modification as carried out on 23 October 2009.

Fig. 6.9 shows the same results using the protective window with modification, carried out on this cruise (4 November 2010).

The comparison of all results shows that the new fixed acoustic array is now significantly improved and ready for use. However, due to the high error ratio by positioning (30 %) it is not recommended to use this system for ROV and AUV. The mobile acoustic array should be used for this purposes.

To conclude, the new acoustic fixed array with the protective window is now calibrated and operational. Modification of the protection window was successful.

Also the mobile array is now recalibrated and can be used.

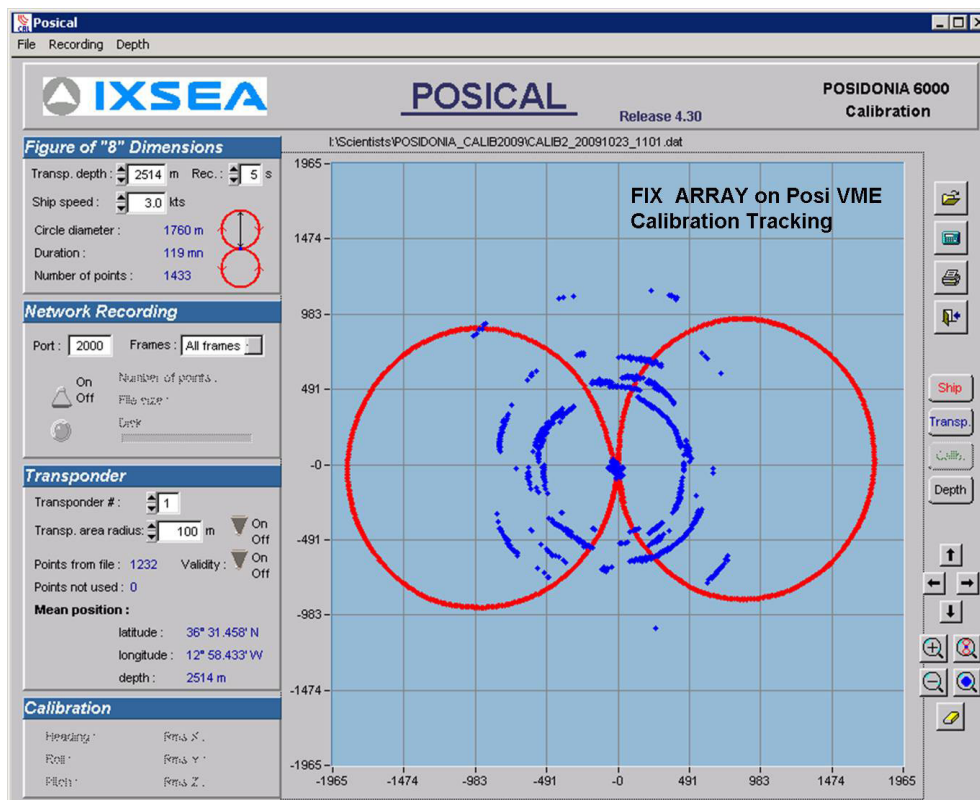


Fig. 6.9: Calibration of the fixed acoustic array during ANT-XXVI/1 (2009-10-23) with window. Red line = ship’s track; blue dots = detected transponder positions.

7. CALIBRATION OF THE NEW ECHOSOUNDER SYSTEM ATLAS HYDROSWEEP DS3

Hans Werner Schenke, Fred Niederjasper, Ralf Krockner, Laura Fillinger,
Ute Gallach, Alexandra Gottschall, Andreas Prokoph, Lukas Schack, David
Ulrich
Alfred-Wegener-Institut

Objectives

During the shipyard time prior to this cruise the swath sonar system HYDROSWEEP DS2 on board *Polarstern* was updated to version HYDROSWEEP DS3. Also the Marine Inertial Navigation System (MINS) was replaced by a new system. During this cruise the necessary calibrations and the Sea Acceptance Test (SAT) were executed as well as adjustments of the processing environment to handle the new data formats. Additionally a new sound velocity profiler, the Midas SVP 6000 by Valeport, was purchased, which was tested and implemented into the processing chain.

This report briefly describes the incorporation and operation of the different devices, the execution of the calibrations their results and quality assessment. The successful operation of the previous echo sounder system HYDROSWEEP DS2 led to the decision to install the new echosounder system Hydrosweep DS3 similarly. The transducers have not been changed but the electronics and software components. The new system operates with transmitting frequency of 15 kHz sending 240 beams at the maximum. Dependent on the signal to noise ratio not all transmitted beams are received back, so the practical number of received beams is decreased. The transmitting swath angle amounts to 120 degrees, which leads to a sea floor coverage of 3.5 times the water depth in case of good backscatter conditions.

The operation application ATLAS Hydromap Online was replaced by ATLAS Hydromap Control, which is also in use for the operation of the Subbottom Profiler Parasound DS3, from ATLAS Hydrographics as well. Both systems are connected within an own local area network to which the operation stations are linked. These operation stations are installed in the same location as for the old system: Two computers are located in the technical office E-550 on E-deck of *Polarstern*, a third is installed on the bridge and a fourth in the winch control room. The echosounder can be operated from all these locations.

For graphical display and archiving of raw data, the software application HYPACK was purchased. Two licences are available which can be shared between the four operation stations. HYPACK system is able to display actual and previous recorded data as well as background data by means of various vector and raster formats. This allows the scientific parties to get a convincing real-time impression of the sea floor topography. HYPACK also consists of tools for system calibration and data editing. For

further processing, e.g. for data cleaning using Caris HIPS/SIPS, three additional PCs are set up in the sonar office E-550.

7.1 Analysis of the distance between MINS and GPS Antennas

Hans Werner Schenke, Fred Niederjasper, Ralf Krockner, Laura Fillinger,
Ute Gallach, Alexandra Gottschall, Andreas Prokoph, Lukas Schack, David
Ulrich
Alfred-Wegener-Institut

Objectives

A 10 m difference between the plotted cruise tracks of the GPS antenna Trimble 1 and the MINS lead to investigations of the distance between both sensors as well as the distance between MINS and GPS Trimble 2. The MINS defines the origin for the ship's navigation coordinate frame and is located very close to the calculated centre of gravity and therefore the impact point of forces like roll, pitch, heave or yaw. The primarily handled variable in this investigation is the difference between the positions of the MINS and one of the two GPS receivers. The expectancy value of this variable is 0 after subtracting the geometric distance between both sensors.

Work at sea

Three sensors were involved in this analysis. The "MINS 2" by Raytheon Anschütz, a strap down inertial navigation system with an accuracy of 0.1 nautical miles combined with GPS as well as two GPS receivers of type Trimble MS750 with an absolute positioning accuracy of approximately 2 m.

For better imagination and interpretation the distances between the sensors were calculated in meters. Therefore the geographic GPS coordinates on the WGS84 ellipsoid as well as coordinates given in the ship's local coordinate system had to be transformed into Cartesian earth centred coordinates. Some assumptions had to be made for this but their influence could be neglected due to the fact that differences were investigated.

Before any data could be analyzed it had to be cleaned from outliers. Some were already removed in the DSHIP database. For the remaining outliers realistic thresholds were defined with the help of variables like the maximum speed of *Polarstern*.

A special source for errors was the GPS Trimble 2 receiver which was known to produce strongly scattered position data. It was repaired during this cruise around the 1 and 2 of November.

The expectancy value of the three dimensional distance detected by coordinates between one GPS receiver and the MINS or between both GPS receivers is zero after subtracting the geometric distance between both sensors. Fig. 7.1.1 shows an example of this distance for the data set *Achten.dat* and the distance between MINS and GPS 1.

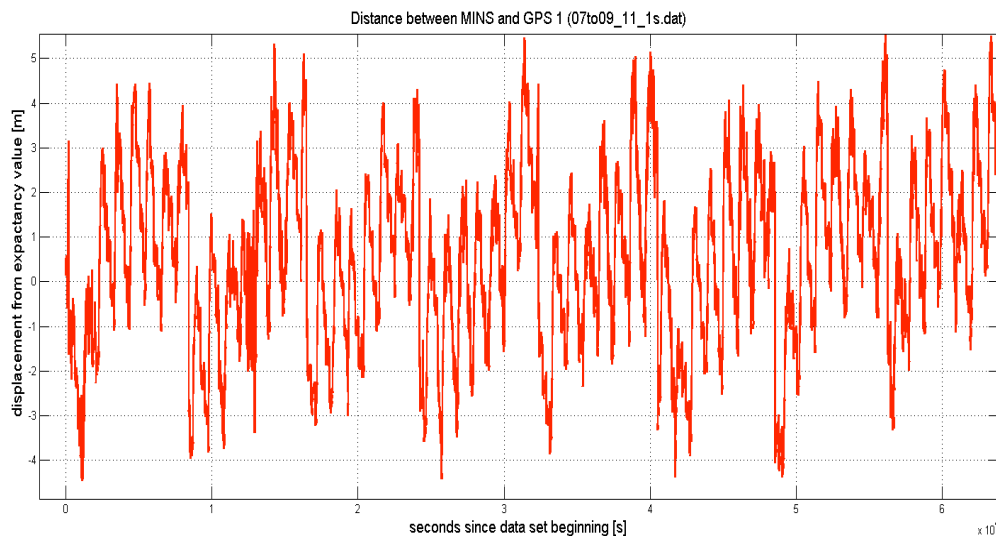


Fig. 7.1.1: Distance between positions given by MINS and GPS1 have been detected to amount to several meters

At first view it is obvious that these data are not white noise as it was expected. Furthermore a statistical chi square test confirmed that this data row is not normally distributed. This systematic behaviour could be correlated to any other variable in the data set. The correlation coefficient was calculated for pitch, roll, heave, speed, acceleration and numbers of satellites in fix.

If the 3D distance is plotted against the seconds since beginning of the data set, the process of the distance can be seen (Fig. 7.1.1). It seems that two or even more frequencies are in the data which are not correlated to any variable considered in this analysis. A Fast Fourier Transformation (FFT) was performed for all data sets on the distance between one GPS receiver and the MINS in meters in order to specify the exact frequency and to see if these frequencies occur in all data sets or not.

Preliminary results

The main goal of this analysis was to determine the three mentioned displacements of distance from the expectancy value 0. Depending on the data set different results were achieved. Table 7.1.1 shows the results and different statistical parameters.

The displacements of the distances to the MINS are explicitly bigger than the inter-GPS displacements. This is indicative for an error source in the MINS.

In all processed data sets the projected distances show no correlation to heading, roll, pitch or heave. This means that the applied projection to Cartesian coordinates is invariant to the orientation of the ship. The assumed correlation with speed could only be proved for one data set (see SVP1.dat in Fig. 7.1.2). A dependency on acceleration describes this effect but this could not be proved for all data sets in this analysis. During the first SVP station *Polarstern* drove 11 kn, stopped down to nearly 0 and accelerated back to 15 kn. For slowing down and accelerating different distances MINS – GPS 1 as well as MINS – GPS 2 occurred with an amplitude of approx. 2.5 m in the range of 4.3 to 11 knots. The GPS 1 – GPS 2 distance remained constant except a small effect with amplitude of approx. 0.4 m.

Tab. 7.1.1: Statistical parameters for distances between devices

Distance	Mean	Standard deviation [m]	Variance [m ²]	95% confidence interval	
	[m]			from [m]	to [m]
MINS – GPS 1	0.269	1.590	2.704	0.258	0.280
MINS – GPS 2	0.339	1.367	1.963	0.330	0.349
GPS 1 – GPS 2	0.020	0.662	0.527	0.014	0.025

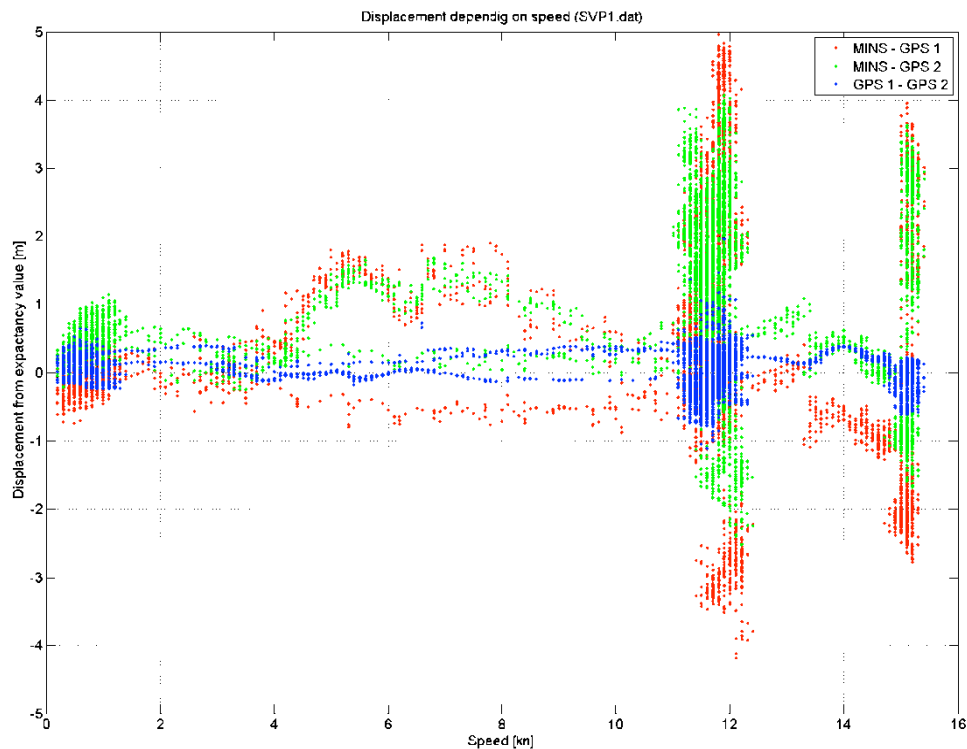


Fig. 7.1.2: Distances depending on speed in SVP1.dat

The red marked frequency of 0.0009336 Hz has an amplitude of 0.497m. This frequency corresponds to an effect that occurs every $0.0009336\text{Hz} \rightarrow 1071\text{s} = 17.85\text{min}$. The next conspicuous frequency apart from the area around 0 is marked in green and shows a value of 0.0001245 Hz with an amplitude of 0.937 m. This corresponds to an effect that occurs every 8032 s according to 134 min.

All significant frequencies from a data set which contains the whole track between 26 October and 11 November are shown in Table 7.1.2. →

Tab. 7.1.2: Significant frequencies of displacement from expectancy value for dataset 2610to1111_1s.dat

Frequency [Hz]	Amplitude [m]	Occurrence [s]	Occurrence [min]
0.0009336	0.497	1071	17.85
0.0001245	0.937	8032	133.87
0.0002489	0.365	4017	66.95
0.0003734	0.232	2678	44.63
0.0004978	0.176	2008	33.47
0.0018667	0.148	536	8.94

The effects with an occurrence of 536, 1071, 2008, 4017 and 8032 seem to be multiples or whole-numbered fractions of the same effect. Because the frequency of $\frac{1}{1071s}$ is the most significant one, this may be assumed to be the “original” frequency.

All data sets were processed like this. Interestingly enough one family of frequencies sticks out in all data sets for the distances which include the MINS position. The distances MINS – GPS 1 as well as MINS – GPS 2 show this frequency and its multiples, but not the distances between GPS 1 – GPS 2. This clearly shows that the 1073 s effect comes from the MINS and not from one of the two GPS receivers. The amplitudes of this frequency are in the same order of magnitude as the standard deviation of the distances MINS – GPS1 and MINS – GPS 2. This could mean that the relatively high standard deviation is caused by the 1070 s frequency.

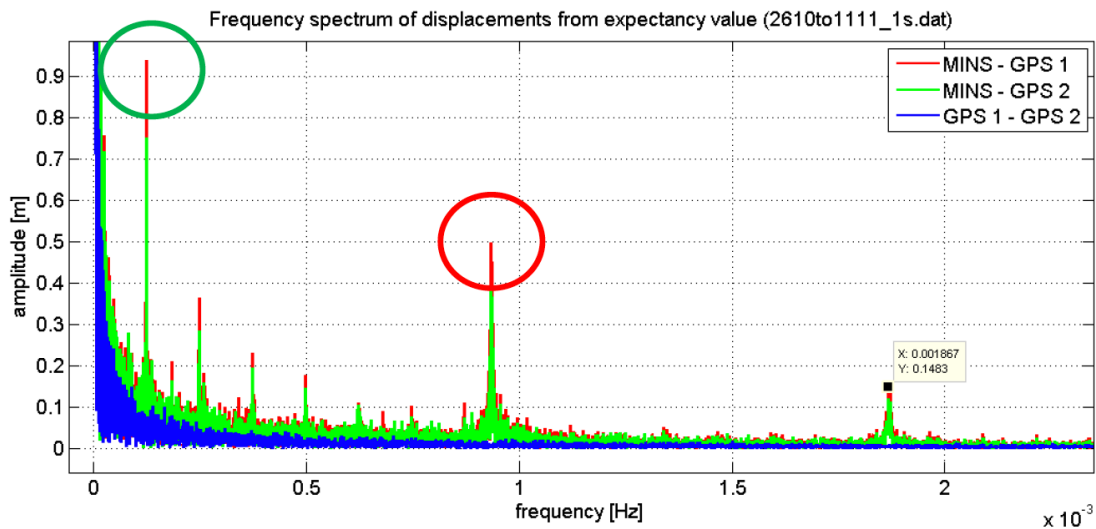


Fig. 7.1.3: In the frequency spectrum of distances two major frequencies can be identified, which may be caused by MINS filters.

7.2 Determination of sound velocity profiles using VALEPORT SVP

Hans Werner Schenke, Fred Niederjasper, Ralf Krockner, Laura Fillingner,
Ute Gallach, Alexandra Gottschall, Andreas Prokoph, Lukas Schack, David
Ulrich
Alfred-Wegener-Institut

Objectives

For the calibration of the Hydrosweep DS3 system an exact knowledge of the sound velocity in the water column is essential. For this purpose two profiles were measured in preparation for the pitch and the roll calibration. The new Valeport Midas SVP 6000 was used successfully during the measurements on 28 and 29 October. On 13 November a third measurement took place, where the collected data was used for the post processing of the previously measured Romanche Gap profiles. Data download and option setting was in all cases accomplished with the manufacturer's software.

The sound velocity of a liquid is determined by its density and pressure. Density of ocean water is primarily influenced by its temperature and salt concentration. These factors are subject to strong variations, due to water layers and other irregularities. Because of the non-linearity of the sound velocity in the water column, it is advisable to perform profile measurements rather than to determine a mean water sound velocity when high precision is needed. The two common methods of sound velocity profile determination are: To carry out a CTD-measurement (conductivity, temperature, depth) and calculate the sound velocity from the measured quantities or to determine the sound velocity directly by means of a sound velocity profiler (SVP).

A sound velocity profiler possesses sensors for temperature and pressure as well as a sound transmitter and receiver in a fixed distance between each other. Measuring the time needed by a single sound pulse needs to reach the receiver, the sound velocity is easily determined.

The used instrument is able to determine the sound velocity in depths down to 6,000 m and in a range between 1400 m/s and 1600 m/s. It was used as a self recording device in our case, even though direct read out through the data download cable is possible and useful for tests.

The device is able to work in three operating modes which are to be chosen by the user during setup. Continuous Mode results in readings at regular intervals. The so called Burst Mode is a programme for longer term deployment sending the instrument to sleep mode between measurements. The profile Mode allows defining a fixed interval (in dBar) for readings, as the instrument is lowered and raised through the water column.

Although the SVP is able to measure at 8 Hz rate and the usual veer speed of the instrument is one meter per second, a 'one measurement every meter' measuring scheme has proofed to result in a reasonable amount of data.

Work at Sea

Data Log Express

The enclosed software package for setup and data download provides a comfortable data access. After the connection to the instrument is established, all necessary options

can be selected. Data can be downloaded and displayed. Various display forms are available and sensors can be chosen separately. The output consists of three different files for every profile: Raw data can be found in the *.000 files in an ASCII-Format, *.bin holds binary data and *.HDR consists of Header Information in plain text again. The *.000 file format can directly be imported to the HYPACK Software.

Since the main work e.g. fixing the instrument to the winch and lowering as well as raising it, is done by the ship's crew, only pre and post processing will be described in the following.

Preprocessing / Preparatory work

A sound velocity profile measurement usually starts with the setup of the instrument. The profiler is connected to a computer via RS232. After establishing communication with the help of Data Log Express' Connection Wizard the setup can be changed.

The profile mode with a sampling interval of 1dBar is chosen. Time is synchronized with the connected PC and metric units are selected. Finally a pressure tare is applied before Self recording mode is chosen in the 'run' menu.

Post processing

In this step the instrument is again connected to a computer using the 'data upload' function of Data Log Express the data can be downloaded set by set. The *.000-file is then eventually made slimmer with the help of a special tool and finally imported to HYPACK for hydrographic measurements yet to come or loaded into Hips and Sips for the post processing of data.

Preliminary results

As easily seen in Fig. 7.2.1 and table 7.2.1 data at Stations PS77/0002-1 and PS77/0005-1 are quite similar. A warm surface water layer is clearly visible and at a depth of about 1700 m the correlation between sound velocity and depth becomes linear, and can therefore be extrapolated easily. The profile of Station PS77/0011-2 is quite distinct from the others. This is mainly due to the much warmer water at the location in the equatorial area, proving the necessity to perform measurements in regular intervals.

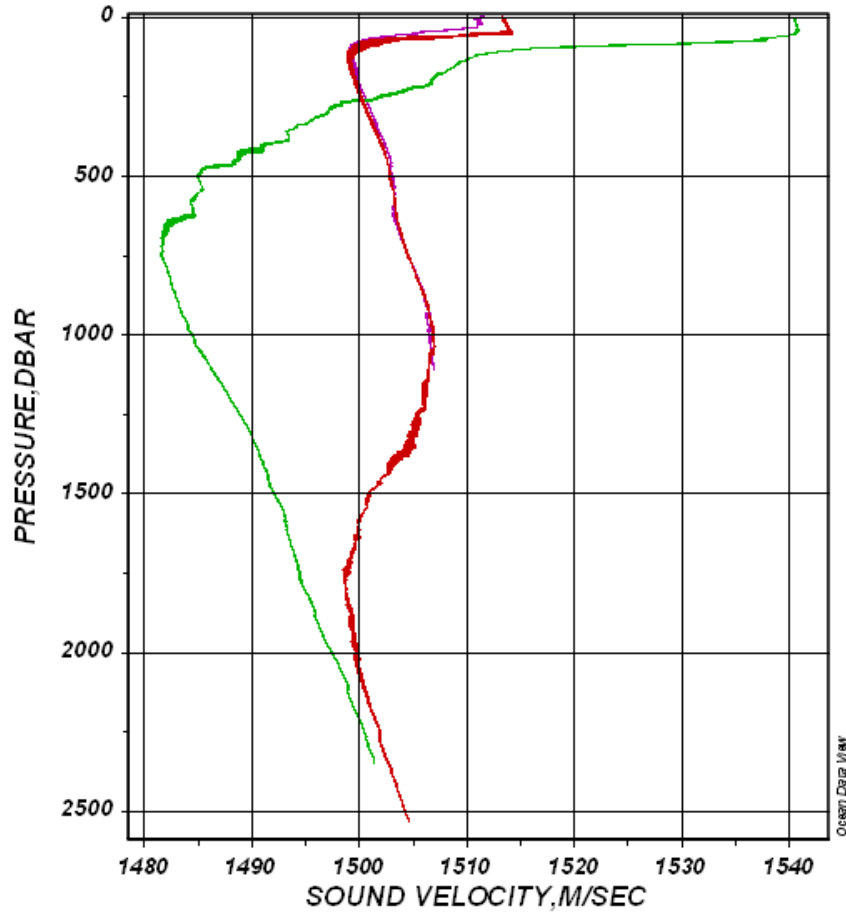


Fig. 7.2.1: Sound velocity profiles at stations PS77/0002-1 (in violet), PS77/0005-1 (in red) and PS77/0011-2 (in green)

Tab. 7.2.1: Sound velocity profiles at stations PS77/0002-1, PS77/0005-1 and PS77/0011-2

Station	PS77/0002-1	PS77/0005-1	PS77/0011-2
Date	2010-10-28	2010-10-29	2010-11-13
Position	46° 06.73' N 4° 13.06' W	45° 49.95' N 4° 47.98' W	0° 13.12' S 18° 25.90' W
SVP in the water	17:50:00	13:20:00	09:04:00
SVP on maximum depth	18:11:00	14:06:00	09:47:00
SVP on deck	18:31:59	15:04:59	10:40:59
Maximum depth	1100 m	2,500 m	2330 m

7.3 Calibration of time latency, roll, pitch and yaw angle

Hans Werner Schenke, Fred Niederjasper, Ralf Krockner, Laura Fillinger,
Ute Gallach, Alexandra Gottschall, Andreas Prokoph, Lukas Schack, David
Ulrich
Alfred-Wegener-Institut

Objectives

In general the accuracy of the calibration of all offsets should be in the same dimension with the accuracy of the motion sensor. After installing a new multibeam system a calibration should be done. In the following this procedure is described for the echosounder system Hydrosweep DS3 on *Polarstern*. At first a coarse calibration was performed using zero as offset for all parameters. In the second step a fine calibration was executed applying the detected offsets of the coarse calibration to improve them. Each calibration, the coarse and fine ones, was executed with the MINS 1 and MINS 2.

The evaluation of the measurements was made with the software Caris HIPS/SIPS and HYPACK. Both software packages detected nearly the same offsets for the calibration. After the determination of the offsets these were applied in the Atlas Hydrosweep Control. Consequently the calibration values in the post processing software, e.g. Caris HIPS/SIPS must be set to zero for further processing.

Work at Sea

Time Latency Calibration: 2010-10-28 10:52 – 2010-10-28 12:56

The first calibration that had to be executed was the latency calibration, because this offset would influence the results of the following calibrations. The latency offset is the time offset between depth measurement and positioning. In this case the latency for the MINS interface in comparison to the Trimble GPS was specified by measuring one profile with the MINS interface and the later one with the Trimble GPS positions directly. To calibrate the system the same profile must be measured twice in the same direction with a different speed of the vessel, in our case 5 and 10kn. The chosen profile must have a steep regular slope. The steeper the gradient of topography is, the higher the resolution of the calibration. The measuring of the profile has to be directed from deep to shallow water.

If there is a latency in the measuring system the slope will be measured at different positions. From the difference of both positions the latency can be calculated:

$$\delta t = \frac{\Delta x}{v_2 - v_1}$$

Δx : Horizontal separation between the two sounding profiles near nadir

v_i Speed of vessel

A time latency of 50 ms for the MINS interface and 700 ms for the Trimble GPS was detected. The used offset in the Hydromap control is that from the MINS, because the positions were generally taken from the MINS.

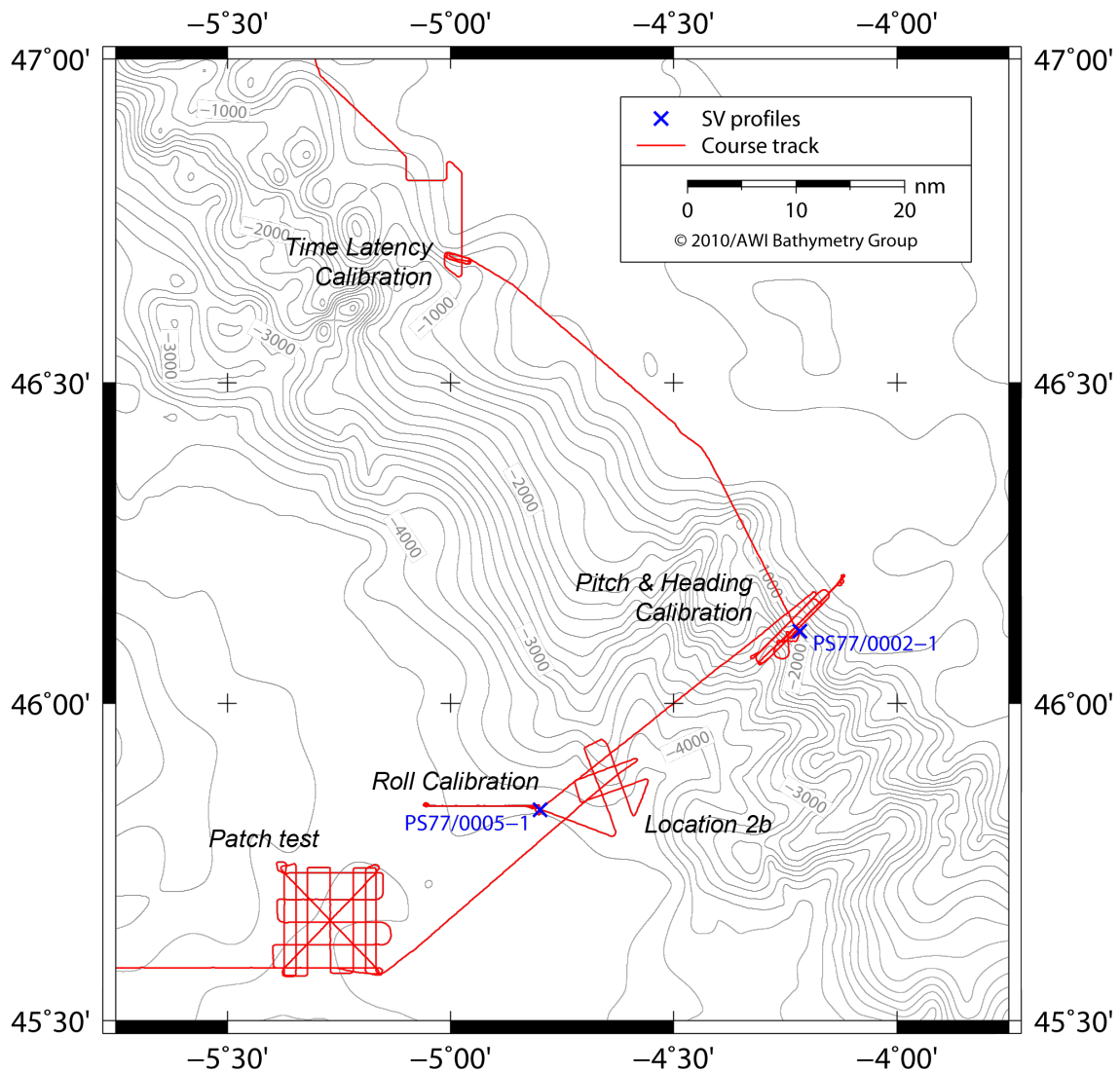


Fig. 7.3.1: Locations of SVP casts and profiles for calibration of orientation angles in the Bay of Biscay

Pitch calibration: 2010-10-28 19:35 – 2010-10-29 8:50

The second step in the calibration process of the multibeam echo sounder was the detection of the pitch offset. For this purpose a sloping seafloor was surveyed, where the gradient of the slope is bigger than the pitch offset. The steeper the gradient is the higher the resolution of the calibration. This profile must be measured twice, in opposite directions with the same vessel speed. Moreover a regular slope is needed for this step of calibration. To calculate the offset the longitudinal displacement along the slope must be measured.

$$\delta\theta_p = \arctan \frac{\Delta x}{2z}$$

Δx : Horizontal deviation between the two sounding profiles near nadir

z : Depth

The result of this measurement was an average offset of -0.16° , but a validation of the result was needed because one value had the opposite direction. This second calibration of the pitch was planned for the Romanche Gap.

Yaw (Heading) calibration

The next step of calibration was the determination of the yaw offset. The yaw offset is caused by the angle between the ships length axis and the axis of the gyro (MINS). For this calibration an underwater obstacle is observed which should be measured in two profiles with opposite directions. The obstacle has to be measured in the overlapping area of both profiles, one time on the portside, the second on starboard. For the calibration the longitudinal deviation of the feature is measured.

$$\delta\alpha = \arctan \frac{\Delta x}{\Delta L}$$

Δx : Horizontal deviation of the feature

ΔL : Distance between the lines

The measurements for the detection of the yaw offset showed no explicit result and the value should be assumed and set to be zero.

Roll calibration: 2010-10-29 15:27 – 2010-10-30 30 02:00

The last step during the calibration was the calibration of the roll angle. For the roll calibration the same profile must be measured in both directions. The differences in the outer beams between both profiles show the roll error.

$$\delta\theta_R = \arctan \frac{\Delta z}{2\Delta y}$$

Δz : Vertical displacement between outer beams of opposite profiles

Δy : Half swath width or distance from nadir to compared point

The best calibration results are possible in a flat area. Moreover it is useful to carry out this calibration in the deepest possible area. Mistakes in the outer beams are proportional to the beam length, making it easier to determine the exact angle.

The mean value for the roll offset was detected to be -0.21° .

Preliminary results

The preliminary results are given in Fig. 7.3.1 and table 7.3.1.

Tab. 7.3.1: Summary of calibrations and corresponding results

calibration				
	type	MINS	results	comment
Latency	--	1	50msec	used result
	--	Direct GPS	700msec	
Pitch	coarse	1	+0,16°	used result
	coarse	1	-0,16°	
	coarse	2	-0,2°	
	coarse	2	-0,2°	
	fine	1	-0,16°	
	fine	2	-0,2°	
	fine	1	-0,16°	
	fine	2	-0,2°	
			-0,16°	
Yaw	no explicit result, offset near zero			
Roll	coarse	1	-0,16°	used result
	coarse	1	-0,16°	
	coarse	2	-0,2°	
	coarse	2	-0,2°	
	fine	1	-0,21°	
	fine	1	-0,21°	
	fine	2	-0,14°	
	fine	2	-0,14°	
			-0,21°	

7.4 Quality determination of the HYDROSWEEP DS3

Hans Werner Schenke, Fred Niederjasper, Ralf Krockner, Laura Fillingner, Ute Gallach, Alexandra Gottschall, Andreas Prokoph, Lukas Schack, David Ulrich
 Alfred-Wegener-Institut

Objectives

After the determination and input of the calibration parameters the measurement quality of the Hydrosweep system had to be reviewed. According tests were performed in the Bay of Biscay visiting the well-known test site "Location 2b" as well as a new site, which was named "Patch test" (see Fig. 7.4.2).

Work at Sea

Location 2b

The double cross at Location 2b (see Fig. 7.4.1) had been measured several times before (ANT-VIII/1, ANT-XV/1, ANT-XXIII/1) and can therefore act as a reference ("ground truth"). The newly measured double cross was compared to the last measurements taken on ANT-XXIII/1 (HDBE, Standard Source Level (239 dB), 120°/120° transmission/receiver, automatic Gain Control with a Start TVG of 18 dB).

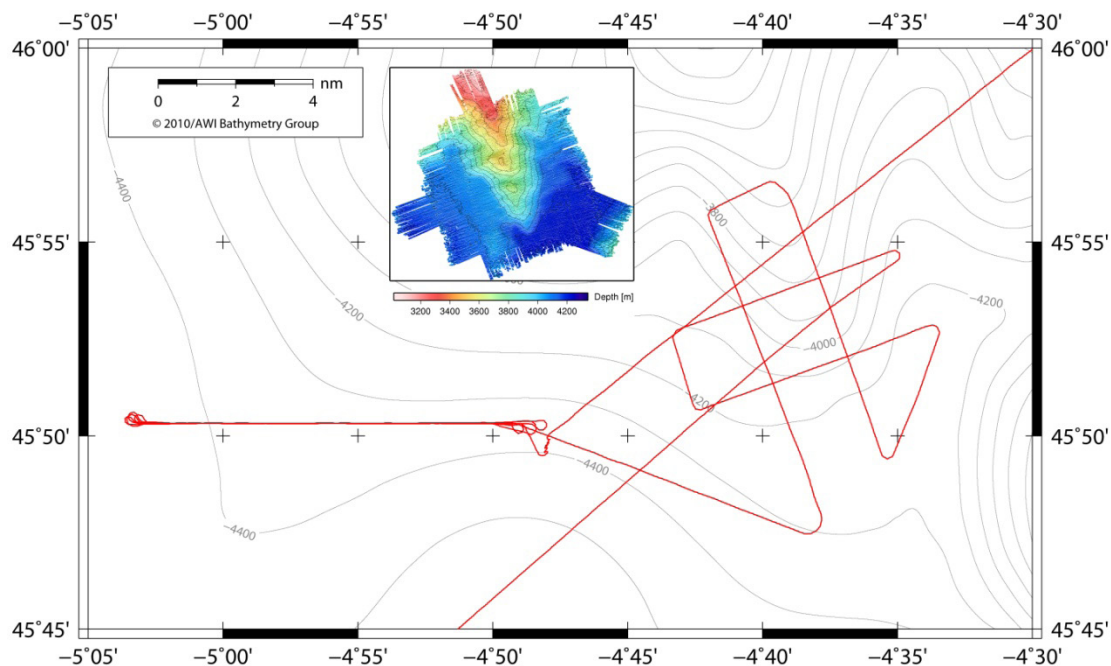


Fig. 7.4.1: Measurements at Location 2b have been performed on this and previous cruises, which can be taken for comparisons and quality assessments. The roll calibration was executed on westerly profile of Location 2b.

To evaluate the digital elevation models from former cruises with the data gathered during ANT-XXVII/1 difference models were calculated and visualized with ArcGIS. Outcomes with a mean difference value of 5.45 m and a standard deviation of 16.75 m were calculated. Regarding the depths of around 4,000 m in the area of investigation these results are reasonable and meet the requirements of the echosounder system.

Patch test

The patch test is a quality control test to estimate multibeam depth accuracy at various angle limits. The test was used to investigate the inner measurement and repetition accuracy of the newly installed and calibrated deep-sea echosounder.

The “Patch test” site (Fig. 7.4.2) was measured according to a standardized procedure. First, a reference surface was created by a test survey with cross lines over a relatively flat bottom (a flat bottom is chosen to minimize the contamination of the depth accuracy test by position error and to achieve a homogeneous surface). The reference surface consists of 10 profiles with an opening angle of 90° (seafloor coverage = two times the water depth). Second, four check lines (two diagonally and two North-South) were measured directly after the reference survey. The edge length of the reference surface is approximately 9 nm, the area covered is about 280 km² with mean depths of around 4,200 m (Fig. 7.4.2).

The analysis of the test was done both with the “Patch Test” tool in CARIS Hips & Sips and the “Beam Angle Test” Tool in HYPACK.

To meet IHO/S44 Order 3 (IHO S44 from 2008: Order 2) criteria the reference surface was computed using a 200 % coverage ($\pm 45^\circ$ aperture) of the 10 profiles.

Order 3 is intended for those areas where the depth of water is such that a general depiction of the seabed is considered adequate. A full seafloor search is not required. It is recommended that Order 3 surveys are limited to areas deeper than 200 metres. The horizontal uncertainty must be better than 150 m +5% of the depth, the maximum vertical uncertainty allowed is calculated by

$$\pm\sqrt{1.0^2+(0.023\times\text{depth})^2}$$

Example: Diagonal check line southwest to northeast (from the CARIS software)

Beam Number	Count	Max (+)	Min (-)	Mean	Std Dev	Order 3 (%)
11 - 21	5	0.000	65.093	-42.285	26.039	100.0
21 - 31	270	70.976	80.742	-19.847	29.848	100.0
31 - 41	798	71.278	66.395	9.413	22.806	100.0
41 - 51	1139	59.768	26.401	18.581	14.332	100.0
51 - 61	1318	53.235	33.736	12.752	11.265	100.0
61 - 71	1389	43.187	24.960	7.696	8.908	100.0
71 - 81	1483	28.782	27.255	1.770	8.197	100.0
81 - 91	1610	25.202	25.492	0.885	7.288	100.0
91 - 101	1715	24.578	33.883	-0.594	6.909	100.0
101 - 111	1803	17.223	25.198	-3.854	6.273	100.0
111 - 121	1850	10.027	37.886	-9.225	6.055	100.0
121 - 131	1762	23.178	21.608	-1.114	5.956	100.0
131 - 141	1668	24.933	18.768	1.837	6.798	100.0
141 - 151	1575	34.642	36.522	5.079	8.485	100.0
151 - 161	1462	36.396	17.986	6.071	8.500	100.0
161 - 171	1397	42.003	26.138	8.439	9.827	100.0
171 - 181	1292	66.192	28.710	13.401	12.979	100.0
181 - 191	1100	63.763	81.673	13.872	16.514	100.0
191 - 201	733	64.982	88.458	-2.528	24.969	100.0
201 - 211	159	55.684	88.866	-26.149	31.135	100.0

It can be recognised that the accuracy of the depth measurements is correlated with the position of the sonar beams: The standard deviation of the outer beams is much higher than the one of the centre beams. The integrated tests of both software packages provided similar results and prove the fulfilment of the IHO Order 3 requirements to

7.4 Quality determination of the HYDROSWEEP DS3

100 %.

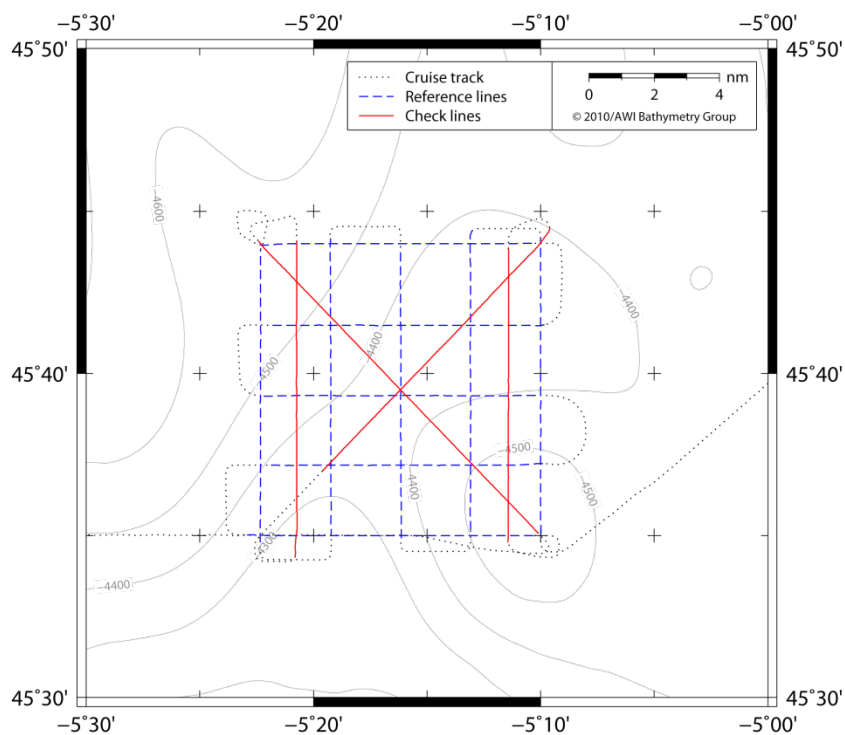


Fig. 7.4.2: Track lines of patch test: The reference lines have been measured with swath angle of 90° to achieve a precise reference surface. The check lines have been measured with full swath angle of 120°. Differences have been calculated for quality assessment.

8. HALOCARBON AIR SEA TRANSECT – ATLANTIC (HALOCAST-A) – FALL

Shari Yvon-Lewis, Lei Hu
TAMU

Objectives

This project is an effort to study the spatial/temporal variability of methyl bromide (CH_3Br) and other halocarbons in the upper ocean in response to the implementation of the Montreal Protocol and its amendments (UNEP, 1995). Assuming that rates of biological production in the ocean have not changed, our CH_3Br model predicts that CH_3Br should be less undersaturated than it was before the phaseout of non-quarantine and preshipment uses (Yvon-Lewis et al., 2009). The anthropogenic chlorofluorocarbons (CFCs) and hydrochlorofluorocarbons (HCFCs) should still be near equilibrium with regard to surface ocean saturation. However, the CFC surface ocean concentrations should be lower and the HCFC surface ocean concentrations should be higher than before the implementation of the protocol. Spatial and temporal trends in the very short-lived species (VSLS) should not be impacted by the Montreal Protocol or its amendments as they are not currently regulated, and many VSLS are thought to be mostly biogenic. During this project, we will gain information on the temporal and spatial variability in these species through measurements made in regions and seasons where we made them a little over 10 years ago.

This study is strongly related to Surface Ocean Lower Atmosphere Studies (SOLAS) goals. Advancing our understanding of ocean/atmospheric chemical coupling requires:

1. A comprehensive data base of the spatial/temporal variability of trace gases in the surface ocean, and
2. An understanding of the factors controlling the surface ocean distributions and air/sea fluxes of these gases.

Understanding sources and sinks is the key to understanding their distributions, and to developing a predictive capability for how they will respond to the coming changes in climate such as changes in sea surface temperature (SST), ocean acidification, changes in salinity, etc.

Shipboard measurements will include underway saturation state measurements and degradation rate constants. Any differences from the predicted saturation state will be used to improve our understanding of the role of the ocean in the global cycling of halocarbons. The long-term goals of this work are to understand the origin and cycling of CH_3Br and other halocarbons in the oceans, and to develop a predictive capability for how the air/sea fluxes of oceanic trace gases will respond to the coming global changes in atmosphere/ocean chemistry and climate.

Work at Sea

We collected and analyzed samples from the underway flowing seawater system and from an air sampling line running to the monkey deck.

- Halocarbon/C1-C3 hydrocarbon air and equilibrator headspace samples were collected and analyzed continuously using a Weiss type equilibrator and a gas chromatograph with mass spectrometer (GCMS) and an FID. An air line ran to the monkey deck for continuous air side measurements, and the equilibrator was used for the water-side measurements with water supplied at 15 L/min from the steel pumping system. The instrument is automated and alternated between air and equilibrator headspace samples.

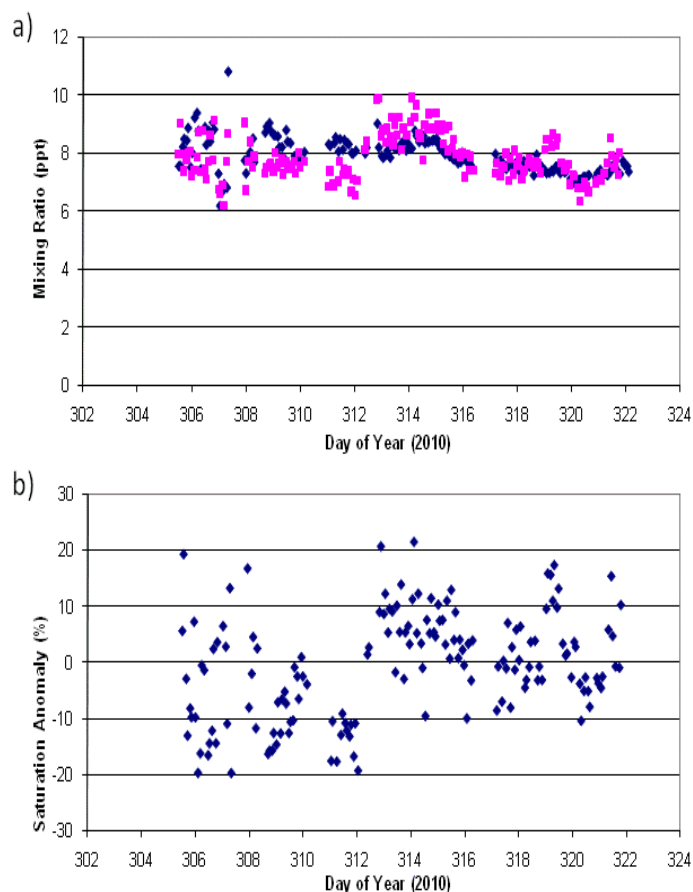


Fig. 8.1: Times series of methyl bromide (a) atmospheric concentrations (◆) and equilibrium surface water concentrations (■) and (b) saturation anomalies.

- Degradation rate constants were measured using water collected once per day from the underway membrane pumping system. Some aliquots of water were

filtered and others were not. All were spiked with ^{13}C labeled CH_3Br or CH_3Cl and the loss was measured over time with a purge and trap GCMS.

- Cyanobacteria samples were collected 3 times per day from the membrane pump flow through system and frozen for analysis at TAMU. (Total samples = 67)
- Nutrient samples were be collected once per day from the membrane pump flow through system and frozen for analysis at TAMU. (Total samples = 24)
- Pigment samples were collected once per day from the flow through system and frozen for analysis at TAMU. (Total samples = 24)
- Dissolved organic carbon (DOC) samples were collected once per day from the flow through system and frozen for analysis at TAMU. (Total samples = 24)

Preliminary Results

We obtained continuous underway air and surface water concentration data for 17 different chemical species; HCFC-22, CFC-12, HFC-142b, CH_3Cl , H-1211, CH_3Br , CFC-11, CH_3I , CFC-113, CHCl_3 , CH_3CCl_3 , CCl_4 , CH_2BrCl , CHCl_2Br , CHClBr_2 , TCE, CHBr_3 . For this project, our focus was on methyl bromide (Fig. 8.1).

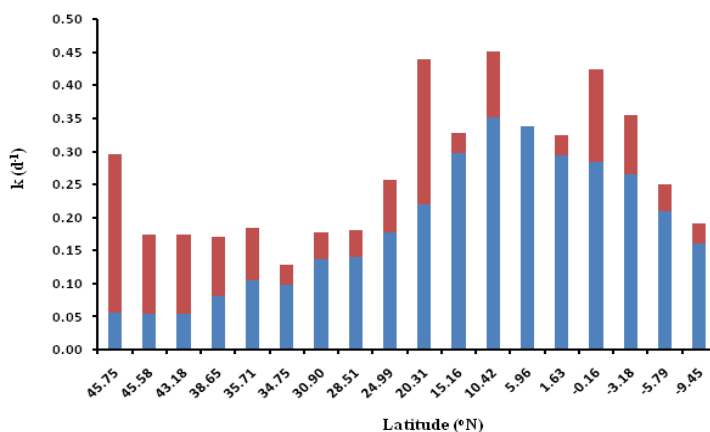


Fig. 8.2: The Latitudinal distribution of methyl bromide degradation rate constants: biological (■) and chemical (■).

The degradation rate constant measurements for methyl bromide show significant biological degradation over the entire latitude range sampled (Fig. 8.2)

The frozen samples will be analyzed back at Texas A&M University. The combined results will be used for modeling of global oceanic uptake and emissions of the various biogenic gases.

References

- UNEP, Report of the seventh meeting of the parties to the Montreal Protocol on Substances that Deplete the Ozone Layer, United Nations Environmental Program, World Meteorol. Org. (WMO), Geneva, Dec., 1995.
- Yvon-Lewis, S. A., E. S. Saltzman and S. A. Montzka, 2009. Recent trends in atmospheric methyl bromide: analysis of post-Montreal Protocol variability *Atmos. Chem. Phys.*, 9, 5963–5974.

9. INVESTIGATION OF BROMINATED AND ORGANOPHOSPHORUS FLAME RETARDANTS AND MONITORING OF LEGACY POPS IN THE ATLANTIC AND THE SOUTHERN OCEAN

Ulla Bollmann¹⁾, Axel Möller
(not on board) ¹Zhiyong Xie¹⁾,
Jasmin Schuster²⁾, Hendrik
Wolschke (not on board) ¹⁾,
¹Zhiyong Xie¹⁾

¹⁾HZG
²⁾Lancaster University

Objectives

Persistent organic pollutants (POPs) can enter the coast, marine and ocean environment by a number of processes, once introduced they are subject to biogeochemical cycling, sinks, and bioaccumulation process. Apart from the discharge of the rivers and runoff, atmosphere is considered to be the primary and most rapid pathway for pollutant transport to the coast and marine environment as a result of their hydrophobic and semi-volatile nature, respectively.

Several leading groups of Environmental Chemistry are joining the *Polarstern* during ANT-XXII to determine emerging and legacy persistent organic pollutants in moderate latitudes of the Northern and Southern hemisphere in proposal to further investigate their up to date levels and air-sea interactions in remote oceans. The research programme is focused on the determination of selected POPs in air and water, which is subdivided into several major groups.

Brominated flame retardants (BFRs), primarily polybrominated diphenyl ethers (PBDEs), have been used to reduce the flammability of various commercial and industrial products the last decades. The global production volume of BFRs was 300.000 tons in 2004 with a continuous increase within the last decades. PBDEs are toxic, bio-accumulative and persistent compounds and have been regulated or banned by national and international regulations, which leads to increasing demand for non-regulated, non-PBDE flame retardants such as hexabromobenzene (HBB) and 1,2-bis(2,4,6-tribromophenoxy)ethane (BTBPE).

Phosphorus flame-retardants (OPFRs), organophosphorus compounds such as tris(2-chloroethyl) phosphate and triphenyl phosphate are widely used as flame retardants as well as plasticizer and in hydraulic fluids with a global production volume (as flame retardant) of ca. 210,000 tonnes in 2004. As a result of international regulations of PBDEs, the production volume of OPFRs is expected to increase, and thus, leads to increasing emissions in the environment.

Current-use pesticides (CUPs); an increased public and regulatory attention during

and 1970s and 1980s resulted in bans for many legacy pesticides and has led to the development and licensing of new pesticides with less persistence. This group of newer compounds is called current-use pesticides. Because CUPs are extensively used worldwide, they are subjected to new concerns regarding the prevalence and effects of these compounds in the environment at low levels.

Among the legacy POPs of interest for this project are polychlorinated biphenyls (PCBs), polychlorinated dibenzodioxins/furans (PCDD/Fs), and polycyclic aromatic hydrocarbons (PAHs). The production of PCBs peaked in the 1960s. First restrictions and bans were established by individual countries in the 1970s and the following decades until it was globally banned in 2001. It was used in closed systems e.g. as a cooling agent in transformers as well as in open system like paints and glues. PCBs were produced as a mixture of different congeners with a varying grade of chlorination. Current sources for PCBs are dumps and old systems. PCDD/Fs and PAHs formed during combustion procedures.

Also part of the monitored legacy POPs are organochlorinated pesticides (OCPs) like DDT and its degradation products DDE and DDD, as well as the chlordane, lindane and hexachlorobenzene (HCB). Even though the pesticides have been officially banned worldwide some are still in use in some countries.

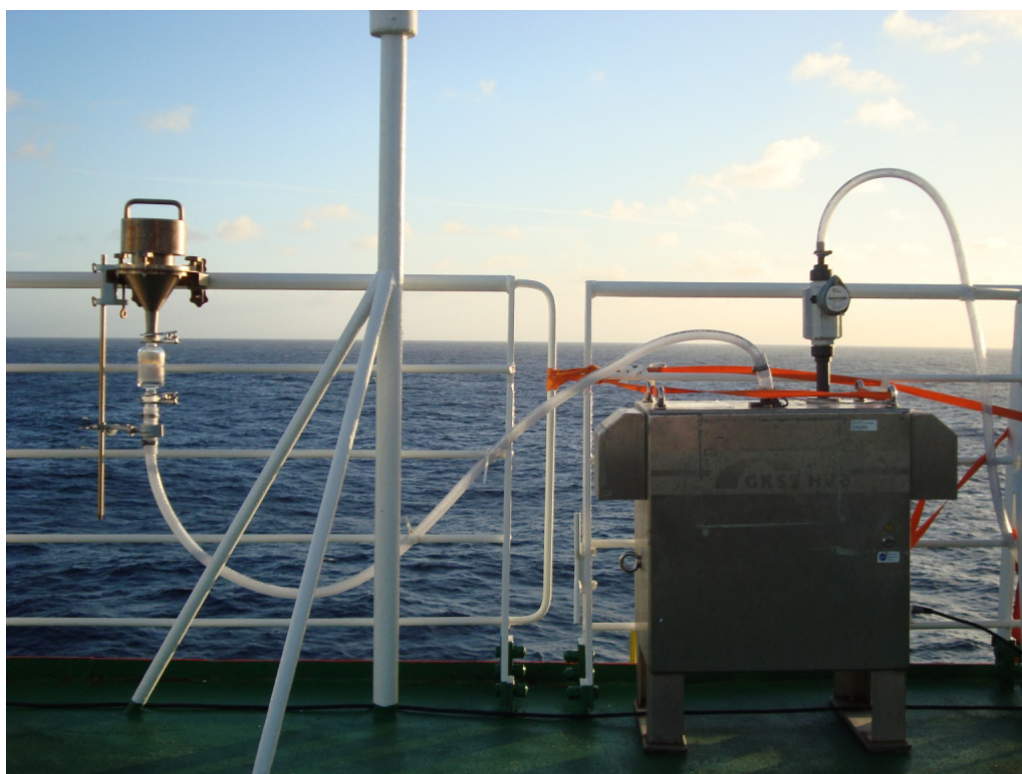


Fig. 9.1: High volume air sampling operated aboard F/V Polarstern during ANT-XXVII-1 (photo by Jasmin Schuster).

9. INVESTIGATION OF BROMINATED AND ORGANOPHOSPHORUS FLAME RETARDANTS AND MONITORING OF LEGACY POPS IN THE ATLANTIC AND THE SOUTHERN OCEAN

ANT-XXVII/1 was quite optimal for these investigations as it ranged from the likely sources (European continent) to remote areas without direct inputs. By combining short-term atmospheric samples and the collections of reprehensive water samples across different region of the North and South Atlantic Ocean, findings are sought as to whether atmospheric transport or ocean current are controlling the transport and setting flux of emerging persistent organic pollutants. Additionally, some other emerging organic pollutants such as non-polybrominated flame retardants, currently used pesticides and organic stabilizers will be investigated for their presence in the Atlantic.

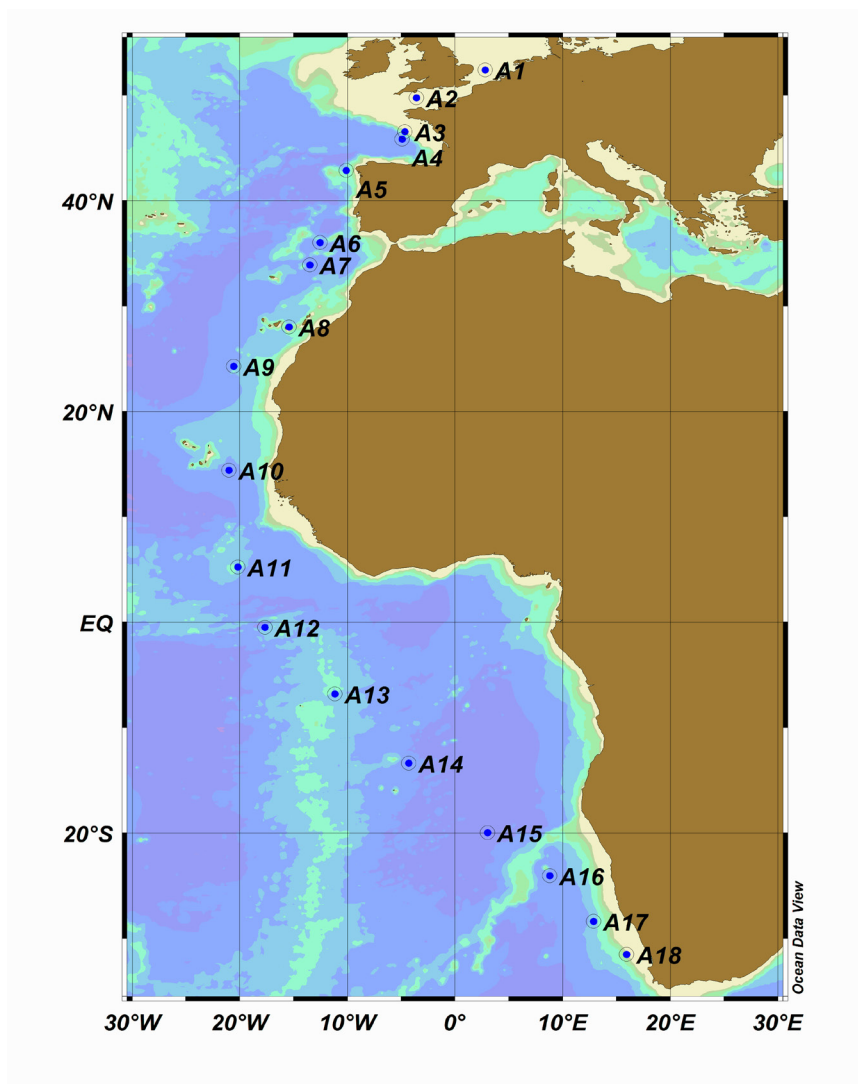


Fig. 9.2: High volume air sampling aboard Polarstern during ANT-XXVII/1

Work at sea

Monitoring studies for POPs concentrations are important to get insights in transport mechanisms and the global cycling. The understanding of the global of fate legacy POPs (i.e. PCBs, PAHs), Dichlorodiphenyltrichloroethane (DDT), Hexa-chlorocyclohexanes (HCHs), Hexachlorobenzene (HCB)) will enable predictions and improved legislations for emerging POPs (i.e. PBDEs, PFCs).

Air samples were collected using a high-volume air sampler operating at a constant flow rate of 500 L min⁻¹. The ship-borne air samples were collected on the upper deck of *Polarstern* (Fig. 9.1). Typical air sample volume was 500 - 1,000 m³. The high volume air sampler consisted of a high volume pump (ISAP 2000, Schulze Automation & Engineering, Asendorf, Germany), a digital flow meter, a metal filter holder and a PUF/PAD-1 or PUF/PAD-2 column. GF/F 8 filter was used to collect atmospheric particles. Samples collected with PUF/PAD-1 columns were used to determine PFRs, BFRs, and dechlorane plus, and samples collected with PUF/PAD-2 will be used to investigate the concentrations of currently used pesticides such as trifluralin, endosufan isomers, and other emerging organic pollutants, respectively (Fig. 9.2). Field blanks were prepared by shortly espousing the columns to the sampling site. Air samples were stored at -20°C in a cooling room.

Water samples were collected using both Keel In-Situ Pump (KISP) and 2 liter sea water solid-phase extraction. KISP was connected to the sea water intake system (stainless steel pipe/Klauss pump) of *Polarstern* (11 m depth). A glass cartridge packed with PAD-2 or PAD-3 was used to enrich the analytes in the dissolved phase, and a glass-fiber filter (GF/F 52) was used to collect suspended particular matters (SPMs). Each sample continually ran for 20 hours to achieve a sample volume of ~1,000 L (Fig. 9.3). 26 2-L water samples were extracted with Oasis Wax cartridges to determine the distribution of perfluorooctanoic acid (PFOA) and perfluorooctane sulfonic acid (PFOS) across the Atlantic Ocean (Fig. 9.4). Additionally, 26 2-L water samplers were extracted with HLB cartridges, which were used to determine dissolved organic matters in sea water. PAD-2 and PAD-3 columns were stored at 0°C, and the Oasis Wax cartridges, and filter samples were stored at -20 °C in a cooling room, respectively.

Lancaster University used a different technology to perform high-volume air sampling and water sampling. Atmospheric samples on *Polarstern* were collected using a High Volume Air Sampler. Particles were collected on a glass fibre filter and POPs were collected using polyurethane foam (PUF) plugs. Samples were collected for 6 h and 12 h periods. 91 atmospheric samples were collected with corresponding field blanks for quality control. This was double the number of samples collected by this institute along the same transect on previous campaigns. This should allow a better resolution of POP concentrations on this transect, as well as more insight of the concentration dependence to diurnal conditions.

Water samples were taken for testing a passive water sampling system especially for research vessels. The passive sampling media, a polyethylene membrane (PEs), was mounted on spiders and deployed in a stainless steel canister. Sea water flowed straight from the tab in the sampler and passed through it with a flow rate of ~5 L/min. Three PEs were deployed at once for a period of 24h. The PEs were spiked with deperation compounds to monitor and calculated the actual water volume sampled. A total of 17 water samples were collected.

Preliminary results

The samples will be further handled in a clean-lab at HZG Research Centre. PUF/XAD-2, PUF/PAD-2, PAD-2 and PAD-3 columns and GF filters were extracted with organic solvents (hexane, dichloromethane, acetone, and methanol) or a mixture for

9. INVESTIGATION OF BROMINATED AND ORGANOPHOSPHORUS FLAME RETARDANTS AND MONITORING OF LEGACY POPS IN THE ATLANTIC AND THE SOUTHERN OCEAN

~24 h. The SPE cartridges were eluted with methanol for PFC measurements, and with hexane/DCM mixture for dissolved organic matters.

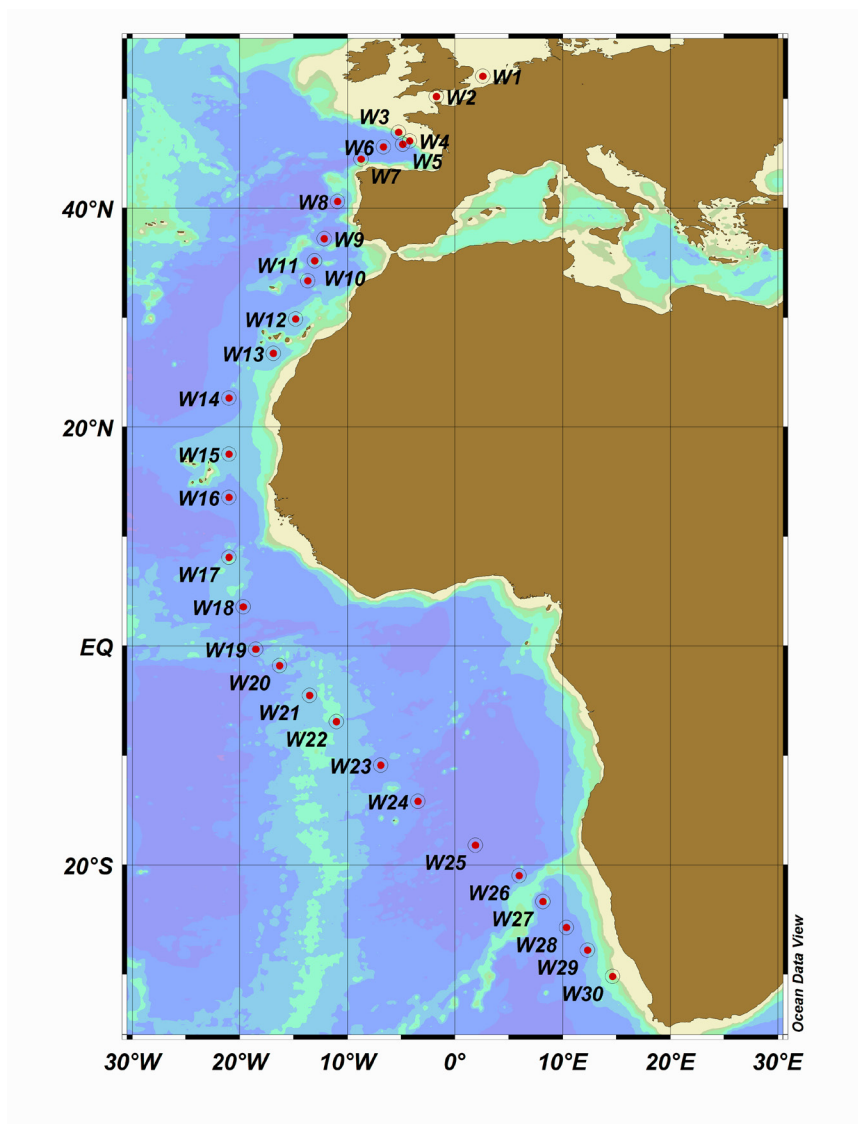


Fig. 9.3: High volume water sampling aboard Polarstern during ANT-XXVII/1

Neutral PFCs were quantified by an Agilent 6890 gas chromatography (GC) coupled to a 5973 mass spectrometer (MS) using positive chemical ionization mode. BFR, PFR and currently used pesticides were determined by GC-MS using negative chemical ionization mode, respectively. PFOS and PFOA and other ionic PFCs were detected using liquid chromatography coupled with tandem mass spectrometers (LC-MS-MS).

Data obtained from this cruise will set up a background of PFCs and BFRs in the North Atlantic. Furthermore, the air-sea gas exchanges of PFCs and BFRs will be investigated to discover the importance of atmospheric transport for the occurrence of these emerging persistent organic pollutants in open ocean.

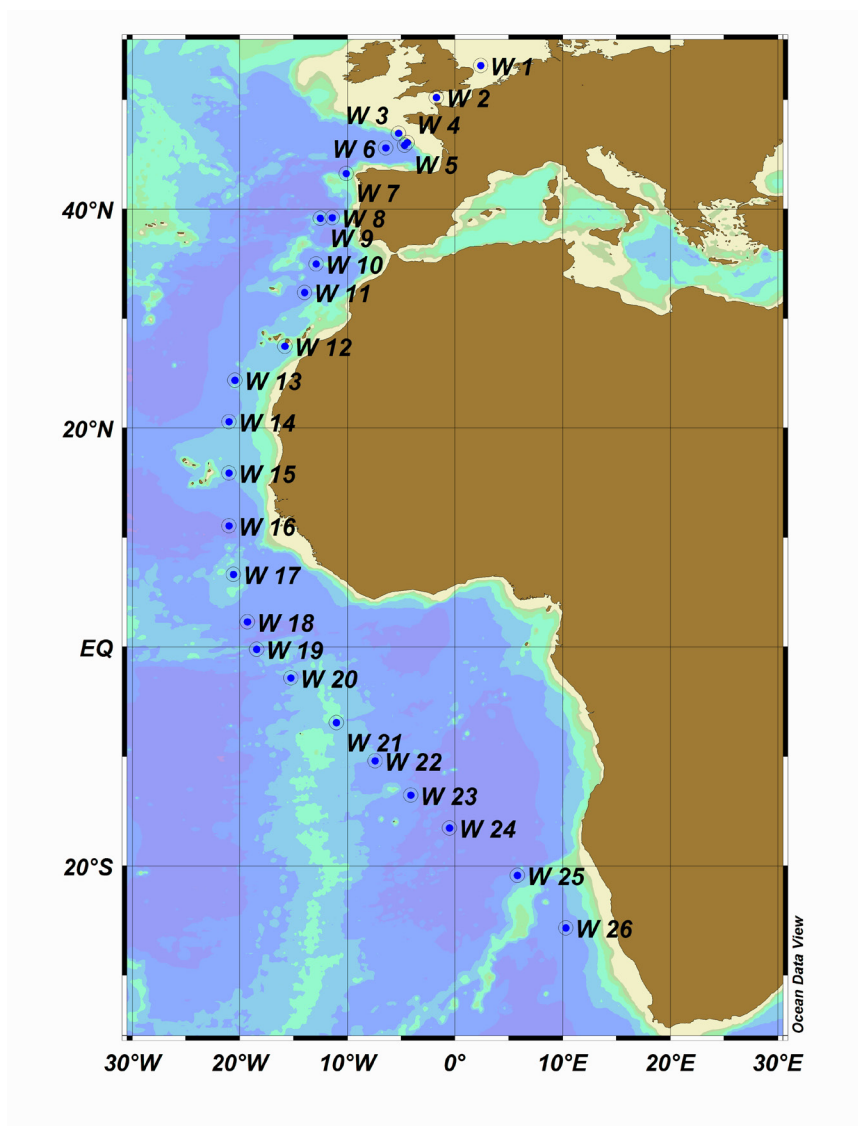


Fig. 9.4: Sampling stations for SPE with WAX and HLB cartridges aboard *Polarstern* during ANT-XXVII/1

Temporal trends of legacy POPs will be analyzed by comparing the air data from this cruise to data obtained in the years 2005 and 2007. Compounds monitored in both air and water samples include PCBs, PAHs, DDT, HCHs, HCB and PBDEs. The samples could not be analyzed on the ship, but have to be analyzed in clean laboratory conditions at Lancaster University.

10. (A) ON-BOARD TESTING OF A NEWLY DEVELOPED SEAGOING MEMBRANE-INLET MASS SPECTRO-METER (MIMS) AND SETUP OF PCO₂/IRON EXPERIMENTS WITH NATURAL SOUTHERN OCEAN PHYTOPLANKTON POPULATIONS; (B) SAMPLING OF POM FOR BIOMARKER ANALYSIS

Klaus-Uwe Richter, Sven Kranz, Ulrike Richter, Meri Eichner, Björn Rost
Alfred-Wegener-Institut

Objectives

Project A was carried out in order to provide lab facilities and properly functioning electronic equipment for the following cruise leg. During ANT-XXVII/2 Southern Ocean phytoplankton communities will be incubated under different CO₂ concentrations in combination with iron depletion and repletion. In view of climate change, Southern Ocean primary producers will face major environmental variations (Tortell et al. 2008). Little information of the response of Southern Ocean phytoplankton on CO₂ increase in combination with iron limitation is currently available. Data on underlying cellular processes of possible responses on these environmental changes do not exist.

To gain such a process based understanding of the phytoplankton in the Southern Ocean, a clean-lab for trace metal free work was installed in a lab-container and a gas-mixing system to provide precise CO₂ gas concentrations was set up, calibrated and tested.

To investigate *in vivo* responses of phytoplankton to changes in CO₂ and iron availability, a sea-going membrane-inlet mass spectrometer (MIMS) with a novel cuvette/inlet system, developed at the AWI, was installed. The MIMS system consists of a custom-made cuvette and inlet system combined with a quadrupole mass spectrometer. Dissolved gas molecules like CO₂ or O₂ permeate through the membrane and are ionized and detected only seconds later in the mass spectrometer. The advantage of this approach is that several processes can be observed and quantified simultaneously. A suite of methods allows quantification of cellular C fluxes, a prerequisite to understand the effect of CO₂ on photosynthesis and other down-stream processes. One method allows distinguishing between CO₂ and HCO₃⁻ as carbon sources and determines the uptake kinetics as a function of C availability or other environmental conditions. In another application, the use of stable isotopes allows measuring photosynthetic processes which are highly sensitive to iron limitation. Stable isotopes also allow the determination of carbonic anhydrase activities, a key enzyme catalyzing the otherwise

slow inter-conversion between CO_2 and HCO_3^- . The MIMS system was first tested for its sensitivity against temperature variations and ship vibration. The system is now configured and the sensitive hardware is working.

For project (B), samples of seawater were taken every 3° latitude along the track. The seawater was immediately filtered and plankton in three size classes of $> 100 \mu\text{m}$, $100 - 20 \mu\text{m}$ and $< 20 \mu\text{m}$ were collected. The isotopic composition of biomarkers in the organic material will be measured back in Bremerhaven. Combined with surface water parameters such as temperature and salinity, results of this project will be implemented in a temperature/salinity proxy for paleoclimatology by Dr. Albert Benthien.

Work at Sea

- We set up the gas mixing system, installed the tubing for the distribution of the gases to the incubation chambers.
- The gas mixing system was calibrated with reference gases.
- The incubation chambers were set up and with the help of the crew of *Polarstern* an illumination system was built up in the container.
- A trace metal free area was set up in the lab-container consisting of a clean-bench attached to a plastic foil tent.
- A 50 m clean sampling tube for pumping seawater to the iron free room was placed through *Polarstern* ready to be connected to a trace metal clean pumped tow fish system, operated on the following transect.
- The MIMS system was installed and tested.
- Abiotic signals were calibrated and biological samples were measured in order to determine the signal to noise ratio.
- Seawater samples between 25 L and 80 L were taken via the ships membrane pump each 3° latitude starting at 47°N till 28°S. In total 26 positions were sampled. Next to filters, accompanying samples were taken for determination of phytoplankton composition and δD of the seawater.

Preliminary results

The systems were installed successfully for the following cruise ANT-XXVII/2.

References

Tortell PD, Payne CD, Li Y, Trimborn S, Rost B, Smith WO, Riesselman C, Dunbar R, Sedwick P, DiTullio G (2008) The CO_2 response of Southern Ocean phytoplankton. *Geophys Res Lett* **35**, L04605, doi: 10.1029/2007GL032583

11. INSTALLATION AND DATA TAKING OF A COSMIC MUON DETECTOR ON *POLARSTERN*

Michael Walter
DESY

Objectives

Goal of the project is the measurement of cosmic particles in dependence on different parameters as air pressure, humidity, temperature and the latitude. On the ocean level we measure mostly muons. They are decay products of elementary particles which are produced in interactions of protons with air molecules in heights of 15 to 25 km. These protons come from the sun or from galactic and extragalactic sources. The sun is a source of relatively low energy protons. Since the sun activity will increase in the coming years, an increase of eruptions will lead to higher particle radiation.

Work at sea

A detector to measure rates of cosmic particles was installed on *Polarstern*. The detector consists of 2 scintillation counters which give a signal if a muon is crossing both.

In the following the different topics of the experiment are summarized:

- Measurement of the number of cosmic muons in dependence on the parameters mentioned above. The rate decreases with decreasing distance to the equator since the magnetic field of the Earth guides the low energy particles to the poles. This effect can be used to estimate the sensitivity of the detector.
- The use of the weather observations on board (especially OCEANET and the weather balloon) for the investigation of the influence of meteorological parameters on the intensity of the cosmic radiation.
- The preparation of a common station consisting of a muon detector (DESY) and a neutron monitor (Univ. Kiel and North-West Univ. South Africa) for long-term investigations of the sun activity and for an early warning system of sun eruptions. Such systems are already installed in different countries and at research stations in Antarctica. The *Polarstern* installation enabled it to extend the measurements to the ocean.

Preliminary Results

The Fig. 11.1 shows the measured number of muons per hour in dependence on the latitude for the time period 2010-11-26 0:00 until 2010-11-24 0:00. The muon rate was normalized to an air pressure of 1,000 hPa.

A clear decrease of the rate is seen going from north to the equator. This geomagnetical cut-off of the muon rate shows that the detector is sensitive also for cosmic particles with lower energy, as e.g. for particles coming from the sun.

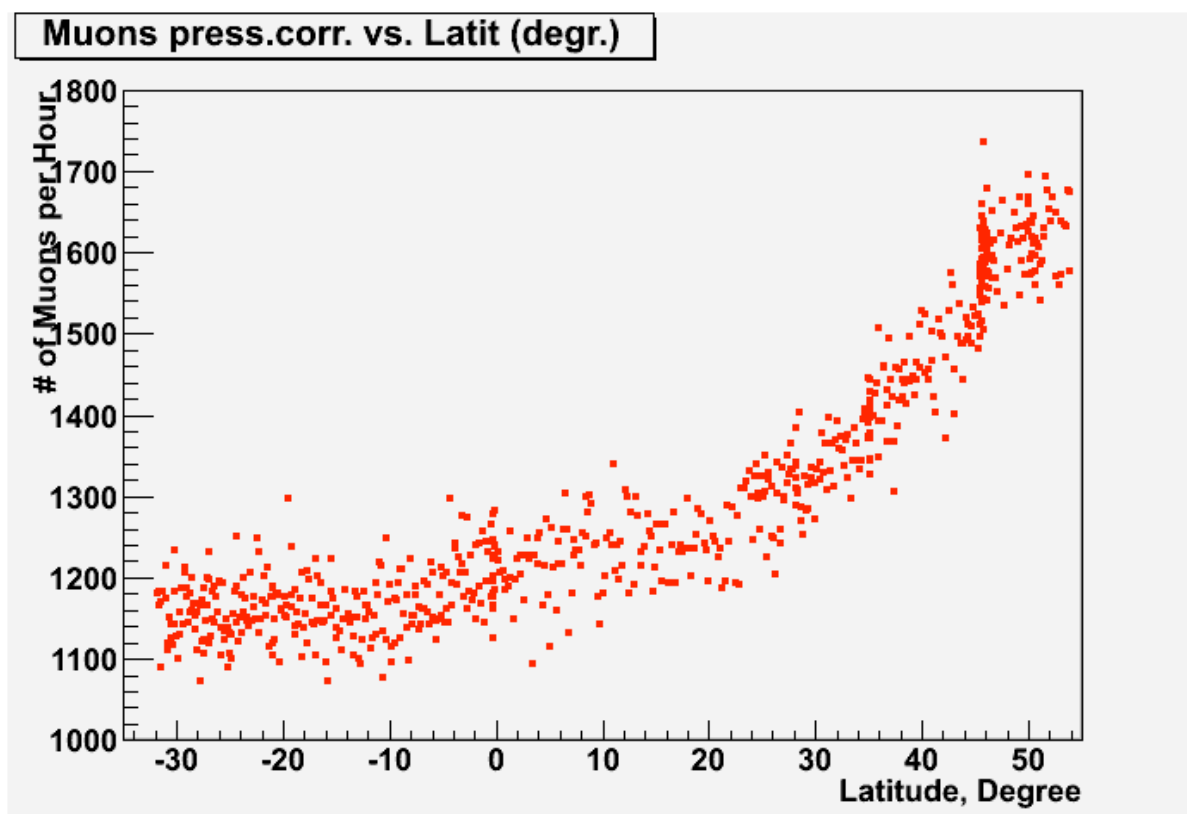


Fig. 11.1: Dependence of the muon rate on the latitude

A post-processing of the data will comprise the following topics:

- an investigation if the observed fluctuations of the muon rate during the day caused by statistical fluctuations, which could be reduced by using larger scintillation detectors,
- the influence of other meteorological parameters than air pressure (e.g. temperature, humidity, cloud density) on the muon rate,
- the data collected at this and at future cruises will be made available via a web-interface at DESY. They also will be used for school and student projects as well as for training programmes of teachers.

12. CAVITY-ENHANCED DOAS MEASUREMENTS OF IODINE MONOXIDE IN THE MARINE ATMOSPHERE

Martin Horbanski, Ulrich Platt (not on board)
IUP

Objectives

It is well known that reactive halogens play an important role in the chemistry of the marine atmosphere (e.g. Von Glasow and Crutzen 2007). Apart from bromine radicals, also iodine compounds emitted from biogenic sources might have the potential to destroy ozone and to form new ultrafine particles. Iodine monoxide at concentrations of around 20 ppt was detected in coastal regions (e.g., Mace Head, Ireland, and the coast of Britain). While coastal regions – in comparison to their areas - are probably much stronger sources of reactive iodine than the open ocean, the latter covers a much larger fraction of the Earth's surface. Thus the contribution of coastal versus open ocean sources to the global budget of reactive iodine is unclear to date.

Most measurements of reactive iodine have been conducted using Long Path Differential Optical Absorption Spectroscopy (LP-DOAS) and Multi-Axis DOAS (e.g. Seitz 2009). LP-DOAS can quantify halogen monoxide radicals at ppt levels by recording their structured absorption using optical path lengths of several kilometres in the open atmosphere. Therefore, the obtained trace gas concentrations are an average along light paths of several kilometres length. However, such measurements are not possible on a ship since they require distances of several kilometres between the telescope and a retro reflector. MAX-DOAS instruments, such as our system permanently operated on the *Polarstern*, observe scattered sunlight using a simple optical setup, but a precise quantification of trace gas concentrations is difficult because the light path is not well defined.

Well-defined optical path lengths of several kilometres can be achieved using Cavity Enhanced DOAS (CE-DOAS) (e.g. Fiedler 2005, Platt 2009). CE-DOAS uses passive optical resonators to provide long light-paths (> 1 km), in a relatively compact setup with resonator lengths in the order of 1 m. Thus CE-DOAS provides point like measurements of trace gas concentrations.

We have developed such an instrument for mobile measurements of iodine monoxide (IO) and nitrogen dioxide (NO₂) and deployed it on the *Polarstern* to perform a precise quantification of the marine IO surface concentrations. A planned combination with our MAX-DOAS system was not possible because a malfunction in its electronics did not allow for a reliable operation.

This cruise also allowed a thorough test of our new CE-DOAS system, before it will

be shipped to Neumayer Station, where it will be used for measurements of iodine monoxide emitted by the snowpack during the summer campaign 2010/11.

Work at Sea

- The CE-DOAS instrument was setup in the scientific working room for first tests.
- The power supply of the instrument was upgraded and the wiring of the power cords were exchanged to allow a stable operation of the instrument at distances greater than 30 m between the instrument and its power supply.
- In order to optimize the wavelength calibration of the spectrometer, the mercury spectral lamp was replaced by a krypton spectral lamp.
- The frame of the CE-DOAS instrument was modified to improve its mechanical stability.
- Calibrations of the CE-DOAS instruments light path were performed by the comparison of measurements in helium and zero-air.
- The instrument was setup on the monkey-deck and first measurements were performed.
- Several attempts were made to repair our MAX-DOAS instrument. The tests performed on this cruise suggest that the malfunction comes from the spectrometer control unit. Unfortunately it was not possible to repair these components during the cruise.

References

- Fiedler, S.E. (2005), Incoherent Broad-Band Cavity-Enhanced Absorption Spectroscopy, PhD thesis, Technische Universität Berlin.
- Platt, U., Meinen, J., Pöhler, D. and Leisner, T. (2009), Broadband Cavity Enhanced Differential Optical Absorption Spectroscopy (CE-DOAS) – applicability and corrections, *Atmos. Meas. Tech.*, 2, 713-723
- Seitz K. (2009), The Spatial Distribution of Reactive Halogen Species at the Irish West Coast, Doctoral thesis, Institute of Environmental Physics, University of Heidelberg, <http://www.ub.uni-heidelberg.de/archiv/9442>.
- Von Glasow, R., and Crutzen, P.J. (2007), Tropospheric Halogen Chemistry, Holland H. D. and Turekian K. K. (eds), *Treatise on Geochemistry Update1*, vol. 4.02, pp 1 – 67.

13. MAPS: MARINE MAMMAL PERIMETER SURVEILLANCE

Olaf Boebel (not on board)¹⁾, Lars Kindermann (not on board)¹⁾, Matthias Monsees¹⁾, Sebastian Richter²⁾, Maria Torres Vega³⁾, Daniel P. Zitterbart⁴⁾

¹⁾AWI
²⁾University Erlangen-Nürnberg
³⁾Develogic
⁴⁾AWI & University Erlangen-Nürnberg

Objectives

The detection of marine mammals in the vicinity of ships to either collect data for cetacean research or for mitigation purposes during the operation of some hydroacoustic instruments is a strenuous, personnel and time intensive task. The MAPS projects aim at making maximum use of ship-whale encounters through systematic logging of opportunistic sightings by the ship's nautical officers (MAPS-vis) and by developing an automatic detections system based on thermal imaging (MAPS-IR).

Whales may be detected by infrared thermography on the basis of the thermal anomaly generated by a whale's blow, which strongly contrasts the cold Antarctic environment. To achieve this, a scanning, high-resolution thermal imaging system, FIRST-Navy, was installed on the ship's crow's nest prior to this expedition. This system, representing the state-of-the-art in infrared imaging, provides 360° thermal images at a 5 Hz full frame refresh rate to computer monitors on the ship's bridge and in the operator's lab.

One purpose of our participation in this cruise leg transiting from Bremerhaven to Cape Town was to further test the associated self-developed software package *Tashtego* and the sensor's endurance under tropical conditions. Furthermore, to estimate the sensor's performance in warm waters, we hoped for ship-whale encounters in the tropics or subtropics to be recorded by the system. However, the main task during this leg was the technical implementation of an additional *PiP* (picture in picture) visual camera system as an extension to the FIRST-Navy infrared sensor, providing close-up pictures of auto-detected whales to allow retrospective species identification. The *PiP* camera system consists of a high-resolution digital color camera with a telelens, mounted on a pan-tilt-unit (PTU). The system shall be automatically triggered and oriented by data from the FIRST-Navy unit.

Complementary to these in-transit marine mammal observations which emphasize the spatial dimension, are stationary, long-term observations of marine mammals with focus on the temporal dimension. Of particular interest are observations in marine mammal breeding grounds. Such observations are hoped to help unraveling the stock structure of a given species. However, visual long-term observations in open ocean regions are impossible to execute. This problem may be overcome by use of passive

acoustic recordings, exploiting the fact that many cetaceans vocalize extensively during their breeding period. To gather information about blue and fin whale presence in their hypothesized Atlantic winter and breeding locations near the Walvis Ridge some hundreds of miles off the Namibian coast, we intend to deploy in this region a deep-sea mooring containing an acoustic recorder to collect continuous acoustic data for at least one year. This mooring complements an array of 10 moorings with similar recording devices to be deployed during cruise leg ANT-XXVII/2 in the Weddell Sea in order to study the whales' migration forth and back to the Southern Ocean.

Work at sea

Operation of the FIRST-Navy thermal imager

The FIRST-Navy sensor head UN 001 was operated continuously for 15 days, starting on 23 October 2010. After 12 hours of operation problems with synchronization between the image acquisition rate and the motor speed occurred. However, uploading of a modified "configuration file" to the FIRST sensor head allowed desynchronizing the rotation and image acquisition, resulting in a defined drift rate of the images. On 2010-11-06, the FIRST sensor head UN 001 was taken out of operation due to problems with presumably the cooling element, as evidenced by sensor temperatures above operating temperatures (80 K) and images turning completely grey. As an at-sea repair of this unit was not possible, the manufacturer and AWI agreed to exchange the sensor head UN 001 with a spare sensor head, UN 002, during the following week. This FIRST sensor head (UN 002) was operational for 26 days until the end of cruise when it was shut down. Detailed information can be found in Table 13.1.

Table 13.1: Timetable showing the operation periods of the FIRST-Navy thermal sensor head.

Start yyyymmdd-hhmmss	End yyyymmdd-hhmmss	Hours operational [h]	Unit number
20101023-180000	20101106-180000	336	1
20101113-140000	20101128-080000	354	2
		∑ 690	

The picture-in-picture camera system

The *PiP* system consists of several components which were assembled and installed during this leg. These are the digital camera (Prosilica GE 4000 C), a remote controllable focus unit (Birger EF232 mount), a tele-zoom lens (Canon 100 - 400 mm 4:5.6L), a pan-tilt-Unit (PTU) (Directed Perception D300-ISM), a 2x level-one GS 0980 router, a Moxa terminal server and a PeakCan Can-to-USB converter. The digital camera provides 5 frames per second with a resolution of 11 Mpixel. Its operation is completely autonomous. Images are polled directly by the computer and stored on its hard drive. Due to the high data rate of 50 MByte/sec the storage process has to operate very efficiently to avoid losing frames. The GE4000C digital camera lacks the ability to

control the focus of the lens, therefore a Birger EF232 remote controllable focus unit was installed. Image data is transferred via an optical cable from the crow's nest directly to the operator's laboratory where the data acquisition and processing for the FIRST-Navy is installed. All *PiP* related software components were installed on the same computer as the *Tashtego* software (which provides data acquisition and processing for the FIRST-Navy images). When the *Tashtego* software automatically detects a whale, this information is exchanged with the PTU controller software (*PiPcontrol*) via a shared memory. The PTU itself is controlled via RS232. Control commands are sent via a virtual serial port (socat) to the Moxa terminal server which is directly attached via RS232 to the PTU. To ensure that the PTU remains oriented towards a certain geo-referenced location, an inertial stabilization software was developed. The PTU was mounted on the crow's nest (Fig. 13.1), close to the FIRST-Navy thermal sensor on 2011-11-06. All necessary cables had already been installed during the previous dock time of *Polarstern*.



Fig. 13.1: The high-resolution camera in its metal housing mounted to the Pan-Tilt-Unit (PTU, black) installed on *Polarstern*'s crow's nest.

Image acquisition and processing

Visual images are directly polled from the digital camera by the *xstream2Mmap* module and stored in a 5 frame ringbuffer as raw image data. This ringbuffer is implemented as a memory mapped file, which resides for performance reasons in a RAMdisk. To temporarily save images, these are written to a larger ringbuffer (8Tb, RAID-0) by the module *xstream2bin* which reads data from the shared memory and writes images in raw format (*.bin) to the harddrive. The raw image data is Bayer-pattern encoded, requiring the application of a *debayer* filter in order to save the image as RGB files. This *debayer* operation lasts more than 200 ms computing time per image, prohibiting

saving images in real-time in a single thread and necessitating saving in raw format. Only when the system is triggered to permanently save a certain set (i.e. period) of images, the *debayer* filter is applied retrospectively, and the images are stored with JPEG compression.

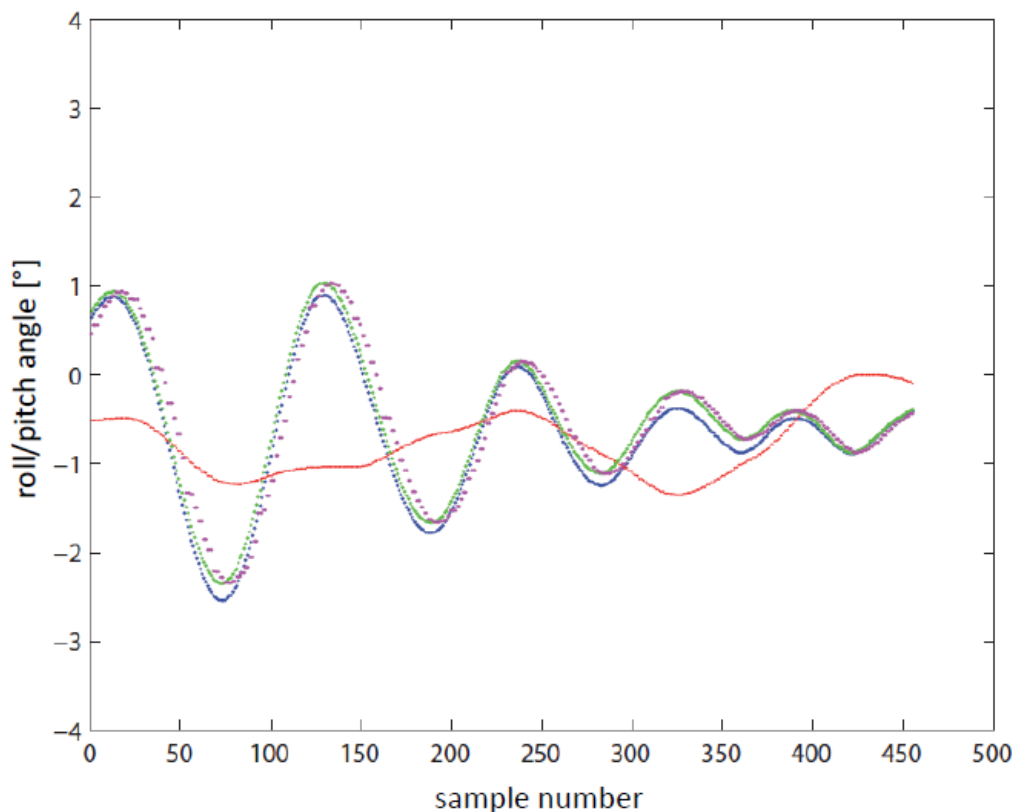


Fig. 13.2: Inertial stabilization of the PiP system. Red: ship roll, blue: ship pitch, green: target tilt value for the PTU, magenta: current tilt value of the PTU.

Positioning and inertial stabilization

To keep the *PiP* camera pointed to a specific spot (i.e. the location of a whale) it is necessary to continuously adjust pan and tilt of the PTU to correct for the ship's movements. Corresponding metadata, like the ship's heading, its position and speed, are received at a frequency of 0.5 Hz from the ship's data management system (Dship) via NMEA strings. When the IR system detects a whale spout, the *PiP* system receives a set of geocoordinates from *Tashtego* to which it shall point the (visual) camera. These coordinates are then translated by the PTU controller software (*PiPcontrol*) to the corresponding PTU pan/tilt position. Subsequently, the PTU's inertial stabilization software module corrects this initial PTU pan/tilt position for the ship's roll and pitch, which are polled from the gimbal of the FIRST-Navy system with a frequency of 20 Hz. This results in stabilized image sequences as shown in Fig. 13.2.

Passive acoustic monitoring

The mooring AWI 247-1 (Fig. 13.3) was deployed at 20° 58.90' S 05° 059.59' E on

20 November 2010 11:40. It contains a SonoVault passive acoustic monitoring (PAM) recorder, (SN 0001, manufacturer delevologic, Germany). This newly developed instrument uses a highly sensitive RESON hydrophone and can record at 24 Bit resolution (19 Bit effective) with up to 20 kHz sampling rate and 16 Bit data (15 Bit effective resolution) with up to 200 kHz sampling. It is equipped with 1 Terabyte of memory (5 memory modules housing 7 32-GB SD-cards each). Optionally, a DSP board can perform various signal processing tasks. In this project, the SonoVault was set to record to 24 Bit WAV format at a sample rate of 5,120 Hz. This allows for three years of continuous sound acquisition. Firmware version 1.1 was uploaded before deployment, the sample-rate was set to 5,120 Hz, the clock calibration to 32,768 and the gain factor to 60. The water depth at this location is 4,288 m and the recorder was placed at a depth of 789 m, i.e. in the SOFAR channel, which ensures a maximum acoustic range.

Preliminary results

Tashtego and PiP software development and implementation

Both, the *Tashtego* and *PiP* software packages were used and tested throughout the cruise. The tests revealed that the computer (Intel i7-860 4 Core) was not powerful enough to handle both (infrared and visual) data streams concurrently. The image acquisition software itself already uses one core for each camera, which resulted in a high image loss rate of the *PiP* system. Therefore *Tashtego* and *PiP* were not used concurrently during this cruise leg. When operated solely, the *PiP* image loss ratio is about 10^{-3} and therefore negligible. During the next cruise leg (ANT-XXVII/2) the computer system will be upgraded with a more powerful machine (12 cores) to overcome this problem. Additionally the *PiP* modules will be integrated into the *Tashtego* software.

Thermal imaging of whale blows

Due to the limited number of whale sightings only two concurrent video sequences were saved during the cruise (see Table 13.2). The data of these two saved sequences have not yet been analyzed; therefore estimates on the sensor performance in warm waters are not yet available.

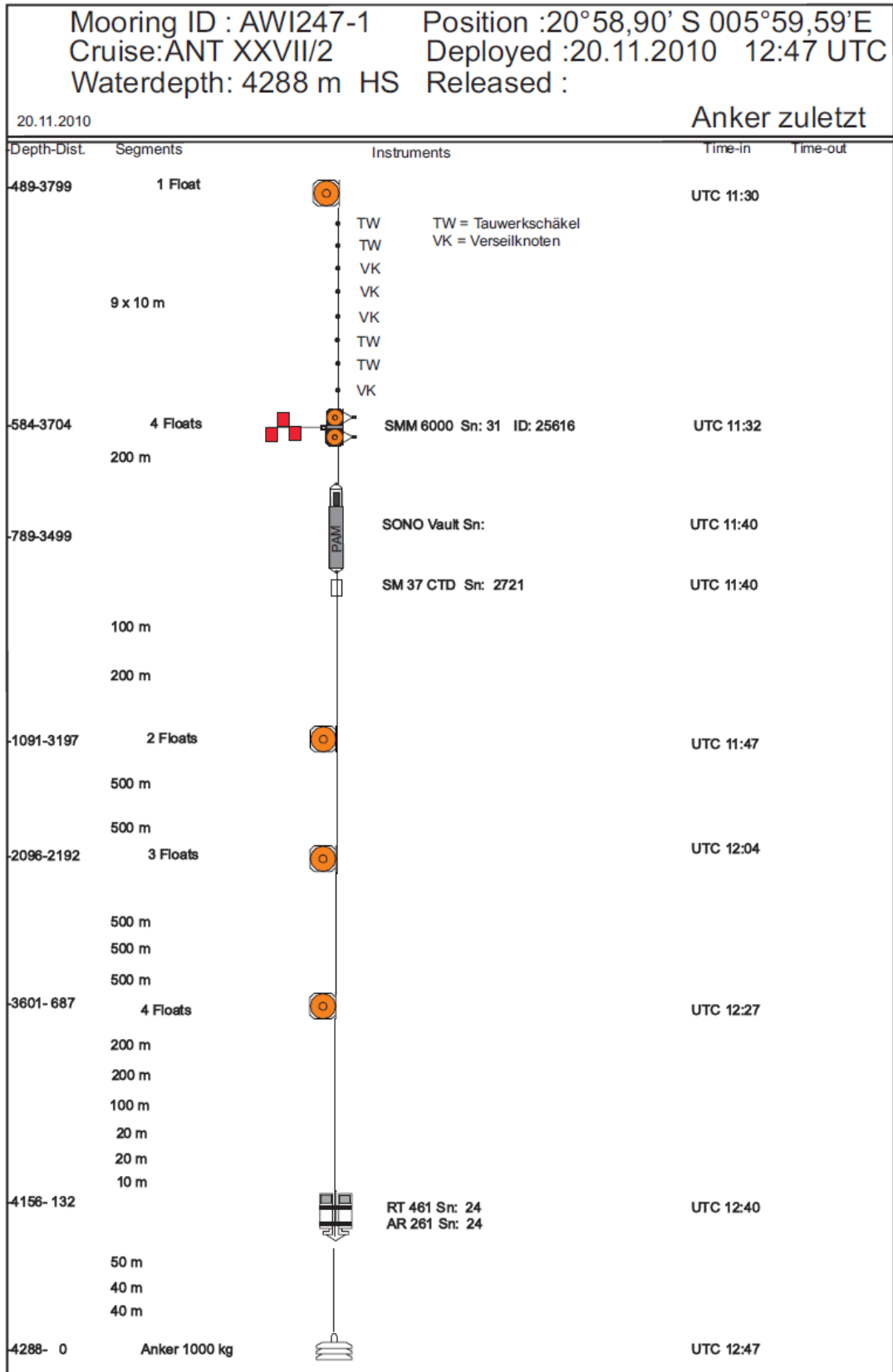


Fig. 13.3: Schematic of mooring AWI 247-1

Table 13.2: List of archived IR sequences during ANT-XXVII/1

Start	End	Sequence
20101024-213000	20101025-000000	Depart Bremerhaven, part1
20101025-050000	20101025-070000	Depart Bremerhaven, part2
20101106-080000	20101106-150000	Las Palmas
20101120-094500	20101120-100500	whale
20101122-161700	20101122-163000	whale

Passive acoustic monitoring

Results from the passive acoustic recordings will only be available after recovery of the mooring. This is planned for fall 2011. It is yet encouraging, that just prior to the mooring deployment an undefined large whale was sighted, and that further sighting were made during the following day, suggesting that the selected mooring position is indeed in an area occupied by large cetaceans.

Acknowledgements

We would like to thank all agencies and institutions, who funded our scientific research. Special thanks go to Master Wunderlich and his crew for their competent and professional support, their friendliness and openness, which made this cruise to a success. And we would like to mention that we appreciated very much all the help we got from the AWI logistics.

APPENDIX

A.1 PARTICIPATING INSTITUTIONS

A.2 CRUISE PARTICIPANTS

A.3 SHIP'S CREW

A.4 STATION LIST

A.1 TEILNEHMENDE INSTITUTE / PARTICIPATING INSTITUTIONS

	Address
Atlas	ATLAS HYDROGRAPHIC GmbH Kurfürstenallee 130 28211 Bremen Germany
AWI	Stiftung Alfred-Wegener-Institut für Polar- und Meeresforschung in der Helmholtz-Gemeinschaft Postfach 120161 27515 Bremerhaven Germany
Bodenseewerke	Diehl BGT Defence GmbH & Co. KG Alte Nußdorfer Straße 13 88662 Überlingen Germany
DESY	DESY Platanenallee 6 15738 Zeuthen Germany
Develogic	develogic GmbH Eiffestr. 598 20537 Hamburg Germany
DWD	Deutscher Wetterdienst Geschäftsbereich Wettervorhersage Seeschiffahrtsberatung Bernhard Nocht Str. 76 20359 Hamburg Germany
Eötvös	Environmental Optics Laboratory, Department of Biological Physics, Physical Institute, Eötvös Loránd University Egyetem tér 1-3. Budapest, 1053 Hungary
Estrato	Estrato: Research and Development, Ltd., Mártonlak utca 13 Budapest 1121 Hungary
FAU	Friedrich-Alexander-Universität Erlangen-Nürnberg Schlossplatz 4 91054 Erlangen/Germany

	Address
HZG	Helmholtz-Zentrum Geesthacht Max-Planck-Straße 1 21502 Geesthacht Germany
IFM-GEOMAR	Leibniz-Institut für Meereswissenschaften an der Christians-Albrecht-Universität, IFM-GEOMAR FB1 und 2 Düsternbrooker Weg 20 24105 Kiel Germany
IfT	Leibniz-Institut für Troposphärenforschung e.V., Leipzig Permoserstraße 15 04318 Leipzig Germany
IUP	Institut für Umweltphysik Universität Heidelberg Im Neuenheimer Feld 229 69120 Heidelberg Germany
Laeisz	Reederei F. Laeisz (Bremerhaven) GmbH Brückenstr. 25 27568 Bremerhaven Germany
Lancaster	Lancaster University University House Bailrigg, Lancaster Lancashire LA1 4YW United Kingdom
MPI	Max-Planck-Institut für Meteorologie Bundesstraße 53 20146 Hamburg Germany
NIOZ	Royal Netherlands Institute for Sea Research Landsdiep 4 1797 SZ 't Horntje (Texel) The Netherlands
TAMU	Texas A&M University College Station, Texas 77843 U.S.A

A.2 FAHRTTEILNEHMER / CRUISE PARTICIPANTS

Name/ Last name	Vorname/ First name	Institut/ Institute	Beruf/ Profession
Alfke	Rolf	Atlas Hydro Bremen	Engineer
Barta	Andras	Eötvös & Estrato	Physicist
Bittig	Henry	IFM-GEOMAR Kiel	Chemist
Boche	Martin	Reederei Laeisz	Engineer
Bollmann	Ulla	HZG Geesthacht	Student
Bumke	Karl	IFM-GEOMAR Kiel	Meteorologist
Eichner	Meri	AWI Bremerhaven	Chemist
El Nagggar	Saad	AWI Bremerhaven	Physicist
Ewert	Jörn	Atlas Hydro Bremen	Engineer
Fillingner	Laura	AWI Bremerhaven	Scientist, bathymetry
Gallbach	Ute	AWI Bremerhaven	Student
Gerchow	Peter	AWI Bremerhaven	Engineer
Gottschall	Alexandra	AWI Bremerhaven	Student
Horbanski	Martin	IUP Heidelberg	Student
Horvath	Akos	MPI Hamburg	Scientist
Horvath	Gabor	Eötvös Uni Budapest	Physicist
Hu	Lei	A&M Uni Texas	Student
Kalisch	John	IFM-GEOMAR Kiel	Meteorologist
Kanitz	Thomas	IfT Leipzig	Student
Kewitsch	Peter	Bodenseewerke Überl.	Engineer
Kleta	Henry	DWD Hamburg	Technician
Kluge	Olaf	Atlas Hydro Bremen	Engineer
Kranz	Sven	AWI Bremerhaven	Biologist
Krocker	Ralf	AWI Bremerhaven	Engineer
Loose	Bernd	AWI Bremerhaven	Technician
Mohr	Wiebke	IFM-GEOMAR Kiel	Biol. Oceanographer
Monsees	Matthias	AWI Bremerhaven	Technician
Niederjasper	Fred	AWI Bremerhaven	Geodesist
Prokoph	Andreas	AWI Bremerhaven	Student
Richter	Klaus-Uwe	AWI-Bremerhaven	Bio-Engineer
Richter	Sebastian	AWI Bremerhaven	Student
Richter	Ulrike	AWI Bremerhaven	Technician
Rogenhagen	Johannes	Reederei Laeisz	Geophysicist
Schack	Lukas	AWI Bremerhaven	Student
Schenke	Hans Werner	AWI Bremerhaven	Scientist
Schuster	Jasmin	Lancaster Uni	Student
Sonnabend	Hartmut	DWD Offenbach	Technician
Springer	André	Atlas Hydro Bremen	Engineer
Steinhoff	Tobias	IFM-GEOMAR Kiel	Chemist
Torres	Maria	Develogic Hamburg	Engineer
Ulrich	David	AWI Bremerhaven	Student
Vielstädte	Lisa	IFM-GEOMAR Kiel	Student
Walter	Michael	DESY	Physicist
Weigel	Benjamin	IFM-GEOMAR Kiel	Student
Xie	Zhiyong	HZG Geesthacht	Scientist
Yvon-Lewis	Shari	A&M Texas Uni	Scientist
Zoll	Yann	IFM-GEOMAR Kiel	Meteorologist

A.3 SCHIFFSBESATZUNG / SHIP'S CREW

Name	Rank
T. Wunderlich	Master
U. Grundmann	1. Offc.
G. Krohn	Ch. Eng.
H. Fallei	2. Offc.
H. Dugge	2. Offc. 3. Offc.
M. Erich	Doctor
A. Hecht	R. Offc.
H.-U. Linzmann	2. Eng.
M. Schäfer	2. Eng.
H. Schnürch	2. Eng.
H. Muhle	Elec. Eng.
A. Winter	ELO
Fabrizius	ELO
F. Himmel	ELO
M. Scholz	ELO
R. Loidl	Boatsw.
L. Reise	Carpenter
A. Becker	A.B.
Schünemann	A.B.
S. Pousada	A.B.
M. Hagemann	A.B.
U. Schmidt	A.B.
M. Winkler	A.B.
U. Wende	A.B.
P. Brickmann	A.B.
J. Prueßner	Storek.
T. Pinske	Mot-man
N. Schütt	Mot-man
K. Elsner	Mot-man
U. Teichner	Mot-man
B. Voy	Mot-man
R. Müller-Homburg	Cook
M. Martens	Cooksmate
F. Silinski	Cooksmate
B. Czyborra	1. Stwdess
M. Wöckener	Stwdess/N.
I. Wartenberg	2. Stwdess
C. Silinski	2. Steward
H.J. Gaude	2. Stwdess
Y.S. Sun	2. Steward
Q.L. Chen	2. Stwdess
K.Y. Yu	Laundrym.

A.4 STATIONSLISTE / STATION LIST PS 77

Station PS77	Date	Time (start)	Time (end)	Position (Lat.)	Position (Lon.)	Depth (m)	Gear
001-1	28.10.10	10:54	10:59	46° 41.86' N	4° 59.22' W	715.0	HydroSweep ParaSound profile
001-2	28.10.10	11:28	11:37	46° 41.84' N	4° 59.01' W	709.5	HydroSweep ParaSound profile
001-2	28.10.10	12:07	12:12	46° 41.86' N	4° 59.17' W	713.3	HydroSweep Para- Sound profile
001-2	28.10.10	12:47	12:55	46° 41.84' N	4° 58.99' W	691.1	HydroSweep Para- Sound profile
002-1	28.10.10	17:50	18:31	46° 6.73' N	4° 13.06' W	1391.9	Sound Velocity Profiler
003-1	28.10.10	19:18	20:13	46° 4.48' N	4° 16.36' W	1973.0	HydroSweep Para- Sound profile
003-2	28.10.10	20:28	21:09	46° 10.95' N	4° 8.26' W	1160.6	HydroSweep Para- Sound profile
003-3	28.10.10	21:50	22:31	46° 6.88' N	4° 14.00' W	984.2	HydroSweep Para- Sound profile
003-4	28.10.10	22:50	23:30	46° 10.87' N	4° 8.38' W	1105.5	HydroSweep Para- Sound profile
003-5	29.10.10	00:03	01:47	46° 6.97' N	4° 13.87' W	1078.8	HydroSweep Para- Sound profile
003-6	29.10.10	02:14	03:58	46° 6.89' N	4° 14.00' W	1063.2	HydroSweep Para- Sound profile
004-1	29.10.10	04:39	05:26	46° 4.39' N	4° 16.97' W	2542.8	HydroSweep Para- Sound profile
004-2	29.10.10	05:35	06:28	46° 9.81' N	4° 11.25' W	2626.6	HydroSweep Para- Sound profile
004-3	29.10.10	06:52	07:38	46° 5.42' N	4° 17.53' W	1044.2	HydroSweep Para- Sound profile
004-4	29.10.10	07:59	08:50	46° 9.37' N	4° 9.90' W	2459.9	HydroSweep Para- Sound profile
004-5	29.10.10	09:08	10:00	46° 4.77' N	4° 18.44' W	2543.6	HydroSweep Para- Sound profile
005-1	29.10.10	13:20	15:04	45° 49.95' N	4° 47.98' W	4201.7	Sound Velocity Profiler
006-1	29.10.10/ 30.10.10	15:26	01:59	45° 50.30' N	4° 49.96' W	4407.6	HydroSweep Para- Sound profile
007-1	30.10.10	03:06	06:41	45° 49.20' N	4° 38.44' W	4104.1	HydroSweep Para- Sound profile
008-1	30.10.10/ 31.10.10	10:00	02:46	45° 34.50' N	5° 9.21' W	4575.1	HydroSweep Para- Sound profile
009-1	02.11.10	13:42	14:04	38° 29.68' N	11° 39.86' W	4875.7	Releaser/Hoisting Test
010-1	03.11.10	18:57	19:58	35° 10.03' N	12° 59.15' W	2464.9	Mooring (short time)
010-2	03.11.10	19:39	21:03	35° 10.43' N	13° 2.34' W	2386.7	Sound Velocity Profiler
010-3	03.11.10/ 04.11.10	21:15	07:42	35° 11.31' N	13° 2.52' W	2398.0	POSIDONIA

Station PS77	Date	Time (start)	Time (end)	Position (Lat.)	Position (Lon.)	Depth (m)	Gear
010-4	04.11.10	07:44	08:27	35° 10.40' N	13° 2.24' W	2365.0	Mooring (short time)
011-1	12.11.10/ 13.11.10	21:48	08:44	0° 1.15' S	18° 35.62' W	7483.6	HydroSweep Para-Sound profile
011-2	13.11.10	09:04	10:40	0° 13.12' S	18° 25.90' W	7465.4	Sound Velocity Profiler
011-3	13.11.10	10:46	13:14	0° 13.06' S	18° 25.88' W	7452.6	HydroSweep Para-Sound profile
012-1	20.11.10	09:10	10:20	20° 53.05' S	5° 49.63' E	4309.8	HydroSweep Para-Sound profile
012-2	20.11.10	11:28	13:15	20° 56.06' S	5° 58.40' E	4248.3	Mooring

Die "Berichte zur Polar- und Meeresforschung" (ISSN 1866-3192) werden beginnend mit dem Heft Nr. 569 (2008) ausschließlich elektronisch als Open-Access-Publikation herausgegeben. Ein Verzeichnis aller Hefte einschließlich der Druckausgaben (Heft 377-568) sowie der früheren "**Berichte zur Polarforschung**" (Heft 1-376, von 1982 bis 2000) befindet sich im Internet in der Ablage des electronic Information Center des AWI (**ePIC**) unter der URL <http://epic.awi.de>. Durch Auswahl "Reports on Polar- and Marine Research" auf der rechten Seite des Fensters wird eine Liste der Publikationen in alphabetischer Reihenfolge (nach Autoren) innerhalb der absteigenden chronologischen Reihenfolge der Jahrgänge erzeugt.

To generate a list of all Reports past issues, use the following URL: <http://epic.awi.de> and select the right frame to browse "Reports on Polar and Marine Research". A chronological list in declining order, author names alphabetical, will be produced, and pdf-icons shown for open access download.

Verzeichnis der zuletzt erschienenen Hefte:

Heft-Nr. 616/2010 — "The Expedition of the Research Vessel 'Polarstern' to the Antarctic in 2009 (ANT-XXV/4)", edited by Christine Provost

Heft-Nr. 617/2010 — "The Expedition of the Research Vessel 'Polarstern' to the Amundsen Sea, Antarctica, in 2010 (ANT-XXVI/3)", edited by Karsten Gohl

Heft-Nr. 618/2010 — "Sozialhistorische Studie zur Polarforschung anhand von deutschen und österreich-ungarischen Polarexpeditionen zwischen 1868-1939", by Ursula Rack

Heft-Nr. 619/2010 — "Acoustic ecology of marine mammals in polar oceans", by Ilse Van Opzeeland

Heft-Nr. 620/2010 — "Cool Libraries in a Melting World - Proceedings of the 23rd Polar Libraries Colloquy 2010, June 13-18, 2010, Bremerhaven, Germany", edited by Marcel Brannemann and Daria O. Carle

Heft-Nr. 621/2010 — "The Expedition of the Research Vessel 'Polarstern' to the Arctic in 2010 (ARK-XXV/3)", edited by Volkmar Damm

Heft-Nr. 622/2010 — "Environmentally induced responses of *Donax obesulus* and *Mesodesma donacium* (Bivalvia) inhabiting the Humboldt Current System", by Daniel Carstensen

Heft-Nr. 623/2010 — "Research in the Laptev Sea region - Proceedings of the joint Russian-German workshop, November 8-11, 2010, St. Petersburg, Russia", edited by Sebastian Wetterich, Paul Pier Overduin and Irina Fedorova

Heft-Nr. 624/2010 — "The Expedition of the Research Vessel 'Polarstern' to the Arctic in 2010 (ARK-XXV/2)", edited by Thomas Soltwedel

Heft-Nr. 625/2011 — "The Expedition of the Research Vessel 'Polarstern' to the Arctic in 2010 (ARK-XXV/1)", edited by Gereon Budéus

Heft-Nr. 626/2011 — "Towards data assimilation in ice-dynamic models: the (geo)physical basis", by Olaf Eisen

Heft-Nr. 627/2011 — "The Expedition of the Research Vessel 'Polarstern' to the Arctic in 2007 (ARK-XXII/1a-c)", edited by Michael Klages & Jörn Thiede

Heft-Nr. 628/2011 — "The Expedition of the Research Vessel 'Polarstern' to the Antarctic in 2010 (ANT-XXVII/1)", edited by Karl Bumke